NUCLEAR SPIN RELAXATION

IN

CONDUCTING LIQUIDS

by

David S. Moore B.Sc.

A thesis submitted for the degree of

Doctor of Philosophy of the

University of Warwick.

School of Physics,

University of Warwick.

March, 1972.

Memorandum

This dissertation is submitted to the University of Warwick in support of my application for admission to the degree of Doctor of Philosophy. It contains an account of my own work performed at the School of Physics of the University of Warwick in the period from January 1968 to March 1971 under the supervision of Professor E. F. W. Seymour. No part of it has been used previously in a degree thesis submitted to this or any other university. The work described in this thesis is the result of my own independent research except where acknowledged in the text. An account of the work on liquid alloys of tellurium has been published in Phil. Mag., (1971), 23, 1249, and an extension of this work in J. Non-Cryst. Solids (1972) 8/9, 256. It is anticipated that an account of the work on quadrupolar relaxation in liquid metallic alloys given in Chapter Five will be published shortly.

David S Moore

D. S. Moore

March 1972

Author's Note

The S.I. system of units has been adopted throughout this thesis. It must be pointed out that in these units the familiar expression for the Knight shift is now

$$S = (2/3)\,\Omega \left\langle |\psi(0)|^2 \right\rangle_F \chi_p^{(v)}$$

However this leads to accepted values of the Knight shift since $\chi_p^{(v)}$ in S.I. units is 4π times its value expressed in c.g.s. units.

Acknowledgements

I would like to express my gratitude to Professor E. F. W. Seymour for his continuing interest in all matters relating to this study, and particularly for his willingness to find time for discussion at all stages in the course of the work. I am grateful to Dr. G. A. Styles for much useful advice and to Dr. E. Claridge who was responsible for the major part of the work in construction of the pulse spectrometer. I would like to acknowledge assistance given in many ways by Dr. D. Brown. I also acknowledge the help of Mr. C. J. Ford who made the suceptibility measurements and Professor S. L. Segel who carried out the relaxation measurements on the Al-Si sample. I thank Professor A. J. Forty for allowing me to use the facilities of the School of Physics and the Science Research Council for providing a Research Studentship.

Finally I wish to thank the members of my family for their continual support and in particular my wife, Jackie, who also was responsible for the production of the manuscript.

ABSTRACT

Measurements have been made of the motions of atoms and conduction electrons in a number of liquid metallic and liquid semiconducting elements and alloys as a function of composition and temperature using the method of nuclear magnetic resonance (NMR). A description of a coherent NMR pulse spectrometer constructed in the course of the work is given.

Nuclear spin-lattice relaxation rate measurements have been made for ^{27}Al in Al-Si, ^{115}In in Bi-In and In-Sb, ^{121}Sb in Bi-Sb and In-Sb, and ^{209}Bi in Bi-In, Bi-Pb, Bi-Sb and Bi-Sn. Where resonance shifts were not already available in the literature these have also been measured (with the exception of that of ^{27}Al). These relaxation rates are compared to those calculated from the resonance shifts using the Korringa relationship. An additional relaxation rate appears showing a broad maximum in the middle of the composition range for all the nuclei observed except ^{27}Al, being as much as eight times as large as the extra rate in the pure metal. This is identified as arising from the fluctuations of the electric field gradients due to the ionic motions interacting with the quadrupole moment of the nucleus. This has led to an extension by Sholl of his theory of electric quadrupolar relaxation in pure liquid metals to the case of liquid alloys to explain these results. The theoretical expression contains two integral terms; the first arising from the two body correlation function, the second arising from the three body correlation function. To fit the theoretical expression to the experimental data it is shown to be necessary to set the second term near to the magnitude of the first but opposite in sign, and then good agreement can be obtained. In order to discuss the data in terms of this theory three simplifying assumptions must be made. It is shown that the assumptions concerning radial distribution functions and self-diffusion

coefficients are reasonable, whereas that concerning the representation of the electric field gradient may not be.

Nuclear resonance shifts and spin-lattice relaxation rates for ^{125}Te in liquid Te-Tl alloys have been measured in the range Te_{100} to Tl_{70}. At 750 K the shift, measured with respect to solid tellurium decreases from + 0.38% to - 0.08% across the composition range whereas the relaxation rate remains approximately constant at $5 \times 10^{3} s^{-1}$ over most of the range. Correlation of the temperature dependences of the total magnetic suceptibility and the shift shows that the changes in shift are principally due to changes in density of states at the Fermi level rather than in the electronic wavefunction at tellurium nuclei. In the region near $TeTl_2$ where the density of states is low the relaxation rate is considerably shorter than that predicted from the Korringa relationship and the observed shift. This is interpreted as due to partial localisation of the conduction electrons.

CONTENTS

CHAPTER ONE

INTRODUCTION

1.1 Conducting Liquids

The behaviour of conduction electrons in solid (crystalline) metals has been very fully described in terms of suitable wavefunctions and energies which are derived using the lattice periodicity. In liquids, where the arrangement of the atoms can only be represented by means of a probability distribution the problem of describing electron behaviour is still far from satisfactory. The destruction of long range atomic order must be expected to remove the sometimes complex energy band structure typical of crystals, leaving a single-sheet spherically symmetrical Fermi surface. However this is not to say that the electrons behave precisely as perfectly free non-interacting particles since they must still be affected by the presence of the ions (and by interactions amongst themselves), and questions concerning the dynamics, wavefunctions and energy - wavenumber dependences of the conduction electrons remain to be completely solved. A recent review of the present state of theory can be found in March (1968).

The most obvious and most thoroughly investigated property which can be expected to throw light on these problems is the electrical conductivity. (The powerful techniques of Fermi surface topology measurements such as the de Hass-van Alphen effect, and of electron density of states measurements through the electronic specific heat require low temperatures and are clearly not applicable to liquids.) Liquids which are classified as conductors or as semiconductors are those whose conductivities exceed a few times $10^{3}\,\mathrm{ohm}^{-1}\mathrm{m}^{-1}$; below this value conduction takes place by ionic motion, whereas above conduction is due predominantly to mobile electrons perhaps assisted to some extent by holes. Electronic

conduction in liquid metals and alloys, i.e. those whose conductivity is comparable to solid metals, has been explained with reasonable success using the nearly free electron (n.f.e.) theory (Faber and Ziman, 1965). The electrons are represented by plane waves which are scattered by weak scattering centres arranged in the same manner as the atoms in the liquid. Under these conditions the electrons have mean free paths which are long compared to the inter-atomic spacing, and the density of states is similar to that for free electrons.

As the scattering of the electrons gets stronger the Born approximation, which is used in the n.f.e. theory as the means of calculating the weak scattering, no longer holds, and so the theory is no longer applicable. Mott (1967) has postulated that as the electron mean free path decreases due to the increase in the scattering the density of states will change. Mott further postulates that if the density of states falls appreciably below the free electron value then electrons in those states become localised, and can only move by means of thermally activated hopping To demonstrate this theoretically a solution of the three dimensional Schrödinger equation with a potential which is a random function of position is required, but as yet no complete solution has been obtained.

When nuclear spins in these materials relax to a lower energy state one of the principal interactions by which their energy is transferred to their surroundings is the direct interaction between the nuclear spin and the conduction electron spin. This work is concerned largely with the measurement of nuclear spin-lattice relaxation rates, and the discussion of the contribution a knowledge of these rates can make to an understanding of electronic behaviour.

1.1.1 Liquid metals The materials in this category, which will be discussed in Chapter Five, all exhibit properties typical of a normal metal. Their conductivities are all of order $10^{6}\,\mathrm{ohm}^{-1}\mathrm{m}^{-1}$,

and the temperature coefficient of the conductivity is usually negative. The composition dependence of the conductivity in binary alloys is satisfactorily explained on the nearly free electron theory. Thermoelectri power values agree with those calculated from free electron theory. Hall coefficients are found to be close to values calculated from a free electron model in pure liquid metals (Cusack, 1963); the situation in alloys where there are less data is much less clear. In some cases there is agreement with the free electron value (see for example Busch and Guntherodt, 1967) whereas in other cases the composition dependence deviates from the free electron calculation (Enderby et al., 1967). Optical properties can be taken, using the Drude formula, to give a value for the effective number of free electrons per unit volume. A summary of these results (Faber, 1966) shows that in a number of pure metals the values agree well with free electron theory. It would appear that the conduction electrons in these liquid metals and their alloys behave as a free or nearly free electron gas.

1.1.2 Liquid Semiconductors Some materials, which will be discussed in Chapter Six, exhibit properties which are reminiscent of solid semiconductors. A summary of transport measurements which have been made on a number of such alloys is given by Allgaier (1969). The conductivity of these liquids range from 3×10^{3} ohm^{-1}m^{-1} for Ga_2Te_3 at a few kelvins above the melting point (Chizevskaya and Glazov, 1962) to 3×10^{5} ohm^{-1}m^{-1} for $AuTe_2$ at a few kelvins above its melting point (Enderby et al., 1967). In almost all cases the conductivity increases with temperature, which implies semiconducting rather than metallic behaviour; although it has been pointed out (Enderby and Collings, 1970) that a weak positive temperature coefficient may appear in some metallic alloys due to the temperature dependence of the partial interference functions describing the atomic dispositions. It is for this reason that

these materials have been termed liquid semiconductors, even though the mechanism by which the conductivity increasesis still uncertain. Another characteristic is that conductivity isotherms as a function of composition in binary alloys usually have sharp minima at or near stoichiometric compositions.

Measurements of the thermopower have also been made on many of these liquids. They are usually large and positive, decreasing in magnitude with increasing temperature; this is behaviour characteristic of conventional p-type semiconductors. However the validity of applying conventional solid state theory must be regarded with considerable doubt since in Cu-Te, for example, the thermopower is positive and its temperature coefficient is negative in the range from stoichiometry to Te_{100} (Dancy, 1965). The description of the stoichiometric liquid as an intrinsic semiconductor where adding excess Te to produce excess n-type carriers does not work since the extrinsic carriers should quickly swamp the intrinsic carriers producing a metallic liquid, but this is not seen to happen in the thermopower. Hall coefficients have been measured for a number of these liquids, and are always negative and several times larger than the value which free electron theory predicts.

It is clear that this class of materials cannot be described by free electron theory nor by conventional semiconductor theory. Theoretical descriptions for these materials are still in an early stage of development, they will be discussed in more detail in section 6.1.

1.1.3 Liquid structure It is clear that since the atomic structure in the liquid influences the behaviour of the conduction electrons, it must be incorporated into any satisfactory theory of electronic properties. The average arrangement of atoms in a liquid may be described by means of the radial distribution function, g(r), which is defined by selecting any atom in the liquid as origin; then the average

number density of atoms in a spherical shell of radius r centred on the origin is given by g(r) times the average number density of atoms for the whole liquid. Measurements of the intensity of X-rays or neutrons scattered from a liquid can in principle yield g(r); methods currently being used, and the problems in deducing accurate g(r) from the experimental data are given by Pings (1969) for X-rays, and by Enderby (1969) for neutrons. Some of the difficulties and experimental values for pure metals are discussed in section 5.5.2. In the case of binary alloys three functions are required and to obtain these experimentally is much more difficult again. These are also discussed in section 5.5.2.

In certain liquid alloys the results of X-ray diffraction measurements have been interpreted as showing the retention of short-range solid-like structure above the liquidus (see, for example, Dutchak and Klym, 1965). If this were to occur it would be expected to increase the inter-atomic correlation time contribution to nuclear spin-lattice relaxation, (see section 1.2.2). For this reason the measurement of nuclear spin-lattice relaxation rates and the identification of an electric quadrupolar contribution can be expected to show up associations between atoms for times in excess of the normal order of magnitude (10^{-12}s). This possibility was one of the original motives for the present research.

1.2 Nuclear Magnetic Resonance

Since the phenomenon of nuclear magnetic resonance (NMR) was first observed by Bloch, Hansen and Packard (1946) and also by Purcell, Torrey and Pound (1946) there have been many publications on different aspects and applications of NMR. The theory is very fully described in a number of books, particularly those of Abragam (1961) and of Slichter (1961) and hence only the background and expressions most relevant to this work will be introduced here.

Nuclei which possess spin angular momentum of maximum aligned value $\hbar\underline{I}$, where I is the spin quantum number and is either integer or half integer, and $\hbar$ is Planck's constant divided by 2π, will also have a magnetic moment $\underline{\mu}$. The ratio of these quantities is called the gyromagnetic ratio, γ, where

$$\gamma = \underline{\mu} / \hbar\underline{I} \qquad \ldots\ (1.1)$$

When in a magnetic field $\underline{B}_o$ the Hamiltonian is $\mathcal{H} = -\underline{\mu} \cdot \underline{B}_o$. If $\underline{B}_o$ is in the z direction

$$\mathcal{H} = -\gamma \hbar B_o I_z \qquad \ldots\ (1.2)$$

The eigenvalues of this are $(\gamma \hbar B_o)$ times the eigenvalues of I_z, and so the allowed energies are

$$E = -\gamma \hbar B_o m \qquad \text{where } m = I, I-1, \ldots, -I.$$

Transitions between these Zeeman energy levels can be induced by supplying radiation of frequency ω_L, known as the Larmor frequency, such that $\hbar\omega_L = \gamma \hbar B_o$. This gives the condition required for resonance, $\omega_L = \gamma B_o$. When the nuclear spins are in thermal equilibrium with their surroundings, the 'lattice', a Boltzmann distribution is achieved so that these levels are not equally populated. Hence a net absorption of energy from the radiation field will occur, since, although the transition probabilities upwards or downwards are equal, there are more spins in the lower energy states. The absorption will cease however when the levels become equally populated unless there exists some means of restoring thermal equilibrium. This is supplied by the interaction between the nuclear spins and the surroundings which allows the nuclei to relax. This process can be characterised by a spin-lattice relaxation rate, R_1, the meaning of which may be illustrated by considering a system of identical nuclei of spin $\frac{1}{2}$ in the presence of a steady field B_o. The nuclei have two possible Zeeman energy levels separated by energy $2\mu B_o$; in thermal equilibrium the number of spins in the lower level, N-, exceeds

the number in the upper N_+ such that $N_+ / N_- = \exp(2\mu B_o / kT)$. If the difference in these two populations, n, is altered to n_i, by (say) the application of an r.f. field of suitable frequency, then the return to the thermal equilibrium value, n_o, when the r.f. field is switched off is given by

$$n_o - n = (n_o - n_i) \exp(-R_1 t) \quad \ldots\ldots (1.3)$$

where t is the time since the field was switched off.

The purpose of this work is to investigate R_1 in different materials and hence to deduce information about the behaviour of the lattice.

The coupling between the nuclear spins themselves allows the maintenance of thermal equilibrium among the spins, the establishment of equilibrium being characterised by a spin-spin relaxation rate, R_2. These processes will now be considered in more detail.

1.2.1 Resonance shifts It has been found that the steady magnetic field required for the resonance of a nucleus in a metal is usually less than that for the resonance of the same nucleus in an insulator (Knight, 1949). This shift, known as the Knight shift, nearly always arises mainly from the s-type conduction electrons; they have a net polarisation due to the external field, B_o, and because of their probability density at the nucleus they produce an extra magnetic field there, proportional to the external field. This is of considerable interest because this shift provides a measure of the contact interaction. Since the conduction electrons make up an important part of the thermal bath (commonly referred to as the 'lattice') which takes up the energy of the nucleus when it relaxes, the Knight shift can give a measure of the magnetic coupling between the nuclear spins and the lattice. Unfortunately experimental measurement of the resonance shift does not lead unambiguously to the contact interaction for there are other

mechanisms which also produce shifts in metals, although these are usually small in comparison. These will be discussed in more detail in section 5.2.

It has been found also that there is a range in the resonance fields for a nucleus in different chemical compounds which are insulators (see for example Proctor and Yu, 1951) and this can add further to the difficulties of extracting the conduction electron interaction. These shifts are known as chemical shifts and arise from the extra field created at the nucleus due to the orbital motion of bonding, or valence electrons. These shifts, which are much smaller than the Knight shifts, under normal circumstances, will be discussed in section 6.2.

A knowledge of the Knight shift is interesting in its own right and it has found many applications in metal physics. The interest in the present work is twofold : first it provides a means of determining the contact interaction which is required for an interpretation of the nuclear spin-lattice relaxation rate; and secondly as will appear later, its value depends on the density of electron energy states at the Fermi level, a quantity of prime importance for an understanding of conduction electron behaviour.

1.2.2 Spin-lattice relaxation The principal interactions by which nuclei relax, and the corresponding relaxation rates will now be considered. On the semi-classical picture what is required is a rapidly fluctuating interaction between the nuclear spin and the lattice. Bloembergen, Purcell and Pound (1948) have postulated that providing the Fourier spectrum of the time-dependent components of the interaction has non-vanishing intensity at the frequency, ω_L, corresponding to the transition between two levels of the nuclear spin then transitions will be induced.

A number of theories have been developed to express R_1 in terms of

the lattice parameters by various mathematical techniques; one of these being the density matrix formalism (Abragam, 1961). The lattice parameters occurring in the interaction Hamiltonian are taken to be random functions of time, and are described by their probability distribution using the density matrix. The density matrix, ρ , is an operator introduced in quantum statistical mechanics to perform the function of the classical density of points in phase space; the matrix elements contain the information required for the description of a statistical ensemble of identical systems. The approach is equivalent to conventional time dependent perturbation theory, but is chosen because it gives a convenient way of computing the thermal equilibrium properties of a system.

If the nuclei are initially in state m, and there is available another state k then d/dt $(m|\rho|k)$ will give the rate of change of nuclear spin population. The time dependence of ρ is given by

$$d\rho/dt = i/\hbar \left[\rho , \mathcal{H}_0 + \mathcal{H}_1\right] \qquad \ldots\ldots (1.4)$$

where $\mathcal{H}_0$ is the Zeeman Hamiltonian,

$\mathcal{H}_1$ is the time dependent interaction Hamiltonian.

$\mathcal{H}_1$ has been taken to be random, which is to say the ensemble average

$$G_{mk}(\tau) = \overline{(m|\mathcal{H}_1(t-\tau)|k)\ (k|\mathcal{H}_1(t)|m)} \qquad \ldots\ldots (1.5)$$

is independent of t, and depends only on τ and the levels m and k. $G_{mk}(\tau)$ is the correlation function since it relates $\mathcal{H}_1$ at time t to its value at a time τ earlier. This leads to a correlation time, τ_c, such that for values of τ shorter than τ_c, $\mathcal{H}_1$ does not change appreciably, but as τ gets longer than τ_c so $G_{mk}(\tau)$ tends to zero.

From the time dependence of the density matrix it can be shown that

$$(R_1)_{mk} = J_{mk}(m - k) / \hbar^2 \quad \ldots\ (1.6)$$

where $J_{mk}(\omega) = \int_{-\infty}^{+\infty} G_{mk}(\tau)\, e^{-i\omega\tau}\, d\tau \quad \ldots\ (1.7)$

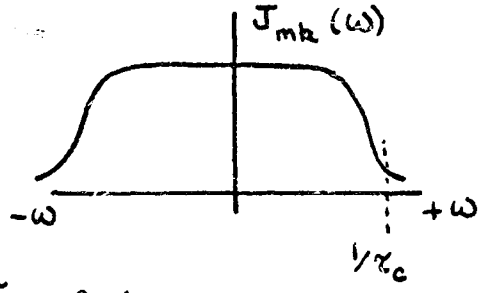

$J_{mk}(\omega)$ is thought of as the spectral density of the interaction matrix, G_{mk}, and will contain frequencies roughly up to $1/\tau_c$.

The inverse of equation 1.7 evaluated at $\tau = 0$ gives

$$G_{mk}(0) = 1/2\pi \int_{-\infty}^{+\infty} J_{mk}(\omega)\, d\omega \quad \ldots\ (1.8)$$

where $G_{mk}(0) = \overline{(m | \mathcal{H}_1(t) | k)^2} \quad \ldots\ (1.9)$

Since $G_{mk}(0)$ does not depend on τ_c the area under the $J_{mk}(\omega)$ curve must be constant so that as $1/\tau_c$ increases $J_{mk}(\omega)$ must decrease, and vice versa. If $J_{mk}(\omega)$ is taken to be approximately constant up to $= 1/\tau_c$, and zero beyond as shown then the area under the curve is given by

$$G_{mk}(0) = (1/2\pi) J_{mk}(0)\ (2/\tau_c)$$

$$J_{mk}(0) \triangleq \overline{(m | \mathcal{H}_1 | k)^2}\, \tau_c \quad \ldots\ (1.10)$$

Thus provided the Larmor frequency, ω_L, is much less than $1/\tau_c$ $J_{mk}(\omega_L) = J_{mk}(0)$ and hence by substituting into equation 1.6 is found that

$$R_1 \triangleq 1/\hbar^2\ \overline{|\mathcal{H}_1|^2}\, \tau_c \quad \ldots\ (1.11)$$

In metals, where the conduction electrons provide the 'lattice', one of the principal interactions is the scalar contact interaction with the spin magnetic moment of the conduction electron. This is the same interaction which leads to the Knight shift as discussed in the previous

section

$$\mathcal{H}_1 = (2\mu_0/3)\ \gamma_e\ \gamma_n \hbar^2\ \underline{I}.\underline{S}\ \delta(\underline{r}) \qquad \ldots. (1.12)$$

The correlation time for this interaction will be of the order of the time for a Fermi surface electron to cross a unit cell, given approximately by $\hbar / E_F$ (Bloembergen 1949) where E_F is the Fermi energy. Since this is of order 10^{-15} s the restriction placed on equation 1.11 is clearly satisfied. Hence from equation 1.11

$$(R_1)_{contact} \simeq 1/\hbar^2 \left\{(2\mu_0/3)\ \gamma_e\ \gamma_n \hbar^2\right\}^2 |\psi(0)|^4 \hbar kT/E_F^2 \qquad \ldots. (1.13)$$

where $|\psi|(0)$ is the electronic wave function evaluated at the nucleus. A factor of kT / E_F has been included to take account of the fact that only electrons within kT of E_F can take part in the relaxation by absorbing the nuclear energy. Other magnetic interactions such as the dipole-dipole coupling and that due to the orbital moments of the conduction electrons are small in comparison to the contact interaction; these will be discussed in section 5.2. In view of the common origin of $(R_1)_{contact}$ and the Knight shift it is not surprising that there should be a simple relation (the Korringa relationship) between the two. This will be found valuable in later chapters in two ways. It can be used as a means of identifying the conduction electron contribution to the total observed relaxation rate. Secondly it can be used to detect deviations from the relation $\tau_c = \hbar / E_F$; in certain materials amongst those which have been classified as liquid semiconductors an enhancement of the relaxation rate has been observed; the explanation for this appears to lie in a partial localisation of the conduction electrons, giving rise to an increase in the correlation time. The evidence for this will be discussed in Chapter Six.

A further important interaction arises for nuclei of spin greater

than $\frac{1}{2}$, i.e. those nuclei which possess an electric quadrupole moment, Q. This moment measures the departure of the nuclear charge distribution from spherical symmetry. The electric interaction with the rapidly fluctuating electric field gradient due to the motion of neighbouring ions also provides a relaxation mechanism. This interaction is expressed by Abragam (1961) from the quadrupolar Hamiltonian to be

$$\overline{|\mathcal{H}_1|^2} = \frac{3(2I+3)}{4\hbar^2 I^2(2I-1)} \overline{\left(\frac{eQ}{\hbar}\frac{\partial^2 V}{\partial z^2}\right)^2} \qquad \ldots\ldots (1.14)$$

where I is the nuclear spin,

e is the electronic charge,

$\partial^2 V/\partial z^2$ is the electric field gradient at the nuclear site.

Since the random diffusional motions of the ion cores in normal liquids occur at frequencies of order 10^{12} Hz, the short correlation time limitation imposed on equation 1.11 is clearly satisfied and it can be used to estimate the quadrupolar relaxation rate. This process, and a more detailed formulation for the rate are discussed in Chapter Five.

It can be seen from the above discussion that (at least under some circumstances) it can be expected that a knowledge of R_1 will provide information about the dynamics both of the conduction electrons and of the ions in liquid conductors.

1.2.3 Magnetic suceptibility Most liquid conductors are either diamagnetic or weakly paramagnetic (see, for example Dupree and Seymour, 1972). The two principal components of the total suceptibility, χ_t, arise from the ion cores and from the conduction electrons. Much interest in measurements of χ_t stems from the possibility of extracting the conduction electron contribution, and hence obtaining information about the electronic structure. The conduction electron suceptibility consists mainly of the spin paramagnetic suceptibility and

the orbital diamagnetic suceptibility. On the free electron model these depend directly on the density of electron energy states at the Fermi level, although in metals the relationships have to be modified in different ways to allow for interactions between the electrons themselves, and between the electron and the ion cores.

The main difficulty in analysing χ_t lies in finding a suitable value for the contribution of the cores; for this there are two approaches. One is to calculate the suceptibility from the free ion wavefunction, the other is to use a direct measurement of a suitable ionic salt in crystalline form or in solution; neither has yet proved entirely satisfactory.

It has been pointed out in section 1.2.1 and 1.2.2 that the contact interaction between nuclei and conduction electrons gives rise to a nuclear resonance shift and spin-lattice relaxation. Hence the observations of these quantities must contain information concerning the electron suceptibility, although as has been indicated the contact interaction part cannot always be easily extracted. However the variations of these parameters, using temperature, or possibly composition, as the implicit variable can lead to a better understanding of conduction electron behaviour.

1.3 Measurement of the spin-lattice relaxation rate

The principles of the technique used in measuring spin-lattice relaxation rates will now be described. When a steady magnetic field, $\underline{B}_o$, is applied to the sample the preferential orientation of the nuclear spins produces a net magnetization, $\underline{M}$, in the direction of the field, conventionally chosen to be the z direction. If an additional magnetic field, $\underline{B}_1$, is now applied, rotating in the xy plane at frequency ω, $\underline{M}$ will precess about the direction of the effective field. It is simpler to consider these processes from a frame of reference which has its z direction in the direction of $\underline{B}_o$ but its xy plane rotating at the same

frequency as $\underline{B}_1$. It can readily be shown that if $\underline{B}_1$ is rotating in the laboratory frame at the Larmor frequency, ω_L, the effective field is in the direction of $\underline{B}_1$. Hence if $\underline{B}_1$ is in, say, the X direction the magnetisation rotates in the yz plane of the rotating frame.

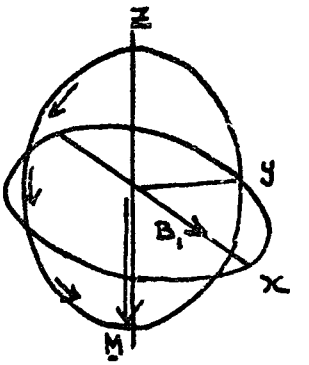

path of M in rotating frame during a π pulse

In this experiment $\underline{B}_1$ is supplied in the form of a pulse at frequency ω_L. The pulses have two lengths, a π pulse is τ_π long such that the magnetization precesses about $\underline{B}_1$ by π, so that it points in the - z direction; and a $\pi/2$ pulse which causes the magnetization to precess about $\underline{B}_1$ by $\pi/2$, into the xy plane. It can be seen that

$$\tau_\pi = \pi / \gamma_n B_1 \qquad \ldots\ (1.15)$$

Thus if a π pulse is applied to the sample the nuclear magnetization is reversed, and this then relaxes towards its original value at a characteristic rate, R_1, by means of the interactions of the nuclear spins with the lattice. The z-magnetization at time t after the π pulse has been applied is

$$M_t = M_o \left\{ 1 - 2 \exp(- R_1 t) \right\}. \qquad \ldots\ (1.16)$$

M_t may be sampled at any time t by applying a $\pi/2$ pulse which will cause the nuclear magnetization to precess about $\underline{B}_1$ into the xy plane. This induces a voltage at frequency ω_L in a receiver coil placed in this plane which will have an initial amplitude proportional to M_t. This voltage will decrease due to the dephasing of the nuclear spins at rate R_2, a process known as the free induction decay (f.i.d.).

If the pulse separation, t, is adjusted until there is zero voltage induced in the receive coil then R_1 can be calculated from $R_1 = \{\ln(2)\}/t$. This however assumes that the factor in the bracket in equation (1.16) is

2, which requires that the π pulse has been accurately adjusted to give a rotation of π. This is difficult to achieve in practice and measurements carried out in this way rely on a single observation; a more accurate method, adopted in this work, is to express equation (1.16) as

$$\ln (M_o - M_t) = - R_1 t + \text{constant} \quad \ldots\ldots (1.17)$$

R_1 is then determined from a series of measurements of M_z as a function of the pulse separation, t. The experimental upper limit imposed by this technique is that $1/R_1$ must be long compared with τ_π, implying a requirement for a large B_1.

There are many other possible methods of measuring R_1; the method described is however one of the simplest and most direct for the rather fast relaxation rates met in the present work. It requires a pulsed NMR spectrometer, the design and construction of which will be described in the next chapter.

References

Abragam, A., 1961, The Principles of Nuclear Magnetism (Claredon Press : Oxford).

Alligaier, R. S., 1969, Phys. Rev., 185, 227.

Bloch, F., Hansen, W. W. and Packard, M. E., 1946, Phys. Rev., 69, 127.

Bloembergen, N., Purcell, E. M. and Pound, R. V., 1948, Phys. Rev., 73, 679.

Bloembergen, N., 1949, Physica, 15, 588.

Busch, G. and Guntherodt, H-J., 1967, Adv. in Phys., 651.

Buschert, R., Geib, I. G., and Lark-Horovitz, K., 1955, Phys. Rev., 98, 1157.

Chizhevskaya, S. N. and Glazov, V. M., 1962, Dolk. An. SSSR, 145, 115.

Cusack, N. E., 1963, Rep. Prog. Phys., 26, 361.

Dancy, E. A., 1965, Trans. Met. Soc. AIME, 233, 270.

Dupree, R. and Seymour, E. F. W., 19 , Physics and Chemistry of Liquid Metals. Ed. S.Z. Beer. (Marcel Dekker : New York).

Dutchak, Ya. I. and Klym, N. M., 1965, Phys. Met. and Metall., 196, 128.

Enderby, J. E., Hasan, S. B. and Simmons, J., 1967, Adv. in Phys., 16, 667.

Enderby, J. E., 1969, Physics of Simple Liquids. Eds. H.N.V. Temperley, J. S. Rawlinson, G. S. Rushbrooke. (North Holland : Amsterdam), Chapter 14.

Enderby, J. E. and Collings, E. W., 1970, J. Non Cryst. Solids, 4, 161.

Faber, T. E. and Ziman, J. M., 1965, Phil. Mag., 11, 153.

Faber, T. E., 1966, Optical Properties and Electronic Structure of Metals and Alloys. Ed. F. Abèles. (North Holland : Amsterdam).

Knight, W. D., 1949, Phys. Rev., 76, 1259.

March, N. H., 1968, Liquid Metals. (Pergamon Press Ltd. : London).

Mott, N. F., 1967, Adv. in Phys., 16, 49.

Pings, C. J., 1969, Physics of Simple Liquids. Eds. H.N.V. Temperley, J. S. Rawlinson, G. S. Rushbrooke, (North Holland : Amsterdam) Chapter 10.

Proctor, W. G. and Yu, F. C., 1950, Phys. Rev. 77, 717.

Purcell, E. M., Torrey, H. C. and Pound, R. V., 1946, 69, 37.

Slichter, C. P., 1961, Principles of Magnetic Resonance (Harper and Row : New York).

CHAPTER TWO

EXPERIMENTAL APPARATUS

2.1 The N.M.R. Pulse Spectrometer

2.1.1 Introduction

The major requirements of the apparatus are:

(a) A pulse sequence generator to provide various trains of microsecond pulses of RF oscillation.

(b) A power transmitter to deliver 5kW output pulse power.

(c) A low noise receiver system to be sensitive to thermal noise in the receiver coil, and to recover from paralysis following the high voltage pulses in a time of 10 μs or less.

(d) In order to permit RF phase-sensitive detection, the pulses must be obtained by gating a CW source so that they are coherent.

The outstanding discussion of pulsed NMR apparatus in the literature is that due to Clark (1964). The high power transmitter described therein was adopted as a basis for the present work. The remaining sections of the Clark system are designed round vacuum tubes and are somewhat dated; alternative solid state circuitry has been designed to replace them.

An additional and very useful coherence within the system is achieved if the pulses that gate the CW oscillator can be time locked to the CW itself; by using this facility all the signal monitoring is much improved. It was therefore decided to build a new apparatus using a crystal controlled oscillator both as the basic CW source and also to drive a chain of decade dividers, the outputs of which can be used as repetition rate triggers for the pulse trains.

2.1.2 General features

An outline of the operation

of the coherent pulse spectrometer as eventually constructed will be given first, followed by detailed discussions of its main components; a block diagram of the spectrometer is given in figure 2.1. Two outputs from the crystal controlled r.f. oscillator are taken, one to the transmitter drive unit, the other via a divider unit to trigger the pulse sequence generator. This generator produces two pulses of variable length, with a variable separation between them, which switch the transmitter drive unit, thus supplying two pulses of r.f. to the transmitter gate. In the transmitter two class B amplifier stages are followed by three class C amplifier stages to produce up to 10kW of r.f. power during pulses. This power is fed to the transmitter coil which is wound in Helmholtz configuration round the sample volume in a similar arrangement to that of Warren and Clark (1968). The receiver coil is wound orthogonal to the transmitter coil and the received signals are fed to a Decca pre-amplifier, then via the suppressor unit to the Decca main amplifier. The suppressor unit, which switches in a large attenuation for the duration of the pulses, is controlled by the pulse sequence generator. The signals from the main amplifier are fed to the phase-sensitive detector, along with the reference signal which is derived from the crystal oscillator, and the detected output is supplied to a PAR CW.1 boxcar integrator. The final noise-averaged signal is displayed on a Telsec chart recorder.

To enable observations to be carried out at different temperatures two independent heater windings are placed on the coil assembly inside a tubular dewar. The temperature is observed by means of two thermocouples, one placed below the sample space, the other above it. Frequencies and pulse separation times are measured using a Venner TSA 6636 counter. The coil assembly is suspended in the centre of a Varian Associates 9" magnet fitted with conical pole faces to give a $1\frac{3}{4}$" gap. The magnetic field is controlled to within 10 μT by a Varian Associates Mark II 'Fieldial' unit.

figure 2.1

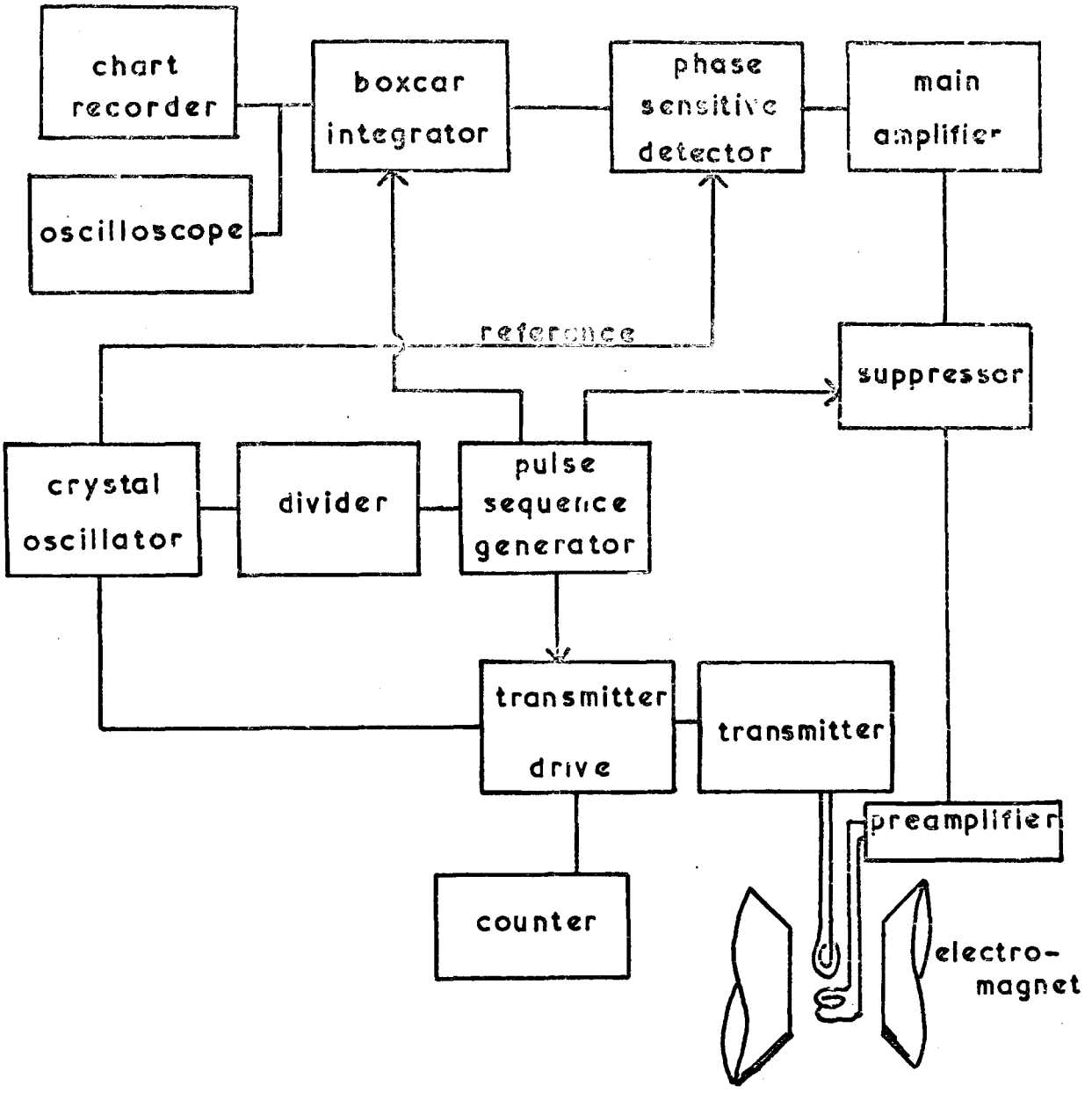

NMR PULSE SPECTROMETER

2.1.3 Pulse generation The spectrometer was initially planned to operate on a single frequency, 9.500 MHz, but it was found useful to have a second frequency available to avoid external interference which was often troublesome, and so a second frequency, 9.000 MHz, was tried successfully.

The master oscillator is a crystal controlled Marconi F 3171 series unit generating one of the above frequencies mounted in a B7G base inside a diecast box. The frequency is monitored to one part in 10^6 by the Venner counter. Two outputs one to the PSD and the other to the transmitter gate unit each have a one-transistor buffer amplifier. A third output is taken to the divider unit. Here the r.f. signal is 'squared' in a gate unit, then fed to the first decade divider unit. There are eight such units each consisting of four Mullard FCJ 101 J.K. flip-flops wired as a synchronous BCD counter. The output of each decade unit is then fed into the input of the next, and also to an eight-way switch which enables the output of any one of the decade steps to be selected. Thus the pulse sequence repetition rate may be varied in powers of 10 from 10^6 per second down to one every 10 seconds. The output is fed via a buffer amplifier to trigger the pulse sequence generator, and is also used to trigger the oscilloscope which monitors the pulses.

The pulse sequence generator is constructed of SGS 900 and 914 micrologic units, see figure 2.2. The input pulse from the divider unit is differentiated and fed via a buffer amplifier to two monostable multivibrators each of which can provide pulses varying from 0.4 μs up to 4 ms in four ranges. The output of the first of the multivibrators gives rise to the first of the variable length pulses, while the output of the second is differentiated and the trailing edge pulse used to trigger a third monostable multivibrator. The output of the third multivibrator supplies the second pulse while the second multivibrator is used to give the variable separation between the pulses. An output from the

figure 2.2

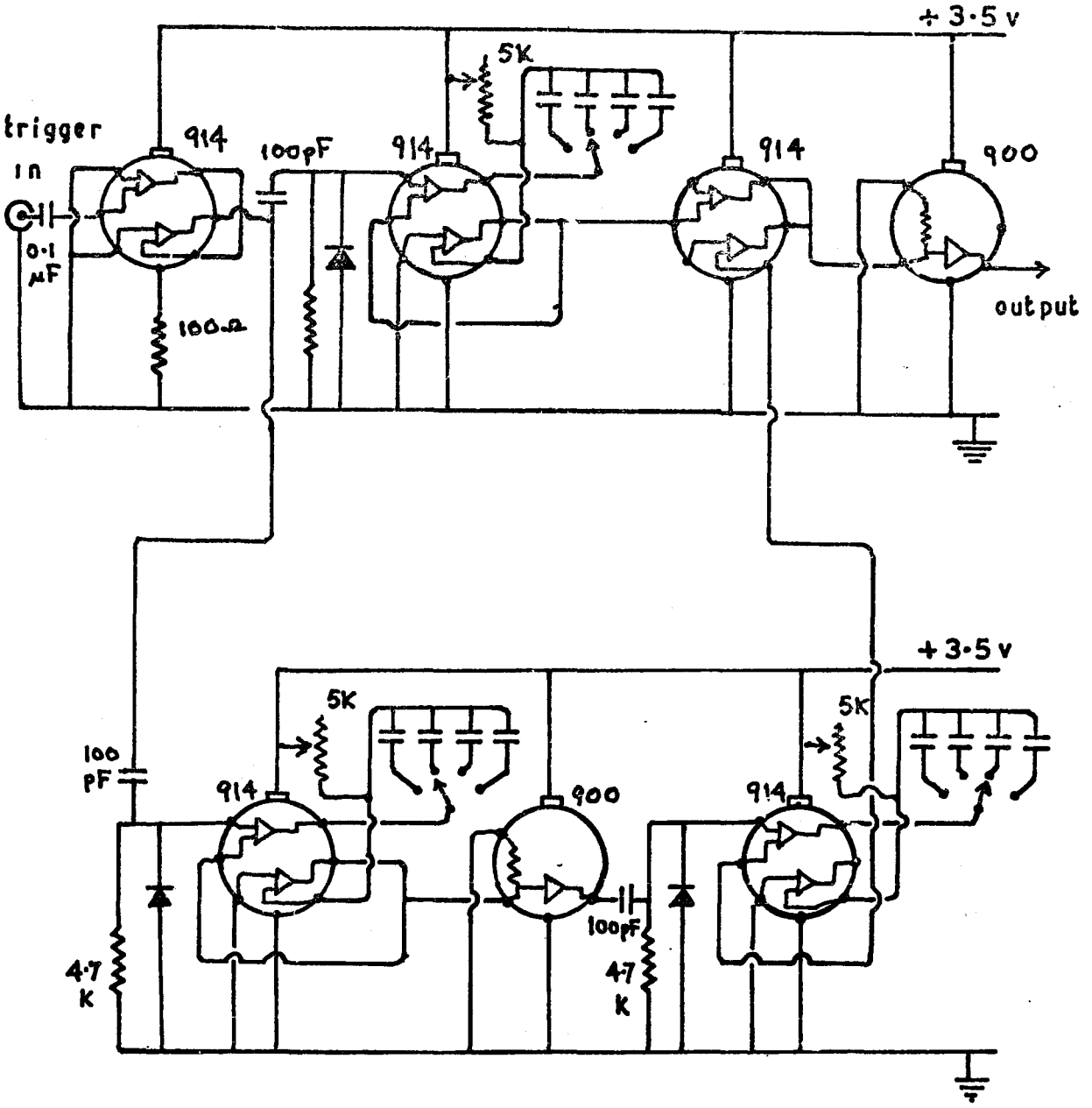

THE PULSE SEQUENCE GENERATOR

second pulse is taken to trigger the boxcar integrator, see section 2.1.4, and then the two pulses are combined in a final buffer stage. The output, which is a two positive-going pulse sequence, is then supplied to the transmitter drive unit. The pulse separation is measured to the nearest microsecond by the Venner counter.

The transmitter drive unit is simply a v 504A transistor gate, which is switched on by the pulses described above to allow the r.f. through to drive the transmitter only during these pulses.

2.1.4 The Transmitter The basic transmitter circuit is very similar to that of Clark (1964), except that the various stages are constructed to operate at a frequency of 9.0 to 9.5 MHz. Tuning facilities are provided only in the final two stages.

The input pulses of r.f. from the drive unit are fed through the Blume gate which ensures that no r.f. is passed to the transmitter except for the duration of the pulses. The final amplifier stage, which consists of two double tetrode 3E29 valves in parallel operating in the class C mode, are constructed on a separate chassis and placed on a frame on top of the magnet. This enables the coaxial cable which couples the output circuit to the transmitter coil to be less than 250 mm in length, minimising cable capacitance.

The HT supply for the final stage is maintained at 3kV by a V405B Fluke high voltage DC power supply. This can only supply currents of up to 30 mA and so an 8 μf capacitor is connected across the supply to ensure that the voltage does not sag during pulses. A short length of wire mounted near to the final tuning capacitor is used to monitor the pulses, the output being taken to a Tektronics 545B oscilloscope. In this way tuning of the final stages can be optimised, and pulse lengths measured. The transmitter is found to supply pulses with rise and fall times of less than 1 μs.

It was found that a considerable amount of external noise observed in the receiver was coming from pick-up by the anode wiring of the final amplifier stage and to overcome this the valves and the associated wiring were enclosed in a copper shield.

Tests were made to find if there was any dependence of the measured values of relaxation rates on the length of the pulses. On reducing the r.f. power level by 30% (and simultaneously increasing the pulse lengths by 30%) the recorded rates were unchanged to within the experimental inaccuracy, so that the pulses were sufficiently short that the simple theory given in Chapter One applies.

2.1.5 The Receiver The receiver system consists firstly of a Decca three transistor preamplifier type I.F. 9.5/3P having a gain of 60dB mounted on the frame over the magnet to keep the input lead short. To provide protection from the direct pick-up from the transmitter coil pulses pairs of crossed FD 100 diodes were added across each tuned circuit in the pre-amplifier. The output from the pre-amplifier is fed through a suppressor unit and a switched attenuator to the main amplifier. The suppressor consists of two double modulators in series, and, on application of the switching pulse from the transmitter drive unit, inserts an attenuation of greater than 60dB for the duration of each pulse and for a controlled time, variable between 5 and 15 μs, beyond the pulse.

The main amplifier is a Decca type I.F. 9.5/3 and is similar in construction to the pre-amplifier, having a gain of 60dB also. Pulse suppression was adequate and so no diodes were added to this unit. The amplified signal is now fed to the phase-sensitive detector, a Hatfield Instruments Ltd. double balanced modulator type M.D.2. The reference signal which is derived from the crystal oscillator is supplied via a switched attenuator and a delay line capable of a delay of up to 0.1 μs,

equivalent to almost one complete cycle at the operating frequencies.

Two outputs are available, the first being the direct output of the phase-sensitive detector. The second is the detector output taken via a transistor amplifier which has a low-pass characteristic and so provides some noise reduction. The first output is usually connected to the boxcar integrator while the second is taken to the oscilloscope to enable resonances to be detected and optimised directly.

2.1.6 The Boxcar Integrator The boxcar integrator, a PAR model CW1, provides a means of improving the signal to noise ratio for the repetitive waveforms. It consists basically of a gate which is opened by a triggering signal from the pulse sequence generator and an integrating circuit having a variable time constant. The integrated output is the average of a large number of repetitions of the input signal and since the average value of random noise voltages tends to zero the output tends towards the synchronous part of the input.

The gate width is continuously variable from 1 μs up to 110 ms and the gate may be opened at some fixed delay beyond the triggering signal by any amount from 1 μs up to 1s. It is also possible to make the gate scan across the input signal to extract the whole input waveform, rather than just one point on the waveform.

Under typical operating conditions with a gate width of 30 μs, an integrator time constant of 3 ms and a pulse sequence repetition rate of 110 per second the signal to noise ratio is improved by about 300 times. The output signal is normally displayed on a Telsec 700 series X-T chart recorder.

2.2 The Coil Assembly

Special attention to probe construction was necessary to achieve both satisfactory electrical and thermal characteristics for use at high

r.f. power and high temperatures.

2.2.1 Construction Initially a main tube consisting of a single thickness of 'fiberfrax' paper (The Carborundum Company Ltd., Rainford, St. Helens, Lancashire) was formed on a slightly tapering glass tube by soaking with fiberfrax rigidiser and allowed to dry; when hard the glass tube was removed. The receiver coil, consisting of 10 turns of 0.5 mm diameter gold wire inter-spaced with Refrasil string (Chemical and Insulating Co., Darlington, Durham), was wound on to this main tube and the leads taken up the sides of the main tube in Refrasil sleeving. Transmitter coil formers consisting of alumina thermocouple tubing (Thermal Syndicate Ltd., Wallsend, Northumberland) of approximately 1.5 mm O.D in 10 mm lengths were cemented direct to the receiver coil at right angles to the turns to fix it, using Aciduma cement (Sankey and Son, Ilford, Essex). The transmitter coil was then wound in gold wire consisting of three turns on each side in Helmholtz configuration using the formers to support the coil and Aciduma cement to fix it, see figure 2.3. The overall length of the coil was about 25 mm, and has an inductance of about 1.1 μH. The coil leads were taken up the main tube enclosed in the alumina thermocouple sleeving and care was taken to maintain about 10 mm spacing between the leads to avoid any possibility of r.f. breakdown occurring. A Pt - Pt 13% Rh thermocouple in 34 s.w.g. in refrasil sleeving inside a fiberfrax paper plug was inserted into the bottom of the main tube, leaving the junction about 20 mm below the centre of the coils. The remainder of the outside of the main tube was then built up to the same diameter as the coil assembly using fiberfrax paper, rigidiser and cement.

It was found that following each pulse strong ringing was occurring in the receiver system with a main frequency of order 150kHz. Since this was clearly not mechanical other coil assemblies were constructed using

figure 2.3

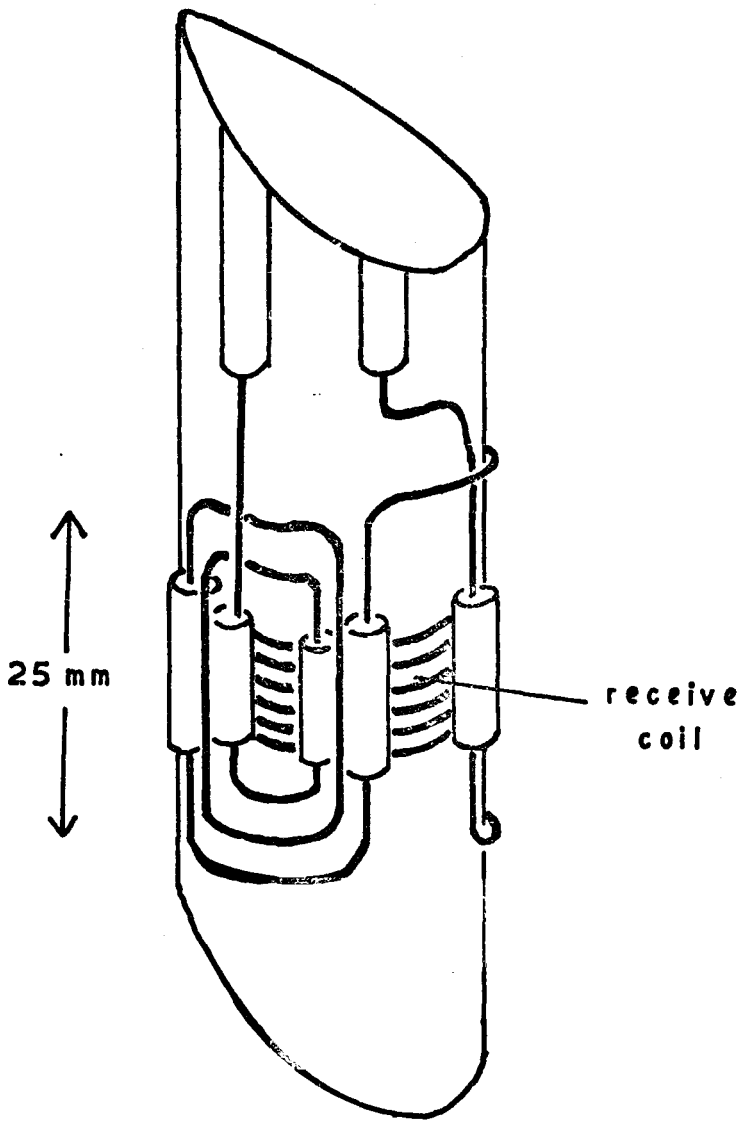

THE COIL ASSEMBLY

transmit and receive coil arrangement

0.25 mm diameter gold wire and also from 0.25 mm diameter platinum wire, but the higher resistances of these wires lowered the Q of the coils without appreciably decreasing the ringing and so they were not used. The ringing appeared to be worse when a sample was in position, or even with an empty sample tube so it was concluded that it originated in the construction material itself. It was overcome by moving the boxcar gate out to beyond where the ringing occurred, about 40 μs beyond the pulse. The rotating magnetic field produced by the transmitter coil at the sample, B_1, measured by finding the length of a $\pi/2$ pulse for ^{27}Al nuclei was approximately 5 mT for the coils constructed in this manner.

The assembly was held in the steady magnetic field by suspending it from the top plate, see figure 2.4. The main coil assembly tube was fed through a hole in the top plate and held in position by means of an O-ring seal. The two coil leads were taken to BNC sockets mounted in the top plate.

Samples were contained in the long straight sample tube made of 10 mm O.D. thin walled silica glass inserted inside the main tube and lowered into the receiver coil. One exception was in the case of Al-Si, where the sample was found to react with the silica glass. In this case a tube of pure alumina was used satisfactorily. The effective sample volume was approximately 1 cm^3. The top of the sample tube was held in a gas tight head connected to a gas handling system, enabling the sample tube to be evacuated and filled with argon if required. In the sample tube head were two lead-through connectors to which a second Pt - Pt 13% Rh thermocouple was connected. This was pushed down inside the sample tube in sleeving so that the junction was within 10 mm of the top of the sample.

2.2.2 Temperature control and measurement To enable relaxation rates to be measured as a function of temperature heater windings

were added. To compensate for the greater heat conduction upwards it was found necessary to use two independent heater windings. A further sleeve in fiberfrax paper, on which two coils were bifilarly wound in 22 s.w.g. nichrome wire with turns spaced 3 mm apart, was added over the coil assembly. Each coil started at the level of the centre of the receiver coil. The top one spread over 80 mm upwards and the leads were taken out through the top plate; the lower coil spread over 80 mm downards and leads were taken out downwards. Each coil was supplied independent of the other from Farnell B 30 stabilised power supply units.

The coils were held in place by two further layers of fiberfrax paper and then the assembly was baked out in a furnace at 900 K for several hours. A tubular dewar in silica glass was placed round the assembly to contain the heat, allowing the lower heater coil and thermocouple leads to be taken out downwards. Finally a copper tube was mounted round the outside of the dewar leaving an airway of approximately 1.5 mm wide, and an Edwards R B.4 compressor was used to draw cooling air up from the bottom over the outside of the dewar and also through cooling channels in the top plate assembly, see figure 2.4.

Sample temperatures were monitored continuously by means of the two thermocouples described, placed above and below the sample and within 10 mm of it. The thermoelectric e.m.f.s were measured to the nearest μV by means of a Tinsley 5590A potentiometer. Temperatures of up to 1150 K were achieved with this furnace and it is probable that higher temperatures could be reached but deteriorating signal to noise ratios imposed this upper useful limit.

2.3 The Magnetometer

In order to measure the steady magnetic field the nuclear magnetic resonance of ^2D was detected. A sample of about 1 cm^3 of D_2O doped with a little manganese sulphate was sealed in a glass phial and a coil of

figure 2.4

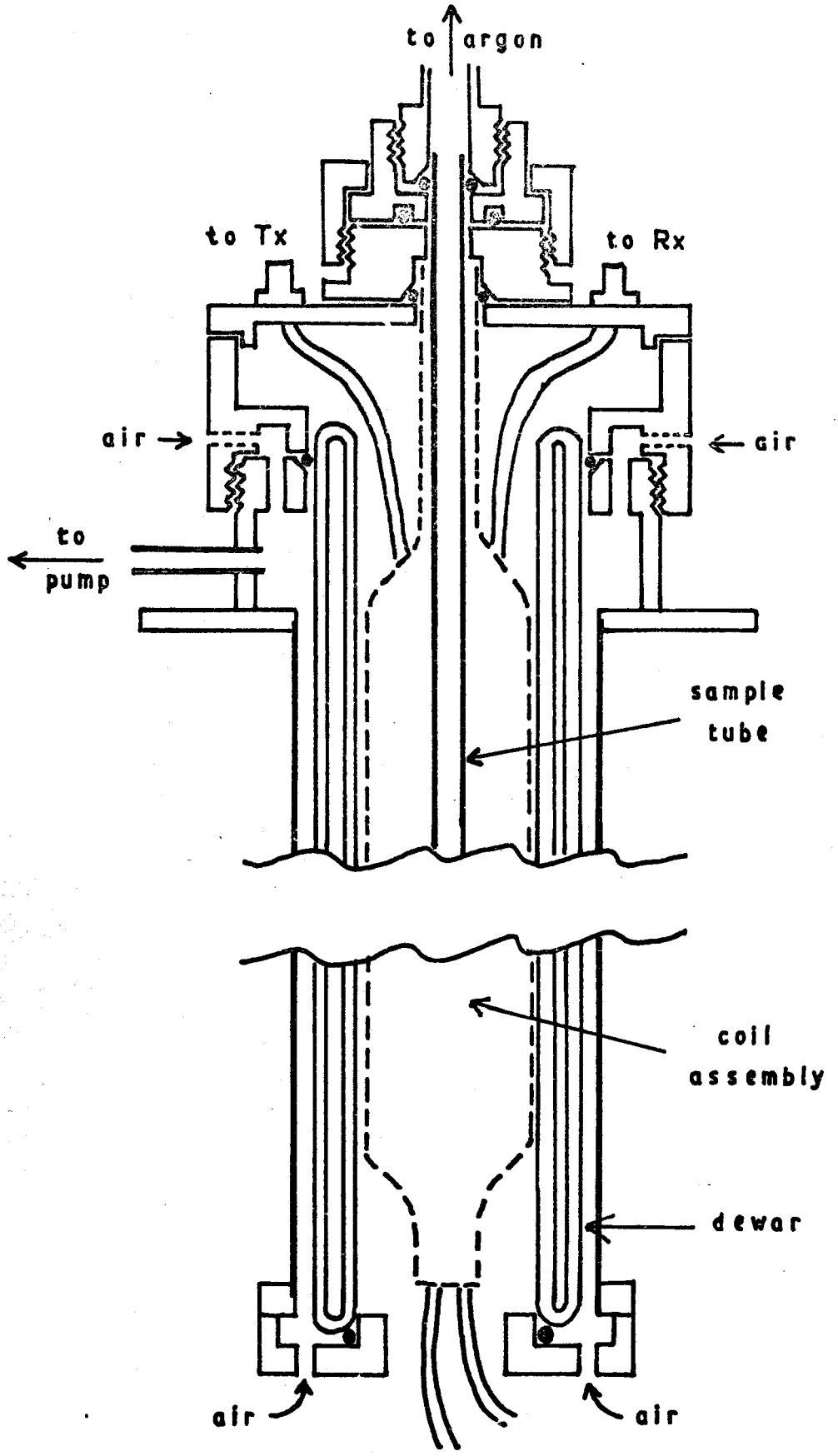

THE FURNACE SYSTEM

copper wire wound on to it. This coil forms part of the tank circuit of a self-oscillating detector circuit.

The circuit employed here (Faulkner and Holman, 1967) is an emitter coupled two transistor oscillator operating in the true Robinson mode (Robinson, 1959). The operating conditions have been chosen to give near perfect limiting, independent of oscillation level, and the circuit has been found to give satisfactory performance over a frequency range of more than two octaves without any adjustment, apart from the tuning capacitor. Nuclear resonance is detected by the absorption of power from the tank coil and the consequent reduction in the circuit Q which gives a drop in the output from the oscillator. The detected output of the oscillator is taken via a 20 dB pre-amplifier to a 60 dB main amplifier, and then via a low pass amplifier to the output terminal for display on the oscilloscope. The oscillator output is also taken via a buffer amplifier to the Venner frequency counter.

To provide a convenient method of displaying the whole resonance the steady field is modulated at 50 Hz by a small field produced by a suitably oriented coil wound on a 30 mm diameter former and placed with the D_2O sample at its centre. The modulating coil is supplied via an adjustable phase-shifting network from a 6.3V a.c. supply, which is also used to drive the timebase of the oscilloscope.

The magnetometer coil assembly is mounted on the rear of the furnace tube on the same horizontal level as the receiver coil. The whole unit is suspended from a top plate attached to v-shaped supports resting on two horizontal rods. When pushed to the back stop the receiver coil and sample are at the centre of the applied magnetic field, and when pulled forward to the front stop the magnetometer coil replaces the receiver coil at the centre of the field.

It is estimated that with the arrangement described measurement of the ^2D resonance frequency enables the steady field to be determined to

within $\pm$ 50 μT.

2.4 Sample preparation

All of the alloys used in this work were prepared from the constituent metals at 99.999% purity, with the exceptions of CuTe and Bi_2Te_3 which were purchased ready prepared. The weight percentages of the individual alloys were calculated from the required atomic percentages using the tables supplied by Hansen (1958). The individual components were then weighed, to the nearest milligram, to make the sample weight approximately 15 grams. In the case of the Te-Tl alloys the thallium components were cut and weighed in an inert atmosphere since Tl oxidises readily in air.

For investigation by N.M.R. satisfactory penetration of the radiation is required. In metals the radio frequency skin effect limits the depth to which the radiation can penetrate. This is overcome in the conventional manner by preparing the samples in the form of powder smaller than the skin depth. For the metals investigated the skin depth is of order of 60 μm, and for the samples of lower conductivities the skin depth is even greater.

The alloy powders, having been prepared by one of the methods described below, were sieved through a 200 mesh sieve and those particles which passed through were thoroughly mixed with quartz powder which had been similarly sieved. The metal alloys were mixed in the ratio one part alloy to two parts quartz, while the alloys containing Tellurium were mixed in the ratio of one part alloy to two and a half parts quartz since they were found to fuse if the smaller quantity of quartz was used.

a) Casting and Grinding. The two components were placed together in a silica glass tube which was connected to a gas handling system, and had a copper cast clamped to its top by an O-ring seal. The air was evacuated from the tube and replaced by argon at a pressure of

about 1/3 atmosphere. The tube was heated until the alloy was molten, shaken for several minutes to ensure complete mixing while continuing to heat and then quickly inverted so that the alloy flowed into the copper cast and solidified rapidly.

Almost all of these alloys were sufficiently brittle to be crushed in a pestle and mortar and then sieved. Those which could not were carefully filed using a specially cleaned file, and the filings washed in dilute HCl and then in water before drying and sieving.

b) Spraying. This method is an improved version of the technique described by Heighway et al., (1970). A broad silica glass tube was drawn out to a fine jet at one side of the bottom and the top of the tube connected to a gas handling system, see figure 2.5. The tube was mounted so that it rested at about 45° to the vertical with the jet uppermost, but it could also be rotated into the vertical position with the jet under the nozzle of the nitrogen tube.

The two components of the alloy to be prepared were placed in the tube, the jet blocked temporarily and the tube evacuated. The tube was then filled with argon to a slight overpressure, the blockage removed and argon allowed to flow out through the jet, the flow being maintained by the overpressure. The tube was heated in the tilted position and agitated until the alloy was molten and thoroughly mixed. The nitrogen gas blast was then turned on, being maintained from the cylinder at a pressure of two atmospheres and the tube rotated into the vertical position. This poured a fine stream of molten alloy into the nitrogen blast, the liquid stream atomised and the particles sprayed into a large glass container whose inside walls were flooded with running water. The sample was filtered from the water and washed thoroughly before drying and sieving.

The advantage of this method is that the alloy particles are produced direct from the molten alloy so that there is little chance of sample

Figure 2.5

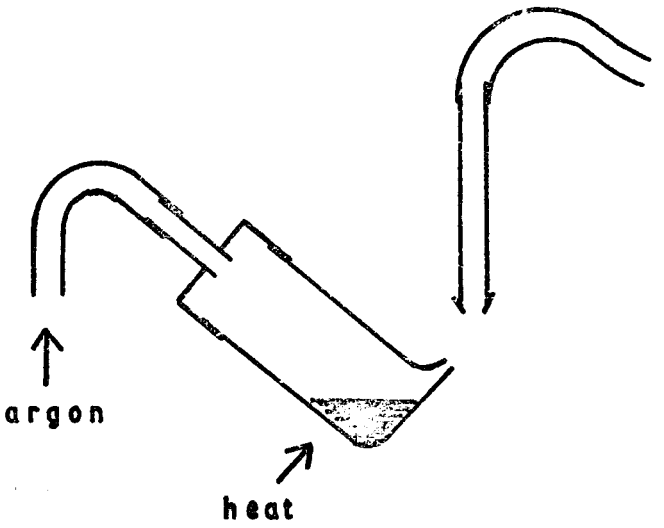

(a) melting position

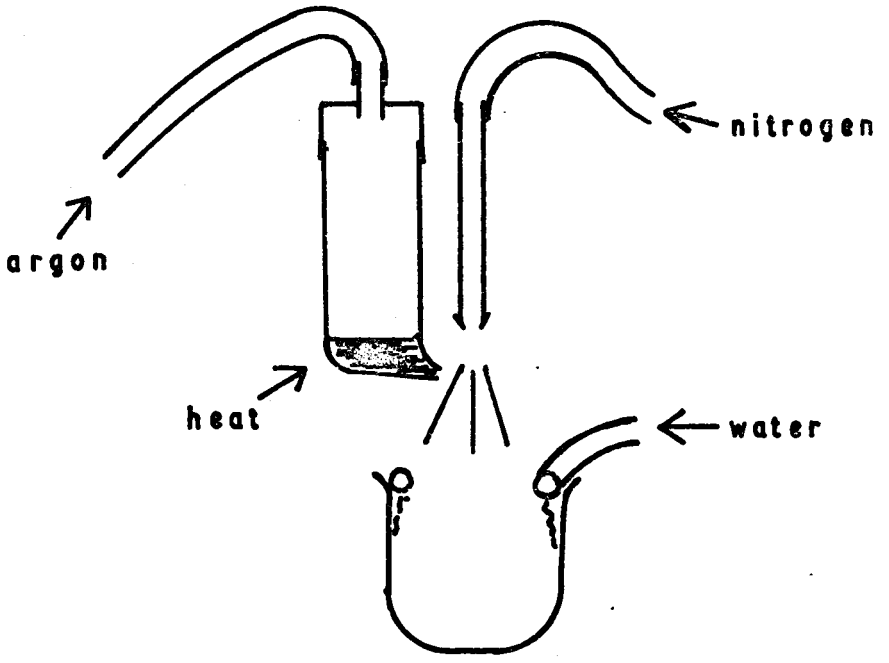

(b) spraying position

THE SPRAYING SYSTEM

inhomogeneity occurring, as could happen in the casting process described above.

c) Composition. The general self consistence of the data together with the agreement obtained with the results of other workers suggests that all of the alloys are near in composition to the values claimed. Analysis of Te-Tl alloys prepared to contain 50 at. % and 32 at. % Te respectively showed that they did in fact contain 45.2 at % and 33 at. %. It seems likely that all of the alloys are within 5 at. % of the stated composition, and that most are correct to within 2 at. %.

2.5 The C.W. Spectrometer

During the period while the pulse spectrometer was under construction a C.W. spectrometer was available, and this was used to carry out an investigation of the composition dependence of the ^{115}In and ^{121}Sb resonance shifts in the liquid In-Sb system.

The basic circuit consists of a coil into which the sample tube is placed, this coil being part of the tank circuit of a Pound-Watkins marginal oscillator constructed by G. A. Styles. The coil is contained inside a heater coil surrounded by a water cooled jacket. The heater coil is supplied from a Roband T112 power supply and the temperature monitored by a thermocouple mounted near the sample tube.

To display the nuclear resonance the steady magnetic field is modulated at 80 Hz by a small field supplied from a Varian VF 16 wide-line spectrometer. The signal from the marginal oscillator is supplied to the phase-sensitive detector in the VF 16 spectrometer along with a reference signal from the modulator. The detected nuclear resonance signal is further improved using a Computer of Average Transients (CAT), in this case a Northern NS 544 digital memory oscilloscope. The CAT has 1024 memory channels which are opened in sequence so that each channel, opened once as the magnetic field is swept through the resonance, stores

a small section of the sweep. Since the coherent signal increases directly with the number of sweeps but the random noise voltage increases as the square root of the number of sweeps, in N sweeps an improvement in the signal to noise ratio of $N^{\frac{1}{2}}$ is achieved. The final resonance signal is displayed on a Bryans series 21000 chart recorder.

The magnetic field is determined using a second coil containing a sample of D_2O mounted on the main assembly as close to the main receiver coil as possible. A second Pound-Watkins marginal oscillator is used to detect the ^2D nuclear resonance in the manner described above. The frequencies of the main nuclear resonance and of the ^2D calibration resonances are measured using a Venner TSA 3436 counter which together with a divider unit is capable of measuring frequencies of up to 10 MHz to 1 part in 10^7.

2.6 The Magnetic suceptibility balance

The magnetic suceptibilities were measured using the well known Faraday technique. The sample is suspended in an inhomogeneous field, and there is then a force on the sample given by

$$F_z = m\mu_0 \chi_{t,x}^{(m)} H_x \left(\partial H_x / \partial z \right)$$

where m is the sample mass,

$\chi_t^{(m)}$ is the mass suceptibility.

The x axis is in the direction of the magnetic field, the z axis is in the direction of the suspension. $H(\partial H / \partial z)$ was determined for this apparatus by measuring the suceptibility of a standard material, silver; see section 4.2.3.

The magnetic field is supplied by a Mullard electromagnet with pole-pieces which has been shaped to provide a large value of $H(\partial H / \partial z)$, but this occurs only over a small volume. To overcome problems of reproducibility the magnet is mounted on a hydraulic jack which is pumped

up; then the hydraulic fluid is released slowly and the magnet sweeps down the sample. The sample is suspended from one arm of a Sartorius microbalance which can measure the force on the sample to within one part in 10^6, with samples which are usually of order 1 gram. The changing force on the sample is monitored and the maximum force noted, to the nearest microgram. To obtain the suceptibility of the sample it is necessary to allow for the suceptibility of the sample holder, a quartz bucket, which often contributes an appreciable part of the total measured force.

A nichrome heater coil wound directly on to a silica tube is fitted over the lower arm of the microbalance and the coil surrounded by fiber-frax paper. Temperature of up to 1400 K can be obtained, and are monitored by means of a chromel-alumel thermocouple mounted inside the furnace tube, having the junction within 4 mm of the sample.

All measurements have been carried out in an atmosphere of argon at a pressure of 400 Torr to inhibit preferential evaporation in any alloy. Above 400 Torr convection currents were found to cause fluctuations observable on the balance.

References

Clark, W. G., 1964, Rev. Sci. Instrum., 35, 316.

Faulkner, E. A. and Holmen, A., 1967, J. Sci. Instrum., 44, 391.

Hansen, M., 1958, The Constitution of Binary Alloys, McGraw Hill.

Heighway, J., Host, I. P. and Styles, G. A., 1970, J. Phys. E : Sci. Instrum., 3, 391.

Robinson, N. F. H., 1959, J. Sci. Instrum., 36, 481.

Warren, W. W. and Clark, W. G., 1968, J. Phys. E : Sci. Instrum., 1, 1019.

CHAPTER THREE

EXPERIMENTAL TECHNIQUE

3.1 The C. W. Spectrometer : Nuclear resonance shift measurements

The sample is continuously irradiated by r.f. radiation, and the resonance condition is detected by an increase in the absorption by the sample. To observe the resonance line the spectrometer frequency is held constant and the magnetic field is swept through the resonance condition. Superimposed on this field is a small modulating field at audio frequency, 80 Hz. Thus the detected r.f. signal will also be modulated and this is passed to a phase-sensitive detector whose output is effectively the differential of the pure absorption line when the phase has been suitably adjusted, enabling the centre of the resonance to be accurately determined.

The magnetic field is set to sweep through the resonance with the sweep range chosen to adequately cover the resonance width. In most cases the signal to noise ratio obtained from a single sweep is insufficient, and so the output of a number of sweeps is then averaged by the CAT (see section 2.5) and the output displayed on an X - T chart recorder. The upper limit to the number of sweeps, and hence to the improvement which can be made in the signal to noise ratio, is set by drift of the magnetic field and of the spectrometer frequency to be of the order of 128 sweeps. The resonance observed on this spectrometer, ^{115}In and ^{121}Sb, were satisfactorily resolved using considerably less than this number.

The field is calibrated by observing the ^{2}D resonance from the D_2O sample. The frequency of the oscillator is adjusted so that the resonance occurs low in the field sweep range, and the output stored in the CAT. The frequency is then re-set to cause the resonance high in the sweep range and the output is also stored in the CAT. These two calibration marks are added to the chart record of the main resonance.

Since the D_2O sample is located at a different position from that of the sample a constant difference between the field at the sample, and that measured by the calibration occurs. This is not important when comparing the resonance field shifts observed in the alloys to that for the same nucleus in the pure metal.

It is found that due to time-constant distortion there is a small difference in the position of the centre of the resonance if the field sweep is operated in the increase mode, as compared to that in the decrease mode. Errors from this source are eliminated by taking the average of an equal number of sweeps in each mode.

3.2 The Pulse Spectrometer

3.2.1 Nuclear resonance shift measurements

It has been pointed out by Clark (1964) that the pulse spectrometer can be used to observe nuclear resonance lineshapes, as well as to measure relaxation rates. This is due to the fact that the steady state unsaturated absorption $\chi''(\Omega)$ is proportional to the Fourier cosine transform of the free induction decay envelope, and the dispersion $\chi'(\Omega)$ is proportional to the Fourier sine transform (Lowe and Norberg, 1957). Hence if the boxcar integrator gate is opened to observe the entire free induction decay then, provided the time constant of the integrator is very much greater than a Larmor period and the receiving system is coherent, the resonance lineshape will be observed as the magnetic field is swept through the resonance condition.

In the initial search for a particular nuclear resonance two adjustments must be made. Firstly the pulse beyond which the resonance is to be observed is adjusted to be a $\pi/2$ pulse. The pulse length may be calculated from B_1, equation 1.15. Secondly the pulses must be several relaxation times apart or else the nuclear magnetisation will become

saturated; in these materials this condition is usually met with the normal operating pulse rate of 100 s^{-1}. Small relaxation rates could also cause a problem in that if the boxcar gate is too wide the signal becomes so spread out that its average size becomes undetectable. Hence the boxcar gate is not usually set to greater than 300 μs and this has not proved detrimental to the observation of nuclear resonances. Unfortunately due to the problems of coil ringing and pulse suppression it is essential to delay the boxcar gate behind the r.f. pulse and so part of the induction decay is not included. In consequence the resonance lineshape observed in this way is distorted and it is not possible to measure linewidths.

The nuclear resonance having been detected, due to phase changes introduced in the system, the resonance may be a mixture of absorption and dispersion. For the Lorentzian lines of interest here it was possible to obtain a pure absorption signal by adjusting the phase of the reference signal (i.e. by altering the delay) until the signal appears symmetrical with respect to the centre of the resonance line.

To measure the position of the centre of the resonance the magnetic field is swept up through the resonance condition and back down again. If it is a strong signal the time constant of the integrator is short and the two resonances are superimposed; if it is a weak signal the time constant will be large and this will introduce some distortion so that the two resonances are each displaced a little, one above and one below the centre. The centre of the resonance is taken as the average over the two resonances seen and the magnetic field is adjusted to correspond to this centre.

To measure the magnetic field the whole assembly is pulled forward placing the magnetometer coil and D_2O sample in to the position occupied by the receiver coil. The magnetometer frequency is adjusted until the ^2D resonance is seen at the centre of the oscilloscope trace. For further

detail see section 2.3. Experimental results are normally the average of four measurements.

3.2.2 Nuclear spin-lattice relaxation rate measurements

Once the resonance has been detected and adjusted in phase as described in section 3.2.1 the field is set to the centre of the resonance. The boxcar gate is reduced in width to sample the height of the decay at the fixed delay beyond the $\pi/2$ pulse. Normally this was set to 30 μs; tests have shown that the observations are not influenced by the gate width, even with fast relaxation rates which are comparable to the reciprocal of the gatewidth.

The field is then switched off resonance by means of a shorting switch connected across a resistor in the field control unit; shifting the field by more than 100 mT. The change in the receiver output gives the magnitude of the resonance, denoted M_o. The pulse separation is then reduced until an appreciable decrease in the signal level is obtained. The magnitude is then measured by switching on and off resonance, and the pulse separation is recorded. The process is repeated for a series of pulse separations, usually eight in all, and finally using a long pulse separation M_o is checked to ensure that there have been no changes in the system. In each case an estimate of the uncertainty is made by noting the average deviation of the receiver output from the value recorded, readily done by observing the chart recorder trace over a period of about a minute. A typical R_1 measurement trace is shown in figure 3.1.

The data are analysed by fitting the best straight line to the graph of the logarithm of signal amplitude against pulse separation (see section 1.3) using the least-squares technique with the values suitably weighted by their uncertainties following Topping (1962). I am grateful to Dr. E. M. Dickson for supplying a computer programme suitable for carrying out this analysis, which yields directly the measured value of R_1. Each

figure 3.1

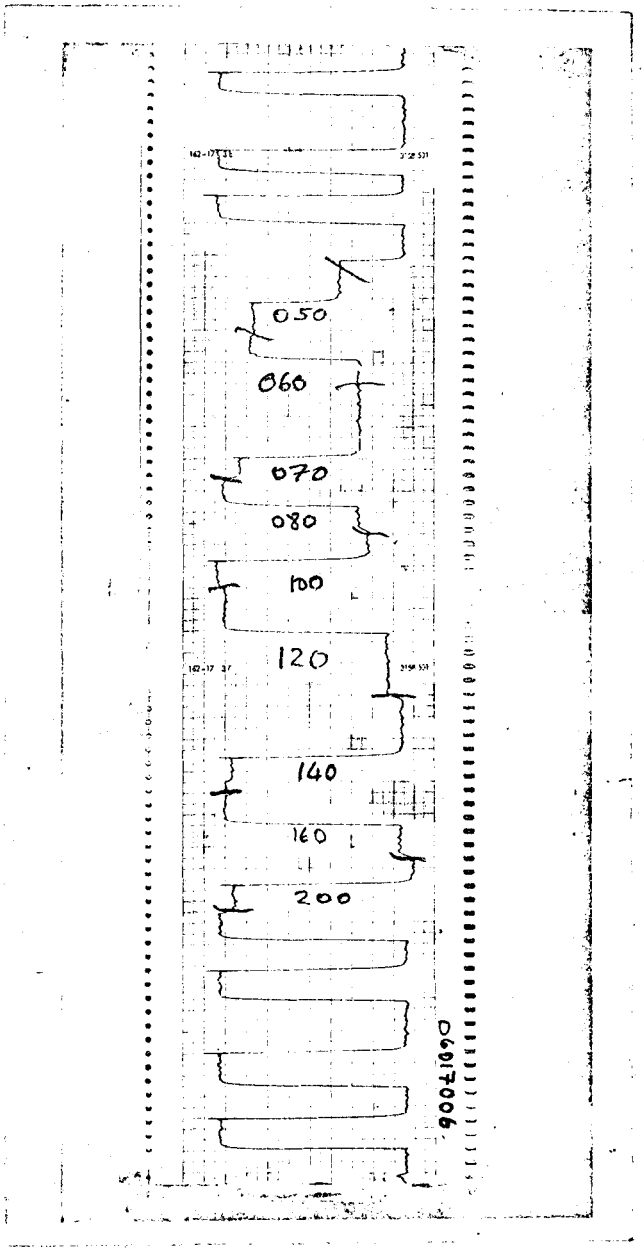

A RELAXATION RATE MEASUREMENT

FOR ^{209}Bi IN $Bi_{50}In_{50}$

the figures on the chart give the pulse

separation times in microseconds

experimental observation consists of the average of six such measurements. As a precaution each set of data is plotted by hand to give an estimated value for R_1.

Considerable difficulty has been experienced in measuring rates in the case of weak nuclear signals. This is due to the fact that under these circumstances the integration time constant is increased to improve the signal to noise ratios, with consequent increase in the time required for the receiver to reach the mean value of the signal. However the output from the receiver arising from other sources, the 'baseline', is subject to random drifting due mainly to external radiation in the bandwidth of the receiver. Under conditions of high gain and small nuclear signals these drifts become relatively large, so that if the period of observation is long the uncertainties become much greater.

For this reason it is found expedient to speed up the estimation of the size of the weakest signals, not by the method described but by sweeping the field through the resonance with a wide boxcar gate in the manner described in section 3.2.1. The baseline is then taken as the signal level at the ends of the field sweep, the signal being the level at the centre of the resonance. This is repeated for a number of suitable pulse separations and the data analysed as normal.

An attempt was made to overcome this problem by the construction of a two channel boxcar integrator, where one channel was intended to sample the signal and the other the baseline 1 ms later; this was unsuccessful in the time available due to technical difficulties.

References

Clark, W. G., 1964, Rev. Sci. Instr., 35, 316.

Lowe, I. J. and Norberg, R. E., 1957, Phys. Rev., 107, 46.

Topping, J., 1962, Errors of Observation and Their Treatment (Chapman and Hall, Ltd.).

CHAPTER FOUR

EXPERIMENTAL RESULTS

4.1 Liquid metallic binary alloys

4.1.1 Resonance shift measurements The principal measurements have been made on the ^{115}In and ^{121}Sb resonances in In-Sb. No measurements on reference compounds have been made; instead the extensive resonance shift results of Warren and Clark (1969) at 900 K for the pure liquid metals namely

$$S\ (^{115}In) = 0.76\%$$

and $$S\ (^{121}Sb) = 0.71\%$$

have been used, in conjunction with the observations in pure In and pure Sb made in the course of this work, to calculate the reference resonance fields, B_{ref}, from the expression

$$S = \frac{B_{ref} - B_{metal}}{B_{metal}} \qquad \ldots\ (4.1$$

The resonance shifts for all other compositions were than calculated using the respective reference resonance fields from equation 4.1. The ^{209}Bi resonance shift reported in $Bi_{50}Sn_{50}$, see table 4.7, has been calculated from equation 4.1 using a value for B_{ref} obtained from the literature (Varian Associates, 1965) : 6.842 MHz/T. The results of shift measurements are given in table 4.1, 4.7 and figure 4.1.

4.1.2 Nuclear spin relaxation rate measurements Where possible the present measurements have been compared to those reported in the literature and in all cases good agreement has been obtained. For example Warren and Clark (1969) have reported measurements

on liquid $In_{50}Sb_{50}$ at 900 K

$$R_1\ (^{115}In) = (14.8 \pm 0.3)\ .10^3 s^{-1}$$

$$R_1\ (^{121}Sb) = (21.6 \pm 2.0)\ .10^3 s^{-1}$$

which are to be compared with results reported in table 4.2 at 900 K

$$R_1\ (^{115}In) = (15.1 \pm 0.2)\ .10^3 s^{-1}$$

$$R_1\ (^{121}Sb) = (21.9 \pm 1.3)\ .10^3 s^{-1}$$

In pure liquid Bi at 620 K Rossini and Knight (1969) report that $R_1 = (16 \pm 2) \times 10^3 s^{-1}$ whereas in this work (table 4.3) it is found that $R_1 = (16.8 \pm 0.3) \times 10^3 s^{-1}$ at 610 K.

The close agreement found in these cases gave confidence in the accuracy of the observations of R_1 made on other systems. The results of the R_1 measurements are given in tables 4.2 to 4.6 and 4.8 to 4.10.

4.2 Liquid binary alloys containing Tellurium

4.2.1 Resonance shift measurements

The resonance shifts reported here for the ^{125}Te nucleus have been calculated from the observed resonance fields using equation 4.1.1 where B_{ref} has been calculated from the value reported by Weaver (1953) for the ^{125}Te resonance in a solution of TeO_2. These results are given in table 4.11, 4.14, 4.15 and displayed in figure 4.2.

4.2.2 Nuclear spin relaxation rate measurements

There was considerable difficulty in making these measurements on the ^{125}Te nuclei due to poor signal-to-noise ratios in all these alloys. The agreement obtained with other experimental observations mentioned in paragraph 4.1.2 indicates that the major part of the uncertainties in the experimental measurements arises from limitations on the sensitivity of the spectrometer. The R_1 results are given in table 4.12, 4.14 and 4.15.

4.2.3 Magnetic suceptibility measurements

The technique used does not give a direct measurement of suceptibility and so the balance has been calibrated using metallic silver as a reference material and values for the Te-Tl alloys have been calculated in terms of the results for silver. It has been taken that

$$\chi_m \text{ (Ag)} = 2.34 \times 10^{-9} m^3 kg^{-1} \quad \text{at } 300 \text{ K}$$

The values obtained for pure Te are considered unreliable due to a high rate of evaporation of the sample at the temperatures of observation; however the Te-Tl alloys all appeared to remain stable, and these are regarded as satisfactory. The results are displayed in table 4.13.

Table 4.1

Nuclear resonance shifts in In-Sb

a) $\underline{^{115}In}$

Temperature (900 ± 10)K

At % In	S %
100	0.760
90	0.804 ± 0.006
80	0.816 ± 0.006
70	0.863 ± 0.006
60	0.894 ± 0.006
50	0.913 ± 0.006
40	0.923 ± 0.006
30	0.931 ± 0.006
20	0.936 ± 0.006
10	0.936 ± 0.006

b) $\underline{^{121}Sb}$

At % Sb	S %
100	0.710
90	0.702 ± 0.006
80	0.690 ± 0.006
70	0.675 ± 0.006
60	0.661 ± 0.006
50	0.646 ± 0.006
40	0.643 ± 0.006
30	0.630 ± 0.006
20	0.621 ± 0.006

figure 4.1

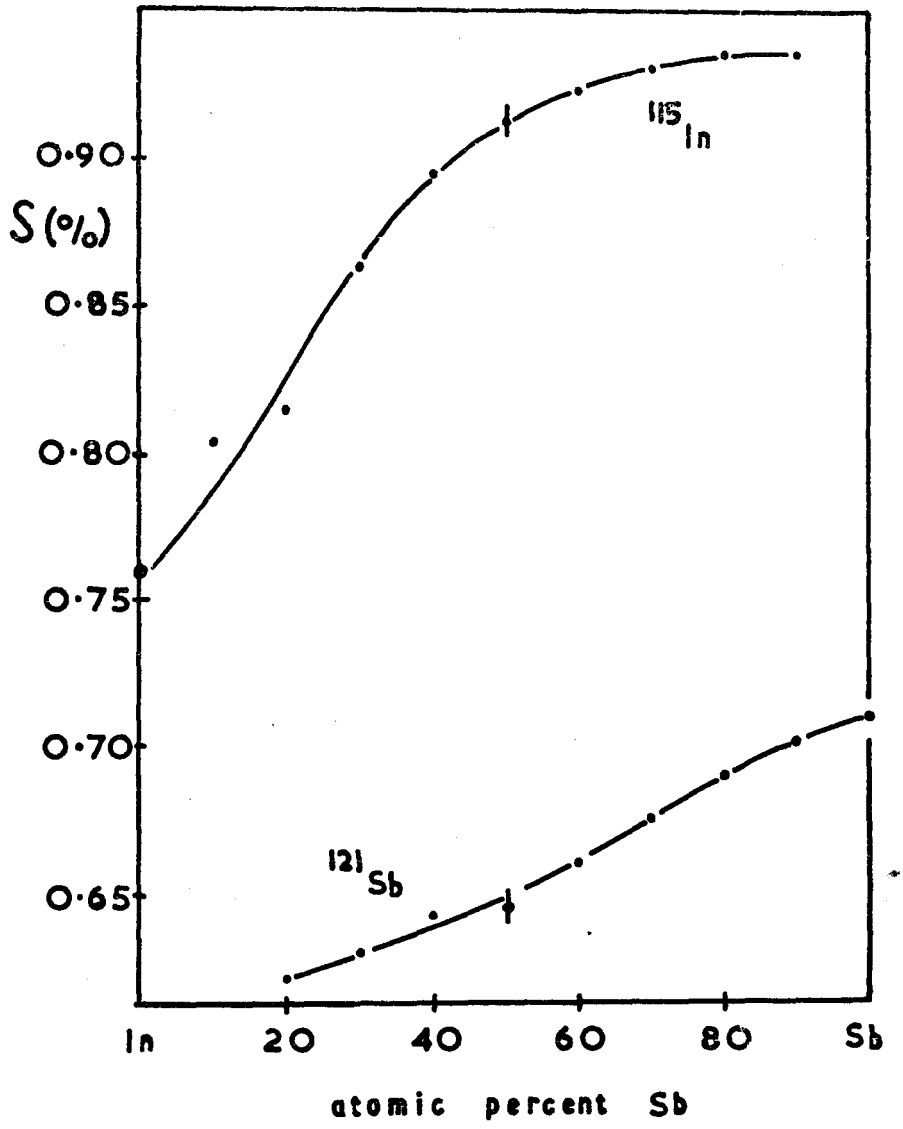

^{115}In AND ^{121}Sb RESONANCE SHIFTS

IN In-Sb AT 900 K

Table 4.2

Nuclear spin relaxation rates in In-Sb

a) ^{115}In

Temperature (900 ± 10)

At % In	R_1 ($10^3 s^{-1}$)
100	9.3 ± 0.2
90	9.8 ± 0.2
80	10.0 ± 0.2
70	12.7 ± 0.3
60	14.2 ± 0.4
50	15.1 ± 0.2
40	15.9 ± 0.2
30	16.8 ± 0.2
20	16.9 ± 0.4

b) ^{121}Sb

At % Sb	R_1 ($10^3 s^{-1}$)
100	10.2 ± 0.2
90	14.1 ± 0.2
80	17.0 ± 0.6
70	19.7 ± 0.6
60	22.1 ± 1.0
50	21.9 ± 1.3
40	21.5 ± 1.0
30	17.8 ± 0.8

Table 4.3

Nuclear spin relaxation rates in Bi-In

a) $\underline{^{209}Bi}$

At % Bi	R_1 ($10^3 s^{-1}$)
100	16.8 ± 0.3
90	18.1 ± 0.4
80	19.0 ± 0.5
70	20.4 ± 0.5
60	20.8 ± 0.7
50	19.4 ± 0.9
40	
30	17.5 ± 0.6
20	16.1 ± 0.5
10	15.1 ± 1.2

Temperature (610 + 5)K

b) $\underline{^{115}In}$

At % In	R_1 ($10^3 s^{-1}$)
100	7.4 ± 0.3
90	7.5 ± 0.1
80	7.9 ± 0.1
70	8.3 ± 0.1
60	8.4 ± 0.1
50	8.7 ± 0.2
40	9.2 ± 0.2
30	9.5 ± 0.1
20	9.5 ± 0.1
10	10.2 ± 0.3

Table 4.4

^{209}Bi nuclear spin relaxation rate in $Bi_{50}In_{50}$

Temp (K)	R_1 ($10^3 s^{-1}$)
909	21.1 ± 1.6
822	21.1 ± 0.8
688	19.8 ± 0.8
616	19.4 ± 0.8
510	19.5 ± 0.3
441	20.0 ± 0.4
400	20.6 ± 1.0
344	23.5 ± 0.6

Table 4.5

^{209}Bi nuclear spin relaxation rate in $Bi_{50}Pb_{50}$

Temp (K)	R_1 ($10^3 s^{-1}$)
905	24.0 ± 1.7
841	22.5 ± 1.0
767	22.3 ± 0.6
705	22.0 ± 0.5
638	20.7 ± 0.5
585	19.5 ± 0.5
523	19.5 ± 0.5
473	19.7 ± 0.5
425	20.6 ± 0.6
401	21.3 ± 0.3
386	23.6 ± 0.5

Table 4.6

^{209}Bi nuclear spin relaxation rate in $Bi_{50}Sn_{50}$

Temp (K)	R_1 ($10^3 s^{-1}$)
567 ± 2	18.3 ± 0.6
523	17.4 ± 0.4
472	16.1 ± 0.3
426	15.1 ± 0.3
381	15.5 ± 0.3

Table 4.7

^{209}Bi resonance shift in $Bi_{50}Sn_{50}$ at 426 K

$S = 1.33 \pm 0.01$ %

Table 4.8

^{209}Bi nuclear spin relaxation rate in $Bi_{50}Sb_{50}$

Temp (K)	R_1 ($10^3 s^{-1}$)
919 ± 2	26.0 ± 1.8
850	24.6 ± 0.8
783	21.8 ± 0.8
754	24.5 ± 0.5
701	23.2 ± 0.8

Table 4.9

^{121}Sb nuclear spin relaxation rate in $Bi_{50}Sb_{50}$

Temp (K)	R_1 ($10^3 s^{-1}$)
919 ± 2	11.2 ± 0.3
850	11.3 ± 0.3
782	10.1 ± 0.3
753	10.6 ± 0.3
705	10.4 ± 0.7

Table 4.10

^{27}Al nuclear spin relaxation rate in $Al_{89}Si_{11}$

Temp (K)	R_1 ($10^3 s^{-1}$)
852 ± 2	0.53 ± 0.1
843	0.43
840	0.45
829	0.48
813	0.43
805	0.43
795	0.42
771	0.40
766	0.45
763	0.43

Table 4.11

^{125}Te resonance shifts in liquid Te-Tl alloys

Alloy (At % Te)	Temp (K)	S %
100	696 ± 2	0.350 ± 0.01
	773	0.395 ± 0.01
	834	0.446 ± 0.01
	880	0.472 ± 0.01
	958	0.468 ± 0.02
	969	0.485 ± 0.01
80	530	0.170 ± 0.02
	556	0.18 ± 0.01
	576	0.22 ± 0.01
	598	0.24 ± 0.01
	611	0.27 ± 0.01
	631	0.28 ± 0.01
	648	0.30 ± 0.01
	709	0.35 ± 0.01
	787	0.39 ± 0.01
	804	0.38 ± 0.01
	825	0.39 ± 0.01
	897	0.41 ± 0.02
60	472	0.05 ± 0.01
	493	0.065 ± 0.01
	513	0.085 ± 0.01
	521	0.09 ± 0.01
	542	0.115 ± 0.01
	606	0.17 ± 0.01
	643	0.195 ± 0.01
	658	0.205 ± 0.01
	731	0.24 ± 0.01

Table 4.11 (Cont)

Alloy (At % Te)	Temp (K)	S %
60	752	0.255 ± 0.01
	826	0.28 ± 0.01
	877	0.305 ± 0.01
45	538	0.05 ± 0.01
	573	0.065 ± 0.01
	649	0.11 ± 0.01
	721	0.15 ± 0.01
	786	0.18 ± 0.01
	860	0.22 ± 0.02
40	847	0.144 ± 0.01
	795	0.115 ± 0.01
	723	0.086 ± 0.01
	700	0.067 ± 0.01
36	665	0.009 ± 0.01
	680	0.016 ± 0.01
	709	0.032 ± 0.01
	732	0.029 ± 0.01
	796	0.045 ± 0.01
	843	0.056 ± 0.01
35	649	- 0.025 ± 0.01
	682	- 0.025 ± 0.02
	737	- 0.011 ± 0.02
	791	+ 0.009 ± 0.01

Table 4.11 (Cont)

Alloy (At % Te)	Temp (K)	S %
34	672	- 0.049 ± 0.01
	715	- 0.032 ± 0.01
	737	- 0.032 ± 0.01
	762	- 0.025 ± 0.01
	788	- 0.018 ± 0.01
	819	- 0.008 ± 0.01
33	639	- 0.114 ± 0.01
	708	- 0.092 ± 0.01
	719	- 0.088 ± 0.01
	754	- 0.075 ± 0.01
	787	- 0.059 ± 0.01
	814	- 0.052 ± 0.01
	841	- 0.040 ± 0.01
31	662	- 0.116 ± 0.01
	689	- 0.093 ± 0.01
	719	- 0.091 ± 0.01
	754	- 0.071 ± 0.01
	780	- 0.065 ± 0.01
	831	- 0.054 ± 0.01

figure 4.2

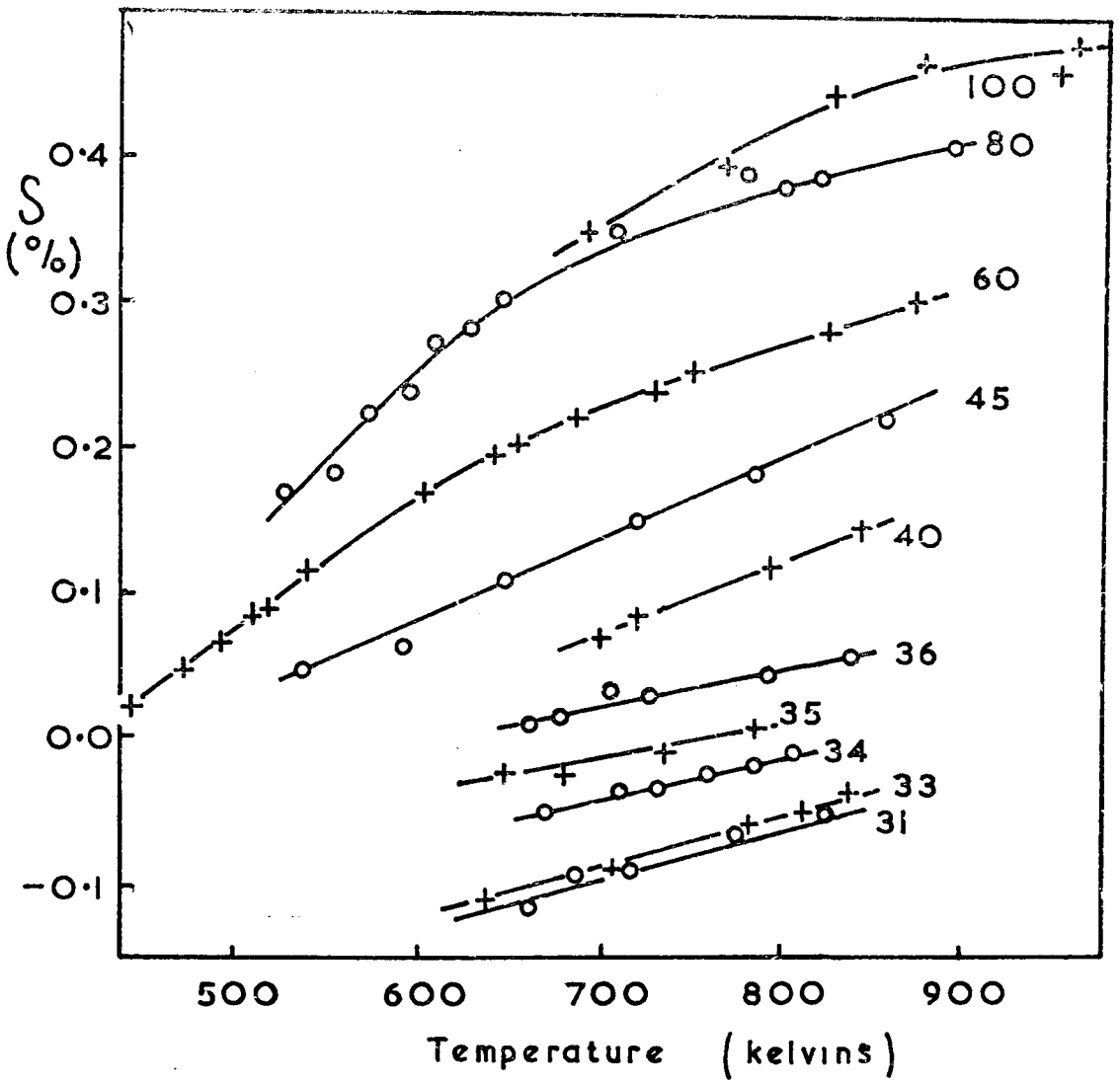

^{125}Te RESONANCE SHIFT AS A FUNCTION OF TEMPERATURE IN SOME Te–Tl ALLOYS

the Te concentration in atomic percent of each alloy is shown

Table 4.12

^{125}Te nuclear spin relaxation rates in Te-Tl alloys

Alloy (At % Te)	Temp (K)	R_1 ($10^3 s^{-1}$)
100	695	5.2 ± 1.1
	778	6.7 ± 1.3
80	523	2.1 ± 0.4
	625	5.4 ± 1.5
60	473	1.8 ± 0.3
	573	3.0 ± 0.7
	690	5.0 ± 2.5
45	563	3.1 ± 0.4
	663	5.0 ± 2.5
40	719	4.3 ± 1.1
36	741	4.6 ± 1.3
35	737	5.2 ± 1.9
34	718	6.7 ± 2.2
33	705	1.0 ± 0.25
	841	1.7 ± 0.3
31	662	0.74 ± 0.2
	831	1.0 ± 0.2

Table 4.13

Total suceptibility of some Te-Tl alloys

Alloy (At % Te)	Temp (K)	Mass Suceptibility ($10^{-9} m^3 kg^{-1}$)
100	751 ± 5	- 0.84 ± 0.1
	773	- 0.73
60	673	- 2.09 ± 0.01
	773	- 1.85
	823	- 1.78
40	723	- 2.37 ± 0.01
	773	- 2.32
	873	- 2.28
36	693	- 2.56 ± 0.01
	773	- 2.53
	843	- 2.49
34	683	- 2.70 ± 0.002
	711	- 2.57
	745	- 2.62
	816	- 2.51
	876	- 2.47
	979	- 2.41 ± 0.008
31	800	- 2.60 ± 0.003
	854	- 2.54
	933	- 2.48
	981	- 2.47

Table 4.14

^{63}Cu and ^{65}Cu resonance shifts and nuclear spin relaxation rates in $Cu_{50}Te_{50}$

a) ^{63}Cu

Temp (K)	S %	R_1 (s^{-1})
700 ± 5	0.038 ± 0.02	1210 ± 60
840	0.038 ± 0.02	1040 ± 30
950	0.038 ± 0.02	900 ± 60
1040	0.044 ± 0.02	910 ± 50
1120	0.053 ± 0.02	900 ± 70

b) ^{65}Cu

Temp (K)	S %	R_1 (s^{-1})
700 ± 5		1080 ± 150
840	0.034 ± 0.02	900 ± 90
950	0.033 ± 0.02	970 ± 70
1040		1090 ± 60
1120		890 ± 60

Table 4.15

^{125}Te and ^{209}Bi resonance shifts and nuclear spin relaxation rates in Bi_2Te_3

Temp (K)	Nucleus	S %	R_1 ($10^3 s^{-1}$)
883	^{125}Te	0.385 ± 0.01	5 ± 2.5
893	^{209}Bi	0.97 ± 0.02	40 ± 20

References

Rossini, F. A. and Knight, W. D., 1969, Phys. Rev., 178, 641.

Varian Associates, 1965, NMR table, 5th edn.

Warren, W. W. and Clark, W. G., 1969, Phys. Rev., 177, 600.

Weaver, H. E., 1953, Phys. Rev., 89, 923.

CHAPTER FIVE

NUCLEAR SPIN-LATTICE RELAXATION IN LIQUID METALLIC BINARY ALLOYS

5.1 Introduction

The most effective interaction by which nuclei in a metallic environment relax is usually the direct contact interaction between the nuclei and the conduction electrons. The same interaction causes a shift of the nuclear resonance position, and these two effects have been combined into a simple relationship by Korringa (1950). It is thus possible to evaluate the relaxation rate due to this interaction from the magnitude of the observed resonance shift. This produces reasonable agreement between observed and calculated relaxation rates for many pure liquid metals, although minor discrepancies arise and these will be discussed later. There are also a few cases, notably Bi, where at temperatures near the melting point there appears to be an extra relaxation rate which increases as the temperature decreases (Heighway and Seymour, 1971).

When the composition dependence of the spin-lattice relaxation rate in binary alloys is examined, in some cases considerable discrepancy is found; there appears to be a large extra rate which reaches a maximum in the middle of the composition range. It was pointed out by Faber (1963) that the nuclear electric quadrupole moment interacting with the local electric field gradients could cause nuclear spin relaxation, and this was confirmed in the case of Ga by Cornell (1967). This quadrupolar relaxation mechanism, which is believed to be the source of the extra rates observed, has been discussed by several authors and a comprehensive expression for the relaxation rate in a pure liquid metal has been given by Sholl (1967). This theory has recently been extended to liquid binary alloys (Sholl, private communication) and the outline of this theory will be given and discussed in the light of available data.

5.2 Magnetic relaxation

5.2.1 The contact interaction

When an external magnetic field is applied to a metal it produces a net polarisation of the s-type conduction electrons, and since they have a probability density at the nucleus they give rise to an extra magnetic field at the nucleus. Thus the field required for resonance is lower than the field required for resonance of the same nucleus in an insulator at the same frequency. This shift of the resonance in metals is known as the Knight shift, and is expressed (Townes, Herring and Knight, 1950).

$$S_s = \Delta B/B_o = (2/3)\,\Omega P_F \chi_P \qquad \ldots\ (5.1)$$

where Ω is the atomic volume,

$P_F = \langle |\psi(o)|^2 \rangle_F$, the probability density at the nucleus, averaged over all Fermi surface electrons,

χ_P is the conduction electron spin suceptibility.

The contact interaction also provides a dynamic coupling between nuclei and conduction electrons enabling nuclear relaxation to take place. This relaxation rate has been expressed (Korringa, 1950)

$$(R_1)_s = (4\pi/9)\mu_0^2 \pi^2 \hbar^3 \gamma_e^2 \gamma_n^2 (\Omega P_F)^2 N^2(E_F)\, kT \qquad \ldots\ (5.2)$$

where γ_e, γ_n are the electron, nuclear gyromagnetic ratios respectively,

$N(E_F)$ is the density of states at the Fermi energy.

These two relationships were combined by Korringa using the assumption of free non-interacting electrons, to give the Korringa relationship

$$\frac{T S_s^2}{(R_1)_s} = \frac{\hbar}{4\pi k} \frac{(\gamma_e)^2}{(\gamma_n)^2} \qquad \ldots\ (5.3)$$

It has been found that agreement between experimental values and the Korringa relationship is not satisfactory, so that electron-electron interaction must be taken into account. It was pointed out by Pines (1955)

that electron-electron interaction leads to an enhancement of the static spin suceptibility and thus to an enhancement of the resonance shift. Later it was shown that the relaxation rate corresponds not to the static but rather to the dynamic frequency and wave number dependent part of the spin suceptibility (Moriya, 1963). Narath and Weaver (1968) have modified the Korringa relationship to take account of these factors, expressing it

$$\frac{T S_s^2}{(R_1)_s} = \frac{\hbar}{4\pi k} \left\{ \frac{\gamma_e}{\gamma_n} \right\}^2 K(\alpha) \qquad \ldots\ (5.4)$$

where $K(\alpha)$ is a function of α, the electron-electron interaction parameter.

The value of $K(\alpha)$ lies between 0 and 1; experimental values for a number of liquid metals are near to 0.7. The calculation of $K(\alpha)$ is a complex problem; Narath and Weaver have evaluated it in two cases, one where the electron-electron interaction potential is approximated to a δ function, the other where the interaction potential has long range. Experimentally determined values of $K(\alpha)$ for the alkali metals are found to lie between the theoretical values found for the two cases. It appears that until more is known about the dynamic part of the spin suceptibility the uncertainty in the magnitude of $K(\alpha)$ remains, and so in this work no attempt will be made to estimate it.

5.2.2 Other magnetic interactions

a) Orbital motion. The orbital motion of the conduction electrons also gives rise to a magnetic field at the nucleus which produces a corresponding shift in the nuclear resonance position. This shift has been expressed approximately by Noer and Knight (1964)

$$S_o = \frac{8}{3} \chi_o \left(\mu_0 / 2\pi \right) \langle 1/r^3 \rangle \, \Omega \qquad \ldots\ (5.5)$$

where χ_o is the orbital suceptibility,

r is the mean radius of the electron orbit,

Ω is the atomic volume.

If as an approximation χ_o is taken as the free electron value of χ_p then a reasonable estimate of an upper limit to S_o can be made. It is found to be small compared to the shift produced by the contact interaction, S_s, except for some transition metals, but may be an appreciable part of S_s for heavy nuclei.

This interaction also produces nuclear spin relaxation. Mitchell (1957) has given an expression for the relaxation rate due to p-electrons in Bloch states, an acceptable model for the near free electrons in liquid metal systems.

$$(R_1)_o = (17/16)\ (\pi Z^2 m^{*2} B^2 / \hbar)\ \gamma_e^2\ \gamma_n^2\ kT \quad \ldots\ (5.6)$$

where $B = \int \frac{\langle |V(r)|^2 \rangle}{r}\, d\tau$,

$\langle |V(r)|^2 \rangle$ is the radial part of the p-wave component of the Bloch wave function,

Z is the number of valence electrons per atom,

m^* is the electron effective mass.

This is a very complex expression to evaluate, but Mitchell has compared this expression with that of $(R_1)_s$ and concludes that this relaxation process will be more than two orders of magnitude less effective than the contact process, providing the s-part is at least half of the conduction electron wave function and so will be neglected.

b) Core polarisation. An additional magnetic field may be produced at the nucleus due to polarisation of the s-electrons in the core by the conduction electrons, creating an additional resonance shift S_{cp}. This shift cannot be easily evaluated since the effects of the s, p and d components of the conduction electrons on each core state must be evaluated individually, and some of these may be negative, producing a reduction in

the overall shift. S_{cp} has been calculated to be -5% of S_s in Li, +16% in Be and +8% in Al (Shyu, Das and Gaspari, 1966). In Cd it is +10% of S_s (Jena, Das and Gaspari, 1970). In In a calculation of S_s is very close to the experimental value of S, and since S_o is expected to be small it is concluded that S_{cp} is less than 1% of S_s (Gaspari and Das, 1968). It appears that there is no correlation between S_{cp} and atomic number; all that can be deduced at this stage is that it is unlikely to be greater in magnitude than 15% of S_s but could be positive or negative in sign.

The existence of this interaction leads to a further relaxation mechanism; there is a Korringa-like relationship between the shift and the relaxation rate but with an inhibiting factor of between one and one fifth, due to degeneracy of non s-states at the Fermi surface (Yafet and Jaccarino, 1964).

$$(R_1)_{cp} \leq \frac{4\pi k}{\hbar} \left(\frac{\gamma_n}{\gamma_e} \right)^2 S_{cp}^2 \, T \qquad \ldots\ (5.7)$$

However even if $S_{cp} = 0.15\ S_s$ then at most $(R_1)_{cp} = 0.02\ (R_1)_s$ which is within the experimental error, and so this relaxation mechanism will be ignored.

c) Other interactions. Because the short correlation time limit has been reached, and because of the smallness of the dipole-dipole interaction this effect contributes little to the nuclear spin relaxation (Bloembergen, Purcell and Pound, 1948). Pseudo-dipolar and indirect exchange interactions similarly are rather small and have reached the short correlation time limit, and so also contribute little to the relaxation.

5.3 Electric quadrupolar relaxation

The interaction between the nuclear electric quadrupole moment, existing when the nuclear spin, I, is greater than one half, and the

fluctuating electric field gradient is also capable of causing nuclear spin relaxation. An expression for this relaxation rate has been given by Abragam (1961) applicable in the short correlation time limit, where the electric field gradient correlation time is very much less than the Larmor period, $1/\omega_L$, which is very well satisfied in the case of liquid metals:

$$(R_1)_Q = \frac{3}{4} \frac{2I+3}{I^2(2I-1)} \left(\frac{eQ}{\hbar}\right)^2 \mathcal{J}(\omega_L) \quad \ldots\ldots (5.8)$$

where Q is the nuclear quadrupole moment,

$\mathcal{J}(\omega_L)$ is the spectral density of the electric field gradient at ω_L.

5.3.1 Isotopic separation This electric quadrupolar rate may be expressed for one chemical species in a particular alloy as

$$(R_1)_Q = C\ F(I)\ Q^2$$

where C is the same for all isotopes of the same species.

The relaxation rate due to the contact interaction, discussed in section 5.2.1, can be expressed in a similar way for one chemical species in a particular alloy as $(R_1)_s = C' \gamma_n^2$. If it is assumed that nuclear spins relax by a combination of these two processes namely $R_1 = (R_1)_s + (R_1)_Q$ and if it is possible to measure the relaxation rates of two different isotopes, X and Y of one chemical species in a particular alloy then, provided that A and B are not the same, where

$$A = \frac{(\gamma_{n,x})^2}{(\gamma_{n,y})^2} \quad \text{and} \quad B = \frac{F(Ix)}{F(Iy)} \times \frac{(Qx)^2}{(Qy)^2}$$

it is a simple matter to resolve the observed relaxation rates $(R_1)_x$ and $(R_1)_y$ into their electric and magnetic components (Cornell, 1967).

$$(R_1)_{sx} = \frac{R_{1x} - B \cdot R_{1y}}{1 - B/A}\ ; \quad (R_1)_{sy} = \frac{(R_1)_{sx}}{A} \quad \ldots\ldots (5.9)$$

$$(R_1)_{Qx} = \frac{R_{1x} - B.\,R_{1y}}{1 - B/A}\,; \quad (R_1)_{Qy} = \frac{(R_1)_{sx}}{B} \qquad \ldots\ (5.10)$$

5.3.2 The Sholl theory for pure liquid metals

The main difficulty in carrying out calculations of Abragam's expression to find if there is agreement with experiment lies in determining $\mathcal{J}(\omega_o)$. In attempting to calculate the electric field gradient at a nuclear site it is clear (Rossini, Geissler, Dickson and Knight, 1966) that the effects of both surrounding ion cores and also the conduction electrons must be considered. Sholl has included the conduction electrons as a screening cloud around the ion cores, and using the theory of linear Hartree screening has expressed the asymptotic form of the screened potential as

$$V(r) = A\,\frac{\cos(2k_f r)}{2(k_f r)^3} \qquad \ldots\ (5.11)$$

where A is the amplitude of the potential.

It has been shown that this asymptotic form is a good approximation up to nearest neighbour distances (Harrison, 1966) and so is likely to be reasonably satisfactory in this case.

An important contribution to the electric field gradient at the nucleus arises from the distortion of its own ion charge distribution by the external field gradient. This has been considered by Sternheimer (1966) who finds that it can be represented by multiplying the external field gradient by a constant, the Sternheimer anti-shielding factor, γ_∞, and the factor has been calculated for a number of ions. The γ_∞ vary from small negative values for metals of low atomic number, for example -4.5 (Na^+) or -9.5 (Ga^{3+}), to large negative values such as -102 (Cs^+) or -81 (Pr^{3+}) for larger atomic numbers, but there does not appear to be any simple relationship to atomic number.

The potential part of the quadrupolar Hamiltonian may be expressed

$$F^{(m)} = \sum_{\lambda} U_m(\underline{r}_\lambda) \qquad \ldots\ (5.12)$$

Where the sum is over all ionic positions, $\underline{r}_\lambda$, other than that of the ion at the origin. The m is an energy quantum number taking integral values between ℓ and $-\ell$; ℓ is 2 for the nuclear quadrupole moment.

$$U_m\ (\underline{r}_\lambda) = C\ V_2\ (r_\lambda)\ Y_{2m}\ (\Omega_\lambda) \qquad \ldots\ (5.13)$$

where $C = (1 - \gamma_\infty)\ (4\pi/45)^{\frac{1}{2}}$

$$V_2(r) = r\ \frac{d}{dr}\left(\frac{1}{r}\ \frac{dV(r)}{dr}\right)$$

Y_{2m} are spherical harmonics,

Ω is the direction of vector $\underline{r}_\lambda$.

The electric field gradient spectral density term is expressed

$$J(\omega) = \int_{-\infty}^{\infty} e^{-i\omega\tau}\ g_{mm'}(\tau)\ d\tau \qquad \ldots\ (5.14)$$

where $g_{mm'}(\tau) = \overline{F^{(m)}\ (t - \tau)\ F^{(-m')}\ (t)}$

and the bar denotes an ensemble average.

Subsituting in this for $F^{(m)}$ from equation 5.12 gives

$$F^{(m)}\ (t - \tau)\ F^{(-m')}\ (t) = U_m\left\{\underline{r}_\lambda\ (t - \tau)\right\}\ U_m^*\left\{\underline{r}_\lambda(t)\right\}$$

and the ensemble average is

$$g_{mm'}(\tau) = \int\int U_m\ (\underline{r}_o)\ U^*_{m'}\ (\underline{r}_1)\ P(\underline{r}_o,\ t - \tau;\ \underline{r}_1, t)\ d\underline{r}_o\ d\underline{r}_1$$

$$\ldots\ (5.15)$$

where $P(\underline{r}_o,\ t - \tau;\ \underline{r}_1,\ t)\ d\underline{r}_o\ d\underline{r}_1$ is the probability of finding ions in $d\underline{r}_o$ at $\underline{r}_o$ at time $t - \tau$, and in $d\underline{r}_1$ at $\underline{r}_1$ at time t; given that there is an ion at the origin.

P is composed of two parts; the first giving the probability of finding an ion in $d\underline{r}_1$ at time t, given the same ion was in $d\underline{r}_o$ at time $t - \tau$. This describes the diffusion of an ion from $\underline{r}_o$ to $\underline{r}_1$, and so is just the product of the diffusion probability and the radial distribution function. The second part gives the probability of finding an ion in $d\underline{r}_1$

at time t and that a different ion is in $d\underline{r}_o$ at time $t - \tau$. This term describes the diffusion of an ion originally at $\underline{r}_o$ to some other part of the liquid while a second ion diffused into $\underline{r}_1$ at time t, and is the sum over all possible starting points of the product of the diffusion probability and the three body correlation function. Since the three particle correlation function is not known the superposition approximation has been used. To get the diffusion probability for each of these terms the method of Oppenheim and Bloom (1961) has been used, taking as a solution to the diffusion equation that for relative diffusion which is equivalent to replacing the self-diffusion coefficient, D, by 2D.

From equations 5.14 and 5.15 $\mathcal{J}(\omega)$ is calculated and substituted into equation 5.8 which gives the quadrupolar rate. This rate contains two terms, one arising from the two particle correlation function (the radial distribution function, g(r)) and the other from the three particle correlation function.

$$(R_1)_Q = \frac{2I + 3}{I^2(2I - 1)} \left\{\frac{A(1 - \gamma_\infty)eQ}{\hbar}\right\}^2 \frac{\pi\rho}{75\,D} \left[I_1 + I_2\right] \quad \ldots (5.16)$$

where $I_1 = \int_o^\infty f(r_o)\, G(r_o)\, dr_o$

$$I_2 = 2\pi\rho \int_o^\infty f(r_o) g(r_o) r_o^2\, dr_o \int_o^\infty G(r_2) dr_2 \int_{-1}^{+1} \left\{g(r_{o2}) - 1\right\} P_2(z) dz$$

$$G(r_o) = \frac{g^{\frac{1}{2}}(r_o)}{r_o} \left\{ \int_o^{r_o} f(r_1) g^{\frac{1}{2}}(r_1) r_1^4\, dr_1 + r_o^5 \int_{r_o}^\infty \frac{f(r_1) g^{\frac{1}{2}}(r_1)}{r_1}\, dr_1 \right\}$$

$$r_{o2}^2 = r_o^2 + r_2^2 - 2 r_o r_2 z$$

ρ is the number density,

$P_2(z)$ is the Legendre polynomial in z where $z = \cos\theta$;

θ is the angle between $\underline{r}_o$ and $\underline{r}_2$.

This equation has been used by Sholl to calculate $(R_1)_Q$ in liquid Ga and liquid In and reasonable agreement with experiment was obtained.

The theory is extended to the case of binary alloys in section 5.3.3. The principal temperature dependence of $(R_1)_Q$ arises from the self-diffusion coefficient, the other terms are only weakly temperature dependent in comparison. The temperature dependence of the $(R_1)_Q$ will be examined and compared to those of self-diffusion coefficients in section 5.4.4.

5.3.3 The Sholl theory for binary alloys

This theory is given in detail in the Appendix and an outline only is given here. When binary alloys are considered the potential which describes the interaction depends on whether the other atom is the same as, or different to the atom at the origin. If there is an A type atom at the origin the possible potentials are V_{AA} or V_{AB}. In calculating how the potential gradient fluctuates the occupancy of $d\underline{r}_o$ at $\underline{r}_o$ is considered together with the occupancy of $d\underline{r}_1$ at $\underline{r}_1$ at a time τ later, so that there are now four possibilities to consider. When the ensemble average is taken there will be four terms of the form of equation 5.15. One of these will be

$$U_m^A(\underline{r}_o)\, U_m^B(\underline{r}_1)\, P_{AAB}(\underline{r}_o, t-\tau; \underline{r}_1, t)\, d\underline{r}_o\, d\underline{r}_1 \qquad \ldots\ (5.17)$$

where $P_{AAB}(\underline{r}_o, t-\tau; \underline{r}_1, t)\, d\underline{r}_o\, d\underline{r}_1$ is the probability of finding an ion of type A in $d\underline{r}_o$ at $\underline{r}_o$ at time $t-\tau$, and an ion of type B in $d\underline{r}_1$ at $\underline{r}_1$ at time t, given that there is one of type A at the origin. As before P_{AAA} and P_{ABB} must include two parts, one depending on the radial distribution function, the other on the three particle correlation function, but in P_{AAB} and P_{ABA} there will only be the three particle correlation function since these two do not describe diffusion of a given atom from $\underline{r}_o$ to $\underline{r}_1$.

The scaling factor, ρ, used on the radial distribution functions is simply a number density and the concentration dependence can be

included in this by means of C, the atomic fraction of A type atoms; the density of A type atoms is then $C\rho$ and of B type atoms $(1 - C)\rho$. Since the three particle correlation function must be expressed by the superposition approximation, terms of second order in C will appear, for example

$$\rho^{(3)}_{AAB}(\underline{r}_o, \underline{r}_2) = C(1 - C)\rho^2 \; g_{AA}(r_o)\, g_{AB}(r_1)\, g_{AB}(r_{o2}) \quad \ldots\ (5.18)$$

where $g_{AA}(r_o)$ is the radial distribution function for A atoms evaluated at r_o, given an A type atom at the origin. Again, following Oppenheim and Bloom (1961) the diffusion probability is included as a solution to the diffusion equation, where the diffusion rates for A and B type atoms are derived separately. This enables a very complex expression for the relaxation rate to be deduced; and is given in full in the Appendix, equation 15. The expression can be made considerably more tractable by some simplifying assumptions.

If it is assumed that

(i) the interatomic potentials are in simple proportion

i.e. $V_{AB} = \alpha\, V_{AA}$

(ii) the radial distribution functions are all the same

i.e. $g_{AA} = g_{AB} = g_{BB}$

and are independent of composition.

This leads to

$$(R_1)_Q = K\left\{\frac{C\, I_1}{D_A} + \frac{(1 - C)\alpha^2 I_1}{D_B} + \frac{C^2 I_2}{D_A} + \frac{(1 - C)^2\alpha^2 I_2}{D_B} + C(1 - C)\alpha I_2\left[\frac{1}{D_A} + \frac{1}{D_B}\right]\right\} \quad \ldots\ (5.19)$$

where $K = \dfrac{2I + 3}{I^2(2I - 1)}\left(\dfrac{A(1 - \gamma_\infty)eQ}{\hbar}\right)^2 \dfrac{\pi\rho}{75}$,

I_1, I_2 are as defined in equation 5.16.

If it is further assumed (iii) that the diffusion coefficients are the same i.e. $D_A = D_B = D$ then

$$(R_1)_Q = \frac{K}{D}\left\{ C\, I_1 + (1-C)\alpha^2 I_1 + C^2 I_2 + (1-C)^2\alpha^2 I_2 + 2C(1-C)\alpha I_2 \right\} \quad \ldots\ldots (5.20)$$

It can be seen that this contains a quadratic expression in C, and it is by using this equation that the experimental observations will be explained. The comparison of the theory with the data will be discussed in section 5.4.

5.3.4 Other theories of quadrupolar relaxation

Borsa and Rigamonti (1967) have used Abragam's expression (equation 5.8) to calculate a value for $(R_1)_Q$. They considered the time dependent inter-pair electric field gradient which arises from screened ionic charges diffusing in the liquid metal, obeying the classical diffusion equation; but the screening was only taken to be exponential in form. They derived an ensemble average by integrating the transition probabilities between the closest distance of approach and infinity. However, they chose the ionic antishielding factor and so neglected the effect of the conduction electrons near to the nucleus being considered. Nevertheless the relaxation rate calculated from this theory gave agreement within a factor of three to the experimental relaxation rate value available for Ga at that time.

This theory was extended to binary alloys (Bonera, Borsa and Rigamonti, 1969); however it predicts only linear dependence on C. This result is incorrect theoretically since, as pointed out by Heighway (1969) they merely added separate contributions to the electric field gradient, each of which contains an ensemble average, rather than taking a new total ensemble average.

A second possible source of the fluctuating electric field gradients

responsible for quadrupolar relaxation has been proposed by Mitchell (1957), namely a direct nuclear interaction with the conduction electron charge, analagous to the magnetic contact interaction. This process utilises the kinetic energy of the conduction electrons at the Fermi surface. An expression was derived by Mitchell for the relaxation rate produced by Bloch electrons. It is distinguished from a diffusion induced relaxation process in that the rate increases with increasing temperature in common with other mechanisms depending on electrons at the Fermi level. The rate has been shown by Mitchell to be comparable to $(R_1)_o$, defined in section 5.2.2.a, and will be neglected for the same reason as $(R_1)_o$ is neglected.

5.4 Analysis of the experimental data

Of the metallic elements in groups IIIa, and Va of the periodic table only Al, Ga, In, Sb and Bi have nuclear spins greater than one half, and thus have electric quadrupole moments, enabling the nuclear spins to relax via the interaction between the quadrupole moment and the fluctuating electric field gradient at the nucleus. Experimentally observed spin-lattice relaxation rates of these nuclei in the pure liquids and binary liquid alloys given in table 5.1 will be discussed.

Some of the data come from measurements of nuclear resonance linewidths. The usual assumptions are made, namely that in liquids the linewidth, ΔB, is due to lifetime broadening and so is proportional to the spin-spin relaxation rate, R_2; and that the dominant process in spin-spin dephasing is the longitudinal spin relaxation rate, R_1, so that R_1 is proportional to ΔB and can be calculated from it. Experimental evidence for the validity of these assumptions will be discussed in section 5.4.1.

The data will be analysed to determine the relative content of magnetic and electric quadrupolar relaxation contributions. When it is possible to carry out isotopic separation of the relaxation rate the

Table 5.1

Element	Alloy	Data source
Al	pure Al	Spokas and Slichter (1959)
	Al-Si	This work
Ga	pure Ga	Cornell (1967)
	Ga-In	Bonera et al (1969)
In	pure In	Warren and Clark (1969)
	Ag-In	Host (1972)
	Bi-In	This work, Styles (1967)
	Cd-In	Styles (1964)
	Ga-In	Bonera et al (1969)
	In-Pb	Styles (1964)
	In-Sb	This work, Warren and Clark (1969)
	In-Tl	Styles (1964)
Sb	pure Sb	This work, Warren and Clark (1969)
	Bi-Sb	This work, Moulson (1966)
	In-Sb	This work, Warren and Clark, (1969)
Bi	pure Bi	This work, Heighway and Seymour (1971)
		Rossini and Knight (1970)
	Bi-In	This work, Styles (1967)
	Bi-Sb	This work, Moulson (1966)
	Bi-Sn	This work
	Bi-Pb	This work, Heighway and Seymour (1971)

magnetic and quadrupolar parts are immediately available; if not it is taken that the quadrupolar rate is negligibly small at the highest temperatures and the experimental Korringa product, TS^2/R_1, is evaluated from values measured there. The Korringa product found in this way can deviate considerably from the value calculated for free non-interacting electrons, due to the value of $K(\alpha)$ and also to the observed shift having

other undetermined contributions S_o and S_{cp}, but it is assumed that their fractional effect will remain independent of temperature. A quadrupolar contribution at lower temperatures can thus be recognised.

5.4.1 Spin-spin relaxation rates Although it has been generally assumed that in liquid alloys $R_2 = R_1$, there is as yet little experimental evidence to support this conclusion. Hanabusa (1965) has shown in the Na-Tl system that provided care was taken to ensure that surface contamination was minimised R_1 and R_2 were the same to within the experimental uncertainties. The R_1 measurements reported here will now be compared with linewidth measurements where available as further confirmation that the two rates are equal.

In the case of pure Bi R_2 is calculated from the linewidth (Heighway and Seymour, 1971) using the usual expression for Lorentzian lines

$$R_2 = \sqrt{3}/2 \quad \gamma_n \Delta B \qquad \ldots\ (5.21)$$

where γ_n is the nuclear gyromagnetic ratio.

This leads to $R_2 = (16.5 \pm 0.2) \times 10^3 s^{-1}$ at 570 K which is to be compared to the value given in table 4.4, $R_1 = (16.8 \pm 0.3) \times 10^3 s^{-1}$ at 574 K.

Turning to alloys, in $Bi_{50}Pb_{50}$ the ^{209}Bi linewidth (Heighway and Seymour, 1971) gives $R_2 = (21.3 \pm 0.5) \times 10^3 s^{-1}$ at 625 K, whereas from table 4.6 $R_1 = (20.7 \pm 0.5) \times 10^3 s^{-1}$ at 638 K and the temperature dependence is such that R_1 will increase as the temperature decreases so that agreement between the two results is again satisfactory.

In Bi-In there are available a set of linewidth measurements over the major part of the composition range for both ^{115}In and ^{209}Bi (Styles, 1967); these are compared to the R_1 data given in table 4.3. The ^{115}In measurements will be considered first; if the R_1 data are extrapolated to 580 K by assuming that R_1 is proportional to temperature then it is found that the R_2 are about 10% larger than the R_1, the discrepancy being greatest in the 40, 50 and 60 at. % In alloys. However since the

experimental uncertainties total around 5%, and since 10% of the observed linewidth is about 15 μT which is of the same order as the inhomogeneity of the steady magnetic field it would be unreasonable to claim that R_2 was not equal to R_1.

When the ^{209}Bi data are examined the discrepancies become rather larger, for example R_2 in $Bi_{50}In_{50}$ was found to be 21% larger than R_1. In this case since R_1 is virtually independent of temperature in this range no extrapolation has been made; the values of R_2 observed at 580 K and those of R_1 at 620 K have been compared directly. A possible explanation for the discrepancy is that it arises from composition inhomogeneity in the samples; the observed R_1 and S would be averages over the sample but if there were a spread of resonance shifts the linewidths would be increased accordingly. If the average range of composition is only ± 1%, from the composition dependence of S (Styles, 1967) in $Bi_{50}In_{50}$ the additional linewidth at 1.4 T is 0.125 mT, which is approximately 20% of the observed linewidth and hence accounts for the difference between R_1 and R_2. This hypothesis is borne out by three things, firstly that this additional linewidth is proportional to the steady magnetic field, and so explains the field dependence of the linewidth which was observed. Secondly S is not composition dependent below 40 at. % Bi and in those alloys R_1 and R_2 just agree within the uncertainty; further the differences between R_1 and R_2 in the other alloys vary in proportion to the magnitude of the composition dependence of S. Thirdly the original samples which were used for both R_1 and R_2 measurements were prepared by G. A. Styles using the method of casting the molten alloy into a mould, then taking a sample of this cast and turning it into a powder, and so might be expected to contain some range of compositions. Fresh samples containing 50 at. % and 60 at. % Bi respectively were prepared using the spraying technique described in section 2.4, but the linewidths measured, although less, agreed with the original measurements to within the experimental

measurements. This implies that alloys prepared by either of these technique will contain a range of compositions of order ± 1%.

If the ^{115}In measurements are examined in the light of this hypothesis a range of ± 1% in composition will produce an increase of some 20% of the linewidth in alloys of 30 to 50 at. % In and there are indeed indications of these in the linewidth measurements. The agreement between ^{209}Bi R_1 and R_2 in $Bi_{50}Pb_{50}$ is also to be expected since the change of the resonance shift with composition is three or four times smaller in Bi-Pb than it is in Bi-In.

It is concluded that R_2 does equal R_1 in liquid alloys but an additional line broadening can arise; giving experimental values of R_2 which can be as much as 20% larger than R_1, depending on how S varies with composition; hence attempts to deduce accurate values of R_1 from linewidths must be carried out with due regard for the composition dependence of S.

5.4.2 Pure liquid metals

a) Aluminium. The only available data report that just into the melt the measured relaxation rate is in agreement with the Korringa product evaluated in the solid over the temperature range 1 K to 930 K indicating that there is no evidence of quadrupolar relaxation.

b) Gallium. Isotopic separation of the relaxation rate data (Cornell, 1967) gives the magnetic relaxation rate for ^{69}Ga and hence the Korringa product as 6.2×10^{-6} s K. The quadrupolar relaxation rate is $(0.6 \pm 0.2) \times 10^{3} s^{-1}$ at 300 K and shows little temperature dependence in the range 300 to 500 K. Sholl (1967) using equation 5.16 has completed calculations of the quadrupolar rate, estimating A and $(1 - \gamma_\infty)$ from the quadrupolar coupling constant and the lattice sums in the solid, and finds that at 300 K $(R_1)_Q = 0.15 \times 10^{3} s^{-1}$. It appears that there has been an underestimate by a factor of about four in the values substituted into

the expression. Since the relative magnitudes of I_1 and I_2 (defined in equation 5.16) can be determined more readily from alloy data, discussion of their values calculated by Sholl will be deferred until section 5.4.4.b.

c) Indium. Isotopic separation of the relaxation rates has not been possible since the abundance of one of the two available isotopes, ^{113}In, is only 4%. The data show near linear dependence over a wide range of temperature implying that quadrupolar relaxation if present is small. Warren and Clark (1969) give the Korringa product as 5.1×10^{-6} s K over the range 430 K to 1200 K. Sholl (1967) has calculated the quadrupolar relaxation rate at 570 K and finds $(R_1)_Q = 1.05 \times 10^3 s^{-1}$, but there is no obvious sign of deviation from the Korringa product value so the quadrupolar rate must be within the experimental error, here $\pm 0.25 \times 10^3 s^{-1}$. Here the theoretical estimate is at least a factor of four too large. Rossini and Knight (1970) report $R_1 = 5.6 \times 10^3 s^{-1}$ in pure In at 403 K, where the liquid has been supercooled by some 26 K. Using the Korringa product from above to calculate the magnetic relaxation rate it is found that $(R_1)_Q = 0.6 \times 10^3 s^{-1}$.

The principal temperature dependence in the quadrupolar relaxation rate comes from the self-diffusion coefficient; using the reported self-diffusion temperature coefficient (Careri et al, 1958) the ^{115}In rate is estimated at 373 K to be $(R_1)_Q = 0.72 \times 10^3 s^{-1}$. Bonera et al (1969) have estimated this rate to be $1.6 \times 10^3 s^{-1}$ but in their estimate the observed resonance shift was used to calculate the Korringa product, along with the factor $K(\alpha) = 0.75$ to allow for electron-electron interaction, and no account was taken of possible core polarisation or orbital contributions to the resonance shift. The value used here for $(R_1)_{magnetic}$ is calculated from the experimentally derived Korringa product and so should be more reliable.

Rossini and Knight (1970) have made estimates of the quadrupolar relaxation rates in several liquid metals using approximations to evaluate

the terms in the Sholl expression. To obtain $(1 - \gamma_\infty)$ for a screened ion they increase the ionic values of Sternheimer (1966) by a factor of three, the integral I_1 is estimated from the value calculated by Sholl for In by comparison of radial distribution functions for the different elements; and the integral I_2 is neglected completely. Using the temperature dependence of the self diffusion coefficient to give the temperature dependence of the relaxation they estimate $(R_1)_Q = 3.2 \times 10^3 s^{-1}$ at 415 K, clearly a considerable overestimate. The relative magnitudes of I_1 and I_2 calculated by Sholl for In will be compared to those deduced from experimental data in section 5.4.4.c.

d) Antimony. From five observations in the temperature range 900 K to 1200 K isotopic separation of the relaxation rates (Warren and Clark, 1969; table 4.2) yields a mean value for the ^{121}Sb Korringa product of 6.6×10^{-6} s K. The quadrupolar relaxation rate decreases from $3.5 \times 10^3 s^{-1}$ to $2.5 \times 10^3 s^{-1}$ as the temperature increases from 900 to 1200 K, so that this process appears to be at least an order of magnitude more effective than in the metals previously discussed.

Rossini and Knight (1970) have estimated I_1 and $F(Q,T,I_1)$ for ^{121}Sb (see equation 5.22) from the calculations of Sholl for ^{115}In as mentioned in section 5.4.2.c. They find that assuming $I_2 = 0$ their estimated values give good agreement with the experimentally determined rate in pure Sb. Since a value of I_2 near to $-I_1$ is required to predict the observed concentration dependence which in turn requires a considerably larger $F(Q,T,I_1)$ to fit the experimental rates it is likely that the value of Rossini and Knight must be underestimated about twenty times.

e) Bismuth. There is only one isotope, ^{209}Bi. Linewidth data (Heighway and Seymour, 1971) and relaxation rate data (Rossini and Knight, 1970; table 4.3) show linear dependences on temperature above 750 K. The limiting gradients agree to within the experimental error, but the linewidths give rather larger R_1 values (see section 5.4.2) and

since there may be some field inhomogeneity contribution to the line-width, the relaxation rate data have been used in preference. The line chosen by Rossini and Knight to fit the data appears to be an upper limit; a choice of $T/R_1 = 37.6 \times 10^{-3}$ s K will therefore be taken as the best fit, which leads to a Korringa product of 6.95×10^{-6} s K.

Below 700 K the observed relaxation rate deviates from the predicted magnetic relaxation rate and an extra, quadrupolar, rate appears and increases as the temperature is decreased into the supercooled region, reaching a magnitude of order $1 \times 10^3 s^{-1}$ at 500 K. The only available estimate of this rate (Rossini and Knight, 1970) gives $(R_1)_Q = 0.9 \times 10^3 s^{-1}$ at 500 K so again there appears to be reasonable agreement, but as previously they have neglected I_2. If an appropriate value is taken for I_2, see section 5.4.4.g this calculation will yield a value for $(R_1)_Q$ which is some twenty times smaller than the experimentally determined rate.

5.4.3 Liquid binary alloys It is clear from the results described above for pure liquid metals that quadrupolar relaxation of the nuclear spins is occuring, and that it appears to be more effective at lower temperatures. However the magnitude of $(R_1)_Q$ is often near, or less than the experimental uncertainty, and so it is difficult to draw quantitative conclusions.

It has been found that alloying can increase the quadrupolar relaxation process by an order of magnitude or more and the new work described in this chapter consists mainly in observing the effects of alloying on the relaxation rate to attempt to get a better understanding of the quadrupolar relaxation process, and perhaps also of the motions of atoms in alloys.

a) Composition dependence. To determine the behaviour of the $(R_1)_Q$ as a function of composition the magnetic relaxation rate is

calculated from the resonance shift using the Korringa product and subtracted from the observed rate. However two possibilities exist, either the Korringa product remains independent of composition, or else it varies with composition due to changes in $K(\alpha)$ caused by alterations in the electron-atom ratio; or in the core polarisation contribution, S_{cp}, to the observed resonance shift. To consider these possibilities the behaviour of the Korringa product as a function of composition must be examined for nuclei where electric quadrupolar relaxation is impossible, i.e. nuclei of spin one half; or where such relaxation is likely to be small.

Considering cases of nuclei of spin one half, the Korringa product for the ^{207}Pb nucleus increases by about 23% on adding 80 at. % Bi, and that for the ^{205}Tl nucleus increases by about 60% on adding 64 at. % In. Both these results come from linewidth measurements with rather large uncertainties so the size of the increase must have considerable uncertainty.

Although the ^{115}In nucleus has a quadrupole moment, the near linear variation of its relaxation rate with composition in several systems implies that electric quadrupolar relaxation in these systems is small. This must be due in part to the high temperatures at which the measurements were made; further reasons will be discussed later. Relaxation rate measurements show that the ^{115}In Korringa product decrease by about 16% on adding 80 at. % Sb (at 900 K) whereas it decreases by only about 10% on adding 80 at. % Bi (at 610 K). Linewidth measurements show that the ^{115}In Korringa product decreases by 31% on adding 80 at % Pb (at 700 K) and decreases by 15% on adding 80 at. % Cd (573 K).

Linewidth measurements have been made on ^{115}In in Ag-In but no isothermal data are available. A decrease in the Korringa product with decreasing temperature is observed in several alloys in the middle of the composition range, indicating the appearance of an additional relaxation mechanism at temperatures below 700 K, presumably quadrupolar

relaxation. If it is assumed that this extra relaxation is small near the ends of the concentration range it is estimated that the addition of 80 at. % Ag reduces the Korringa product by about 30%. Due to the possibility of quadrupolar relaxation still being present this figure must be an upper estimate.

An examination of the ^{115}In and ^{205}Tl linewidths and shifts in In-Tl should indicate whether the Korringa product changes have a common origin. The ^{115}In Korringa product decreases by about 20% on adding 74 at. % Tl, whereas if it changes in the same way as the ^{205}Tl product described above it should decrease by about 30%. The uncertainties in the observations are too large to draw a firm conclusion but the fact that they both change in the same direction implies that there might be a common origin, and since they have the same valency this cannot arise from a change in the electron-atom ratio.

Only in the case of In is there sufficient data to examine the effect of different elements on its Korringa product. The results are summarised by displaying a section of the periodic table, and displaying below each element the percentage change in the ^{115}In Korringa product caused by adding 80 at. % of that element in In.

Table 5.2

Changes in the ^{115}In Korringa product

I a	II a	III a	IV a	V a
Ag - 30%	Cd - 15%	In	Sn	Sb - 16%
		Tl - 22%	Pb - 31%	Bi - 10%

The changes are apparently not related to the valence difference and so it is unlikely that changes in electron-electron interaction due

simply to changes in electron density are sufficiently large to be observable in comparison to uncertainties in the data or to the effect of other factors which are causing the changes. It is concluded that the changes observed must arise from changes in the core polarisation or orbital contributions to the measured resonance shift.

It will therefore be essential to consider two possible variations in the magnetic relaxation rate with composition, one where the Korringa product is considered to be constant, the other where it varies in a similar fashion for each constituent of an alloy system; the above results do not enable a conclusion to be drawn as to which is the better course of action.

b) Temperature dependence. It is assumed that the Korringa product will remain constant, independent of temperature, and any small changes due to volume changes, being inside the experimental error, will be ignored.

5.4.4 Composition dependence of $(R_1)_Q$ The data will be analysed by comparing the predictions of the Sholl theory, together with the calculations for Ga and In (Sholl, 1967) to the experimental results. Some adjustments have to be made to obtain reasonable agreement and these together with the values required to fit the theory to the experimental results for Sb and Bi, where no calculations have been made, will be discussed.

As a first step the three simplifying assumptions described above (section 5.3.3) will be made and the relaxation rate will be taken as given in equation 5.20. This is now re-expressed

$$(R_1)_Q = F(Q,T,I_1) \left\{ C + \alpha^2(1 - C) + \left[C + \alpha (1 - C)\right]^2 I_2/I_1 \right\} \quad \ldots\ (5.22)$$

Before proceeding a few remarks will be made concerning the influence of the parameters α and I_2/I_1 on the composition dependence of the

relaxation rate. i) α. When α equals one the relaxation rate is constant, independent of composition. As α increases above 1 the gradient of the curve from C = 1 is positive and increases as α increases; as α decreases below 1 the gradient of the curve from C = 0 is positive, increasing as α decreases although much less rapidly than when α is greater than one. Below around α = 0.05 it has little influence on the predicted rate.

ii) I_2/I_1. If I_2 is less than about half I_1 the variation is near linear with composition, $(R_1)_Q$ arising mainly from the I_1 term; it is only as I_2 approaches $-I_1$ that any curvature appears. The composition dependence gets progressively more curved with a peak in the middle of the range as I_2/I_1 tends to - 1. This is in agreement with the general form of the experimentally determined composition dependence. If I_2 approaches $+I_1$ a pronounced dip in the middle of the composition range will occur, but there has been no experimental evidence of this form of composition dependence. Since $(R_1)_Q$ in the pure metal is given simply by $F(Q,T,I_1)\{I_1 + I_2\}$ it is clear that I_2 cannot exceed $-I_1$ without predicting a nagative relaxation rate.

iii) The combination of the two effects gives, for I_2/I_1 near - 1, and α greater than 1, a curve which peaks at C < 0.5, the magnitude of this peak increasing as α increases. The rate at low C does not drop below the rate at C = 1.

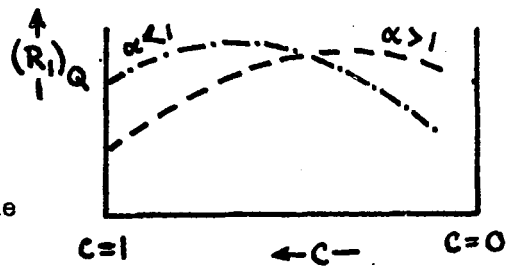

If I_2/I_1 is near -1 and α<1 the curve peaks at C > 0.5, and the magnitude of the peak increases as α decreases. The rate at low C does not rise above the rate at C = 1.

a) <u>Aluminium in Al-Si</u>. An attempt has been made to see whether by alloying ^{27}Al quadrupolar relaxation could be made large enough to be observable. Although as will be demonstrated in the following

sections quadrupolar relaxation is expected to be greatest in alloys of around C = 0.5, $Al_{89}Si_{11}$ was selected since in the solid this is an eutectic composition, and is well known to show considerable supercooling. Quadrupolar relaxation is observable at temperatures near the solidus, being most marked in the supercooled liquid, and it has been possible to supercool this alloy by 70 K below its melting point. However as can be seen from table 4.10 no appreciable deviation from T/R_1 = constant was found even at the lowest temperatures, indicating that the relaxation was principally magnetic in origin. This is not surprising since both anti-shielding factors and quadrupole moments, see equation 5.19, are small in light elements.

The observations give $T/R_1 = (1.8 \pm 0.1)$ K s which when compared to that for pure Al (Spokas and Slichter, 1959) of $T/R_1 = (1.85 \pm 0.05)$ K s indicates that the contact interaction in Al changes little on alloying with Si.

b) Gallium in Ga-In. The composition dependence of the ^{69}Ga relaxation rate at 373 K shows a small peak in the middle of the range, see figure 5.1.a. Since the ^{115}In relaxation rate shows a marked peak, see figure 5.2, it is not possible to deduce how the Korringa product changes with composition and so it is taken that the product remains constant. When the magnetic part has been subtracted off, the quadrupolar rate is seen to peak at around 55 at. % Ga, and the values at low C do not fall below that at C = 1; the general form suggests $\alpha > 1$ and I_2/I_1 close to - 1.

Sholl (1967) has calculated values for I_1 and I_2 for ^{69}Ga in pure Gallium at 300 K, but finds that I_2/I_1 is about - 0.7, which would give near linear variation of relaxation rate with composition. To get any agreement with the observed curvature a value of I_2/I_1 of about - 0.95 must be taken. This would require the size of $F(Q,T,I_1)$ (see equation 5.22) calculated by Sholl to be increased by a factor of five to allow

figure 5.1.a

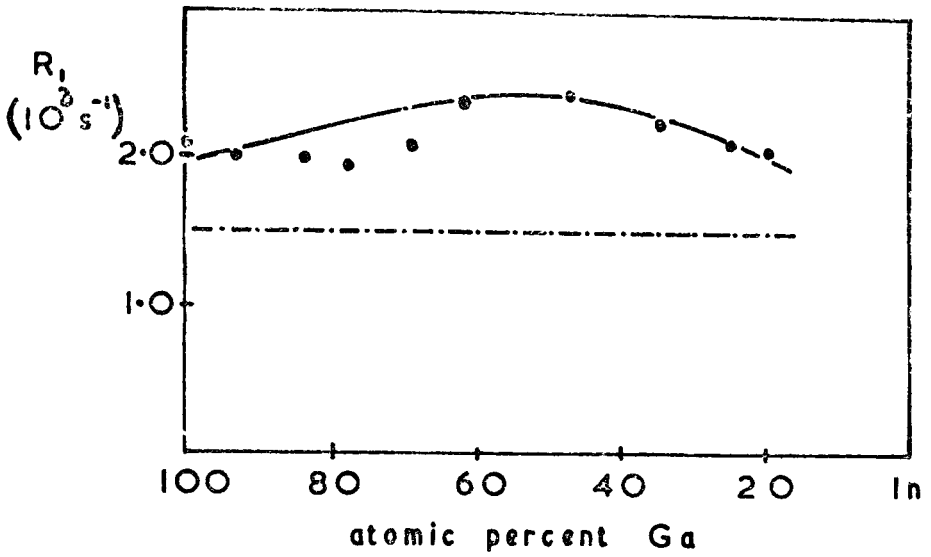

^{69}Ga R_1 IN Ga–In AT 373 K

calculated magnetic relaxation rate ——·——

figure 5.1.b

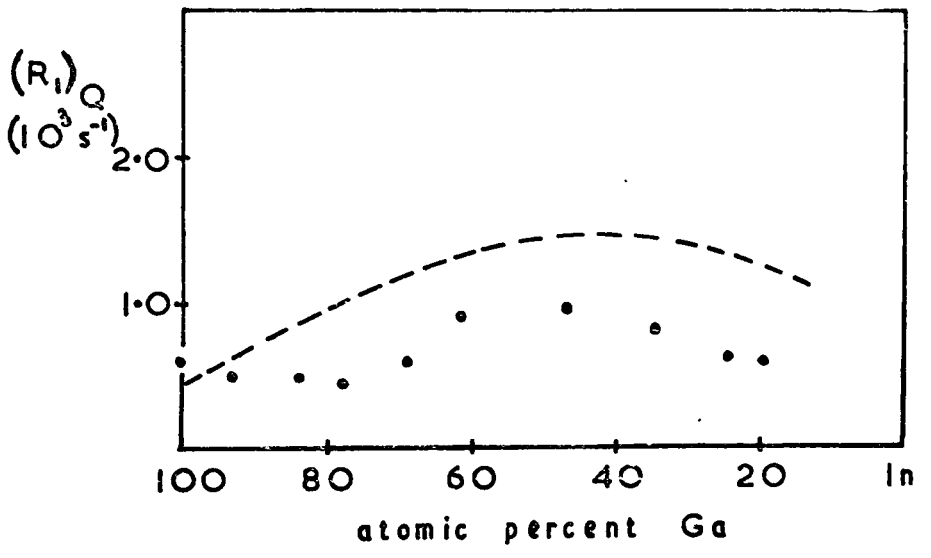

^{69}Ga $(R_1)_Q$ IN Ga–In AT 373 K

Sholl theory prediction – – – – –

for the change in $I_1 + I_2$; hence because of the factor of four described in section 5.4.2.b the new expression must be multiplied by about twenty to obtain agreement with experimental observations in pure Ga. The quadrupolar relaxation increases by a factor of two or three on going from pure Ga to around 50 at. % Ga and this implies that α is near 1, and no more than 1.7.

Comparison of the observed ^{69}Ga relaxation rate in pure Gallium at 373 K $(1.8 \pm 0.1)\ 10^3 s^{-1}$ (Cornell, 1967) and $(2.1 \pm 0.2)\ 10^3 s^{-1}$ (Bonera, Borsa and Rigamonti, 1969) indicates that the uncertainties in these measurements are, if anything, underestimated. Since the quadrupolar relaxation rate is small throughout the composition range the experimental uncertainties are of order $\pm$ 30%, and together with the uncertainity in the magnetic relaxation rate indicates that no further conclusions can be drawn from these data. The theoretical prediction from the simplified Sholl alloy relaxation rate using $\alpha = 1.7$, $I_2/I_1 = -0.95$ and $F(Q,T,I_1) = 20 \times F(Q,T,I_1)_{\text{Sholl calc.}}$ is shown in figure 5.1.b.

c) Indium in Ga-In. Here the ^{115}In nuclear spin relaxation rate shows a marked peak in the composition dependence at 373 K, see figure 5.2, due to the presence of quadrupolar relaxation. No deductions about the possible composition dependence of the Korringa products can be made so it is assumed that the ^{115}In product remains constant. Since at 7 at. % In the calculated magnetic relaxation rate agrees closely with the observed rate it is possible to claim that the Korringa product cannot decrease with decreasing In content because this would lead to a calculated relaxation rate which would be greater than the observed rate.

When the magnetic relaxation rate has been subtracted off the quadrupolar relaxation is a curve which peaks at around $C = 0.65$ and decreases to small values at $C < 0.2$. This is the general form for $\alpha < 1$ and I_2/I_1 near to -1. The temperature of observation, 373 K, is too far below the melting point of pure In to enable the resonance to be observed

figure 5.2

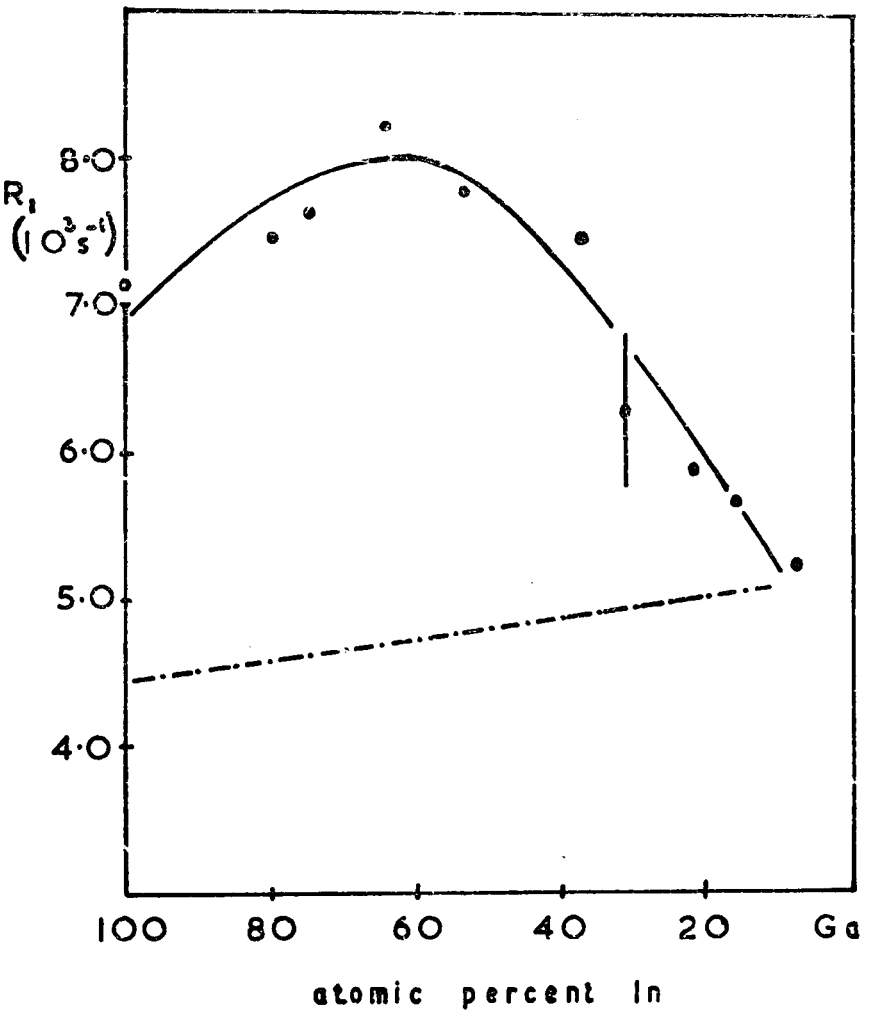

^{115}In R_1 IN Ga–In AT 373 K

calculated magnetic relaxation rate.....

Erratum The point at 100 % In in the above diagram is wrongly plotted. The correct value is $R_1 = 5.2 \times 10^3 s^{-1}$.

in the pure metal, so that the rate must be extrapolated in temperature, see section 5.4.2.c.

Sholl (1967) has also calculated I_1 and I_2 for pure In at 573 K, and finds that I_2/I_1 is about - 0.46; using any likely value of α with these values for I_1 and I_2 an almost linear decrease in quadrupolar relaxation with decreasing In concentration is predicted. Since I_2 is a much more difficult integral to evaluate it is more likely to be incorrect; if it is nearly doubled to make $I_2/I_1 = -0.89$, then with the original value of $F(Q,T,I_1)$ calculated by Sholl the quadrupolar relaxation rate for pure In becomes $0.7 \times 10^{+3} s^{-1}$ at 373 K. Table 5.3 shows some calculated values for quadrupolar relaxation at different compositions using different choices of α along with the above values for I_1, I_2 and $F(Q,T,I_1)$.

Table 5.3

Predicted ^{115}In quadrupolar relaxation rates (in $10^3 s^{-1}$)

C \ α	0.02	0.1	0.2	0.316	0.5	Experimental
1.0	0.7	0.7	0.7	0.7	0.7	0.7
0.8	1.6	1.3	1.1	1.0	0.8	2.8
0.6	1.9	1.5	1.3	1.1	0.8	3.5 ± 0.5
0.3	1.5	1.2	1.0	0.8	0.6	1.3

Below $\alpha = 0.02$ the rates change little with α, and from the above table it is clear that the curvature is insufficient to fit the data. It is therefore necessary to modify the value of I_2 further to make it nearer to $-I_1$ and so to increase the curvature. This will decrease the overall magnitude of the predicted rates and so it is necessary to increase the value of $F(Q,T,I_1)$. The Sholl alloy expression (equation 5.22) has been evaluated for each of several values of α using a series of values of I_2/I_1. The factor $F(Q,T,I_1)$ has been chosen for each curve to make the

predicted rate at C = 1 become 0.7 x $10^3 s^{-1}$. The predicted curves are then compared to the data and a best fit for each α value selected. For $\alpha > 0.5$ the predicted curve is clearly too flat, below $\alpha = 0.1$ the values seem physically unlikely. Three α values 0.2, 0.31 and 0.5 along with $I_2/I_1 = -0.97$ and $F(Q,T,I_1) = 24 \times 10^3 s^{-1}$ all give reasonable fits, see figure 5.3, and of these $\alpha = 0.3$ appears the best. While none of these curves fit the data well at low values of c the data are least reliable there, and since, if the Korringa product does change with composition it has been shown above that this can only lead to an increase in the estimate of the quadrupolar relaxation at low c, this does not appear to be a serious discrepancy.

If the value of $F(Q,T,I_1)$ calculated by Sholl is extrapolated to 373 K it is found to be about four times smaller than that required to fit the values for I_1 and I_2 chosen there to the experimental results.

d) Indium in Bi-In. The quadrupolar relaxation rate in In is given above by $(0.6 \pm 0.2) \times 10^3 s^{-1}$ at 400 K, the ^{115}In quadrupolar rate in $Bi_{50}In_{50}$ is $(2.7 \pm 0.3) \times 10^3 s^{-1}$. From the ratio of these values, and using the value of I_2/I_1 derived in section 5.4.4.c, it is possible to evaluate α. It is however possible to fit two values of α, one greater than one, the other less than one. The only means of distinguishing them is their composition dependence, and this is unknown at present since most of the quadrupolar rates are within current experimental uncertainties at the temperature of observation of the data, 580 K. It is only possible to state that either $\alpha = 0.3 \pm 0.15$ or else $\alpha = 1.5 \pm 0.15$. $\alpha = 0.3$ is chosen since for Bi in Bi-In has already been evaluated at $\alpha > 1$.

e) Antimony in In-Sb. The experimental data show clearly the presence of quadrupolar relaxation, see figure 5.4. The ^{115}In relaxation rate data are almost linear, see figure 5.6.a, and because the temperature of observation is high (900 K) it is reasonable to assume that

figure 5.3

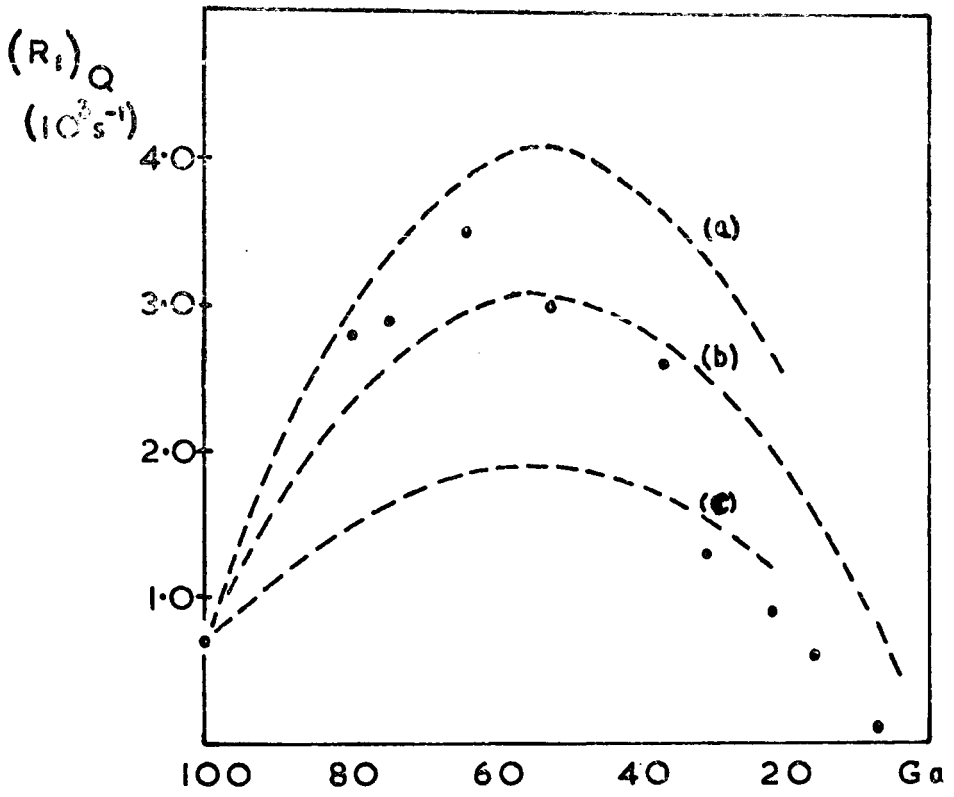

^{115}In $(R_1)_Q$ IN Ga–In AT 373 K

Sholl theory predictions ----

(a) $\alpha = 0{\cdot}2$ (b) $\alpha = 0{\cdot}3$ (c) $\alpha = 0{\cdot}5$

figure 5.4

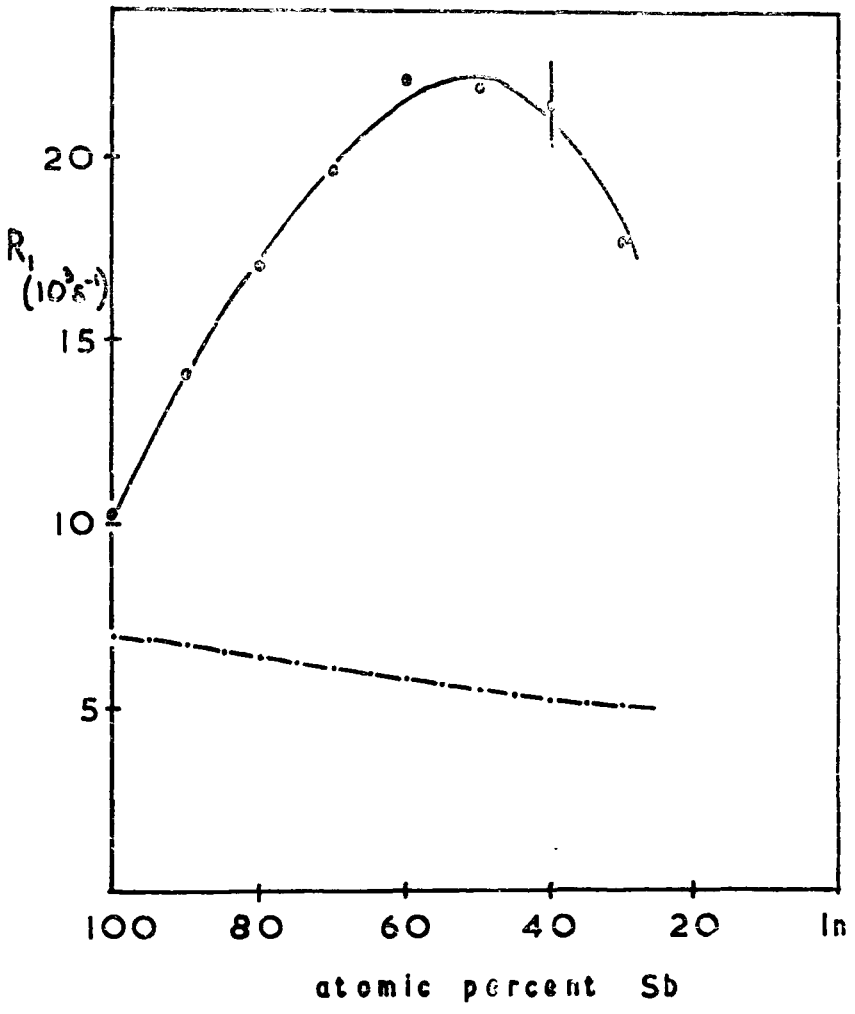

^{121}Sb R_1 IN In – Sb AT 900 K

calculated magnetic relaxation rate ——·——·——

quadrupolar relaxation has become negligibly small compared to the magnetic relaxation. The ^{115}In Korringa product decreases by about 20% as the In content decreases to zero, so if the ^{121}Sb product behaves similarly it should increase by around 25% as the Sb content decreases from 100% to zero. This leads to an estimate of the ^{121}Sb magnetic relaxation rate in $In_{50}Sb_{50}$ of $(R_1)_M = (5.3 \pm 1.3) \times 10^3 s^{-1}$; isotopic separation by Warren and Clark (1969) in $In_{50}Sb_{50}$ yields for ^{121}Sb $(R_1)_M = (7.8 \pm 3.0) \times 10^3 s^{-1}$ at 900 K. To predict the value given by Warren and Clark the ^{121}Sb Korringa product will have to decrease by 25% on going from 100 to 50 at. %, and not increase as suggested above; however this is considerably larger than any of the changes of the ^{115}In Korringa product on alloying as discussed earlier, and would therefore appear that $(R_1)_M$ obtained by isotopic separation is overestimated. Since the uncertainties in the two $(R_1)_M$ values overlap no firm conclusion can be drawn as to whether the two Korringa products have a common behaviour.

The assumptions that the ^{121}Sb Korringa product varies similarly to that of In, or that it remains constant, give two sets of quadrupolar relaxation rate data which are only six percent different at most. Since this is within the experimental uncertainty the data will be taken as the average of the two Korringa predictions. The general form of the quadrupolar relaxation rates indicates that $\alpha > 1$, and so for a number of different values of α the predicted composition dependences have been evaluated using several values of I_2/I_1 near to - 1. The value of $F(Q,T,I_1)$ has been chosen to normalise each curve to the data at C = 1; the best fits for those curves which fit the data are shown in figure 5.5. Of these the curve for $\alpha = 1.7$ and $I_2/I_1 = -0.96$ appears to give the best fit, requiring $F(Q,T,I_1)$ $8 \times 10^4 s^{-1}$ to fit the data.

f) Antimony in Bi-Sb. The ^{121}Sb quadrupolar relaxation rate at 920 K in $Bi_{50}Sb_{50}$ is estimated to be $(3.2 \pm 0.6) \times 10^3 s^{-1}$, see table 4.9. This is similar to the rate in pure Sb at this temperature

Figure 5.5

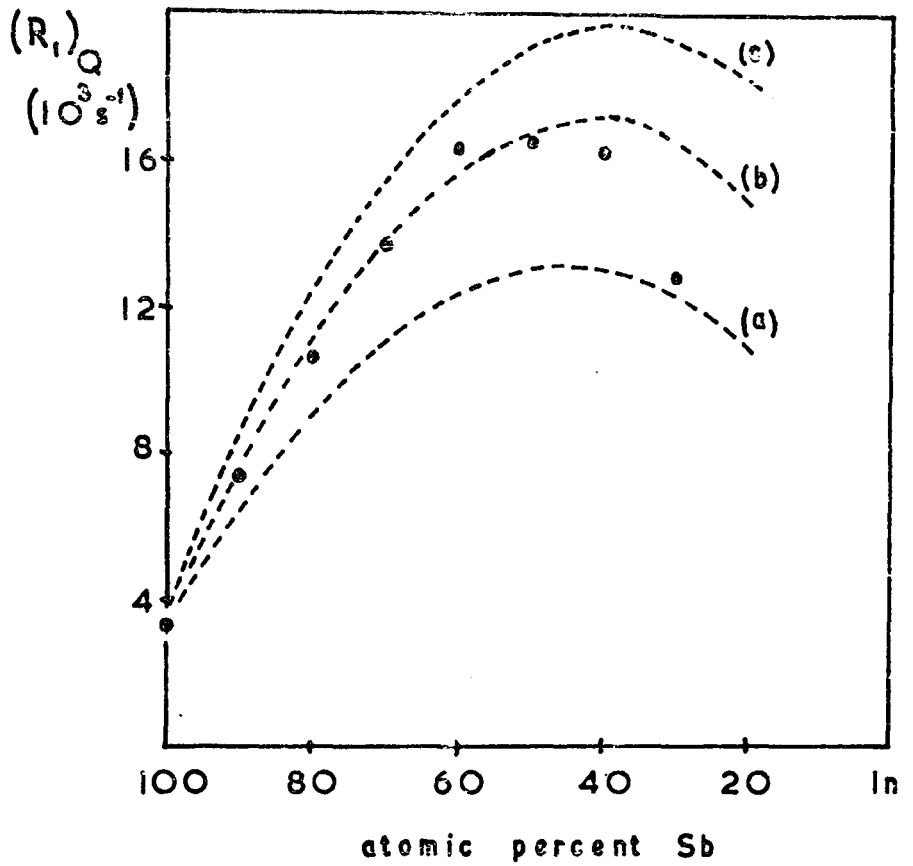

^{121}Sb $(R_1)_Q$ IN In–Sb AT 900K

Sholl theory predictions ------

(a) $\alpha = 1{\cdot}4$ (b) $\alpha = 1{\cdot}7$ (c) $\alpha = 2{\cdot}0$

Figure 5.6.a

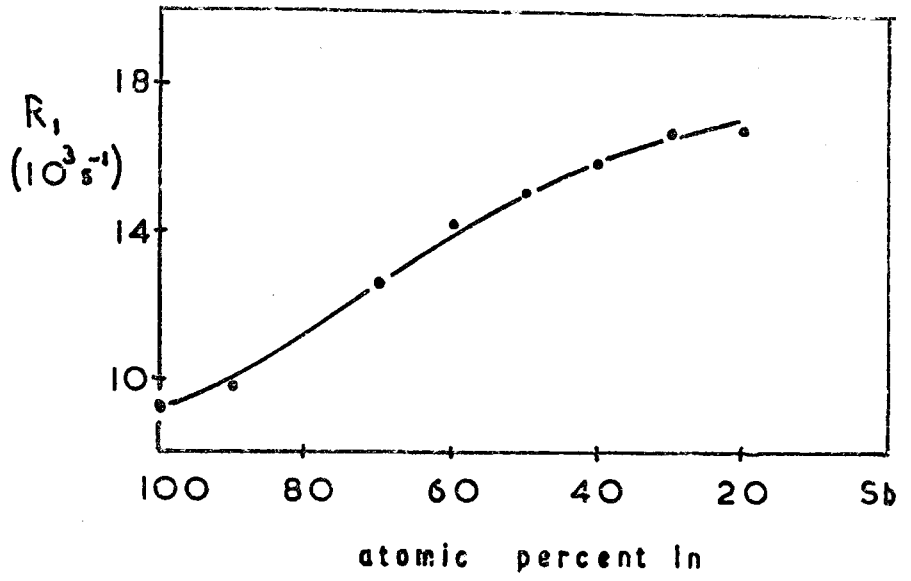

^{115}In R_1 IN In–Sb AT 900 K

figure 5.6.b

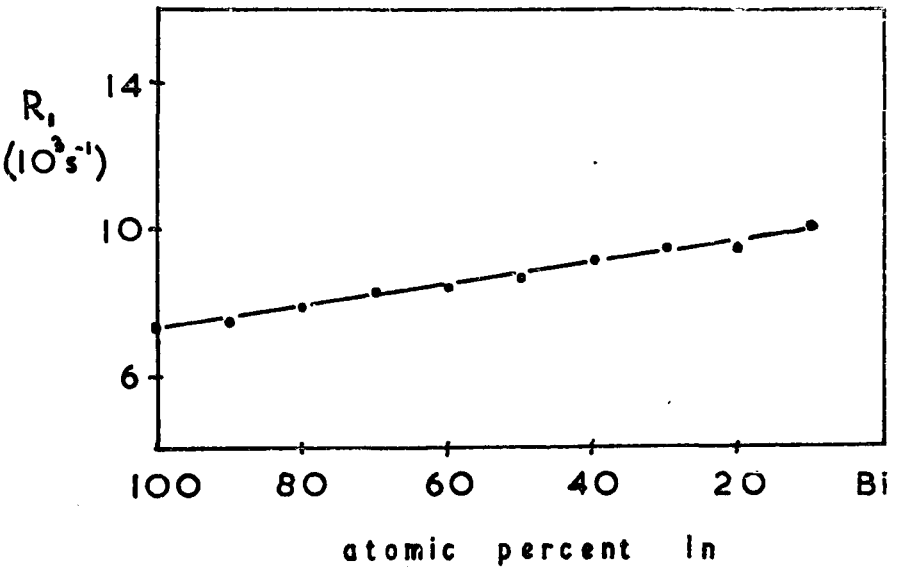

^{115}In R_1 IN Bi–In AT 615 K

$(3.3 \pm 1.0) \times 10^3 s^{-1}$, and using the values of $F(Q,T,I_1)$ and I_2/I_1 derived for Sb above it is probable that α is less than one. $\alpha = 0.65$ predicts that the rate at $C = 0.5$ is 1.2 times the rate at $C = 1.0$, whereas $\alpha = 0.5$ makes it 1.9 times the rate at $C = 1.0$. It is concluded that in this system $\alpha = 0.65 \pm 0.15$.

g) Bismuth in Bi-In. The ^{209}Bi nuclear spin relaxation rate also shows the presence of quadrupolar relaxation, see figure 5.7, and again the ^{115}In relaxation rate at the temperature of observation (610 K) shows little evidence of any quadrupolar relaxation, see figure 5.6.b. The two sets of quadrupolar relaxation rate data derived on the two assumptions for the behaviour of the Korringa product are clearly different, and will be dealt with as separate cases. Since again there are no calculated values with which to make a comparison a selection of possible α and I_2/I_1 values have been tried, each predicted curve being normalised by adjustment of $F(Q,T,I_1)$. Since the quadrupolar rate for pure Bi is small and not accurately known the curves have been normalised to the value at $C = 0.5$; $7.5 \times 10^3 s^{-1}$.

i) Korringa product independent of concentration. The predicted curves for $I_2/I_1 = -0.96$ and $\alpha = 2$, 2.5 and 3 all fit the data within the experimental error, but $\alpha = 2.5$ gives the best fit, see figure 5.8. This requires $F(Q,T,I_1) = 11 \times 10^3 s^{-1}$.

ii) Korringa product varying similarly to that of In. The experimental curve is slightly more peaked than in case i). The best fit now appears to be between $\alpha = 2.5$ and $\alpha = 3$. The slightly larger value of α increases the predicted rate to match the experimental curve without increases of $F(Q,T,I_1)$ or of I_2/I_1.

Rossini and Knight (1970) have also estimated $F(Q,T,I_1)$ for pure Bi; again they appear to have underestimated by some twenty times.

h) Bismuth in Bi-Pb. The data here again show the presence of quadrupolar relaxation, see figure 5.9, and so should provide a test

figure 5.7

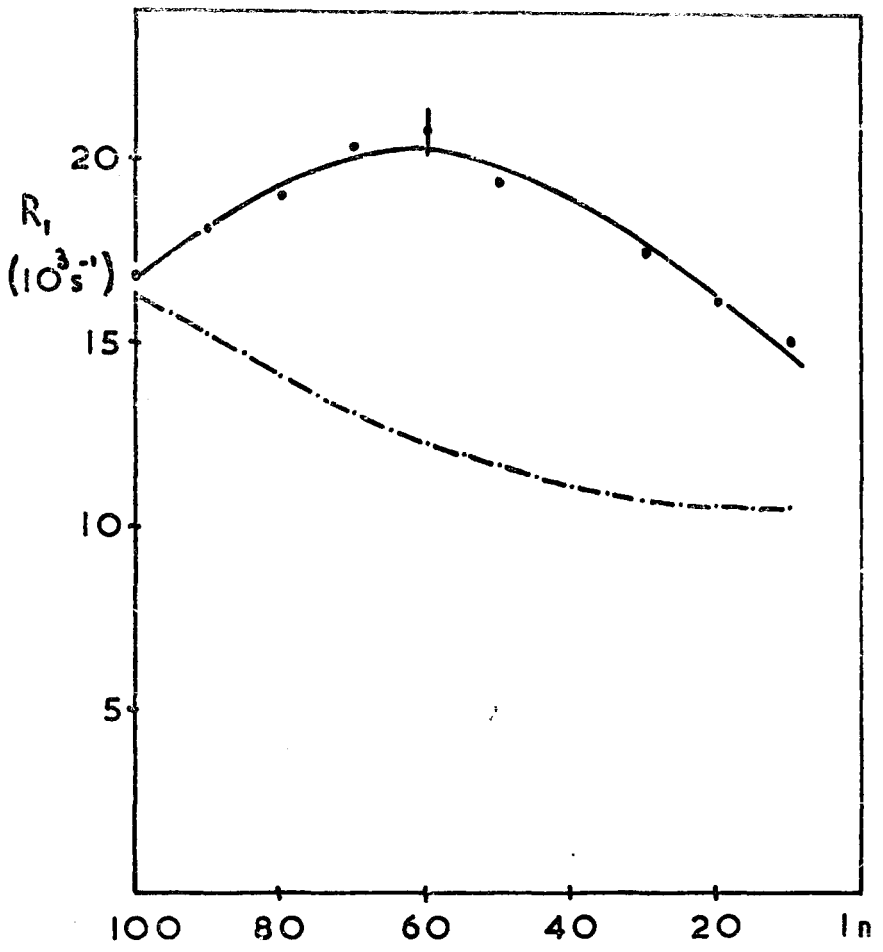

^{209}Bi R_1 IN Bi–In AT 615 K

calculated magnetic relaxation rate–·–·–·–

(Korringa product constant)

figure 5.8

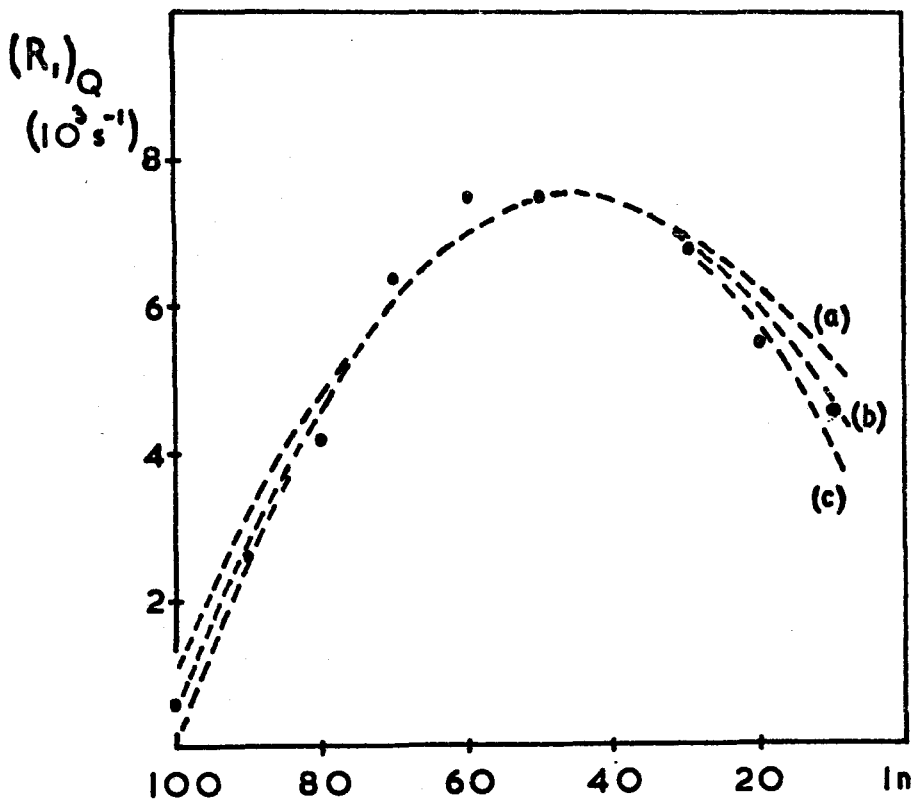

^{209}Bi $(R_1)_Q$ IN Bi–In AT 615 K

Sholl theory predictions -------

(a) $\alpha = 2{\cdot}0$ (b) $\alpha = 2{\cdot}5$ (c) $\alpha = 3{\cdot}0$

figure 5.9

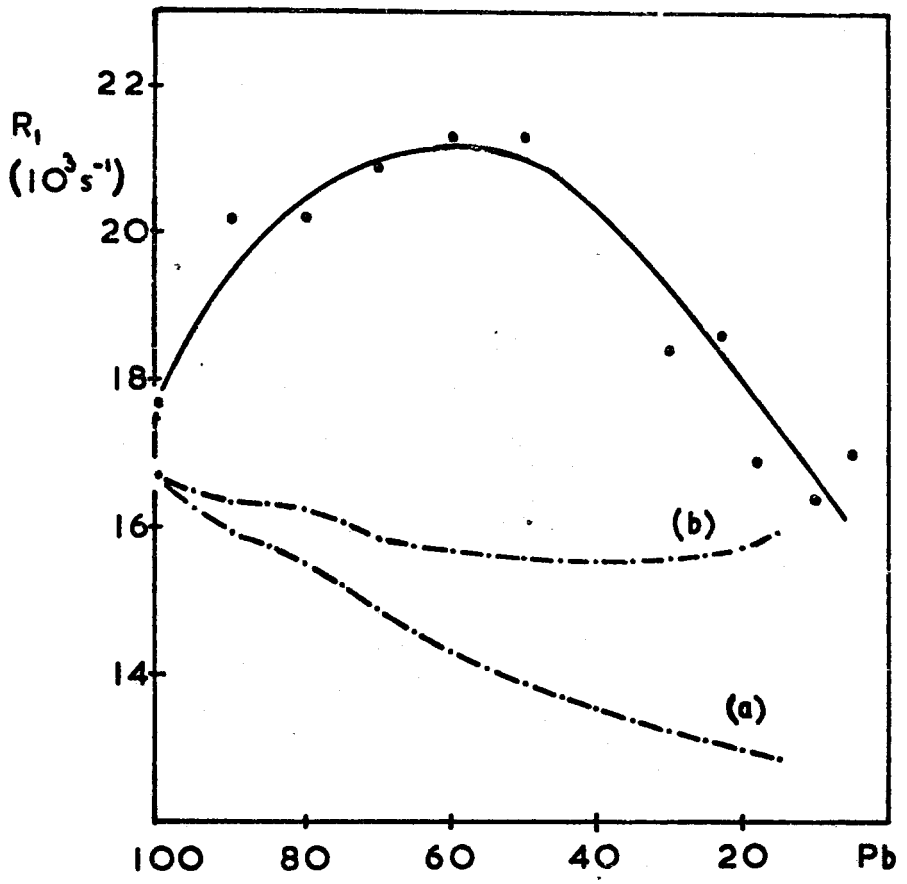

^{209}Bi R_1 IN Bi–Pb AT 625 K

calculated magnetic relaxation rate —·—·—·—

(a) Korringa product constant

(b) Korringa product varying similarly to that of Pb

for the Sholl theory, and the simplifying approximations, since the values of I_1, I_2 and $F(Q,T,I_1)$ deduced for ^{209}Bi above should carry over into this system with only α altering in value. The temperature of observation, 625 K, is comparable with that in the previous section and so the magnitude of $F(Q,T,I_1)$ should remain unchanged.

The ^{207}Pb nucleus has no quadrupole moment and so the behaviour of its Korringa product may be determined unambiguously; it is found to increase by about 30% across the composition range C = 1 to C = 0. The uncertainties are larger here than in most other cases since the ^{207}Pb nuclear resonance is particularly weak. The two sets of data derived on the assumptions that the Korringa product remains constant, or that it changes similarly to that of the ^{207}Pb nucleus are widely different in character. In the first case the form of the composition dependence is similar to the previous section with $\alpha > 1$, but the second case has the form of $\alpha < 1$.

i) Korringa product constant. Here using the values for the values for I_1, I_2 and $F(Q,T,I_1)$ from above the best fit is for α between 2 and 2.5, but these do not fit the experimental data at low C, being rather too large. If I_2/I_1 is increased within the limit of uncertainty, to - 0.97 this increases the curvature, and improves the fit at low values of C; but requires an increase in α to compensate. It is deduced that $\alpha = 2.5 \pm 0.5$ with $I_2/I_1 = -0.97$, see figure 5.10.a.

ii) Korringa product varying similarly to that of Pb. The general form here is that of $\alpha < 1$ and several values were tried; although a fit to the region $1 > C > 0.5$ could be found, the curvature could not be made great enough to fit at low C. The magnitude of $F(Q,T,I_1)$ required to normalise the curves at C = 0.5 is roughly twice that used in i) above. Possible fits for $\alpha > 1$ were also tried but again it could not be made to agree at low C, see figure 5.10.b.

i) <u>Bismuth in Bi-Sn.</u> The ^{209}Bi quadrupolar rate has been

figure 5.10.a

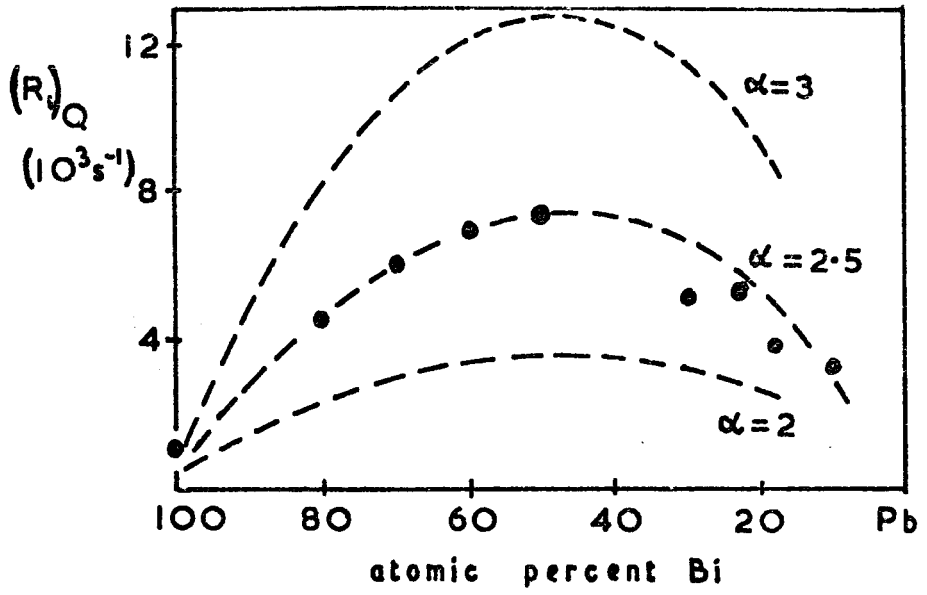

^{209}Bi $(R_1)_Q$ IN Bi–Pb AT 625 K

(Korringa product constant)

Sholl theory predictions ----

figure 5.10.b

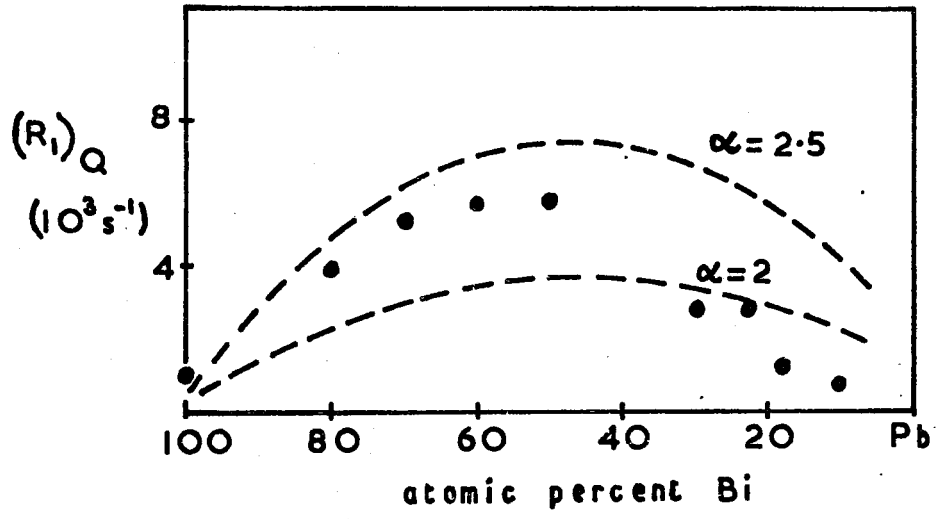

^{209}Bi $(R_1)_Q$ IN Bi–Pb AT 625 K

(Korringa product varying as that of Pb)

Sholl theory predictions -----

measured in $Bi_{50}Sn_{50}$, see figure 5.13.b, and is compared with the quadrupolar rate in pure Bi. From the ratio of these two at 610 K it is estimated that $\alpha = 1.7 \pm 0.3$, although as has been pointed out the value could be less than one, and since no composition dependence is available no definite choice can be made. However since the ^{209}Bi α value is greater than one in Bi-In the same choice is made here.

j) Bismuth in Bi-Sb. The ^{209}Bi quadrupolar rate in $Bi_{50}Sb_{50}$ is shown in figure 5.14.a, and by comparison of this rate with that in pure Bi at 610 K it is estimated that $\alpha = 2.5 \pm 0.4$; choosing $\alpha > 1$ for the same reason as used in section 5.4.4.i.

k) Summary of $(R_1)_Q$ for Bi. ^{209}Bi quadrupolar relaxation rates at 610 K are tabulated for several alloys of C = 0.5, the values being taken from the best fits to the data, and only in the case of $Bi_{50}Sb_{50}$ has it been necessary to extrapolate. The value in pure Bi is also given.

Table 5.4

^{209}Bi $(R_1)_Q$ (in $10^3 s^{-1}$) for $Bi_{50}X_{50}$ at 610 K

In		Sn	Sb
(a)	(b)	(a)	(a)
7.2 ± 0.5	8.2 ± 0.5	3.4 ± 0.6	9.5 ± 1.5
		Pb	Bi
		(a) (b)	
		6.3 ± 0.5 4.9 ± 0.5	0.6 ± 0.3

(a) Korringa product constant (b) Korringa product varying

From this it can be seen that there is little dependence on the difference in valence between the two constituents.

5.4.5 Temperature dependence of $(R_1)_Q$ Quadrupolar

relaxation is found to be greatest at compositions near the middle of the range in the alloy systems discussed, and so as part of this work an investigation of the temperature dependences of the relaxation rate has been made in the 50 at. % alloy of several systems. The upper temperature limit is set by deteriorating signal to noise ratios at around 900 K, and since several of these alloys have relatively high melting points in these cases only a few data have been obtained, with consequent reduction in accuracy.

The temperature dependence of the Sholl formulation (equation 5.22) arises mainly from the self-diffusion coefficient; the radial distribution functions change much less rapidly with temperature. There is still much doubt as to the correct form of the self-diffusion temperature dependence (see for example Nachtrieb, 1967) but it has been common for the results of self-diffusion experiments to be analysed in terms of an Arrhenius behaviour. For this reason the quadrupolar relaxation rates have been analysed here by plotting $\ln(R_1)_Q$ as a function of $(\text{temperature})^{-1}$. The dependence obtained are compared to those obtained from self-diffusion experiments where these are available.

a) Indium in $Bi_{50}In_{50}$. The appropriate Korringa product for ^{115}In in this alloy, which has been evaluated from the limit to which T/R_1 tends to high temperatures, is 4.9×10^{-6} s K. From this the magnetic relaxation rate at each temperature of observation has been calculated and subtracted from the observed relaxation rate. When $\ln(R_1)_Q$ is plotted as a function of $(\text{temperature})^{-1}$, it is just possible within the experimental error to fit a straight line, see the broken line in figure 5.11.

Self-diffusion data are available (Petrescu, 1970) and these show two temperature dependences; above 400 K it is given by $\exp(-1370/T)$; and below 400 K to the melting point (383 K) the self-diffusion coefficient appears to be independent of temperature. Equally it is possible to fit the relaxation rate data to two dependences, $\exp(1400 \pm 300/T)$ above 400 K and $\exp(550 \pm 200/T)$ below 400 K as shown by the full line

figure 5.11

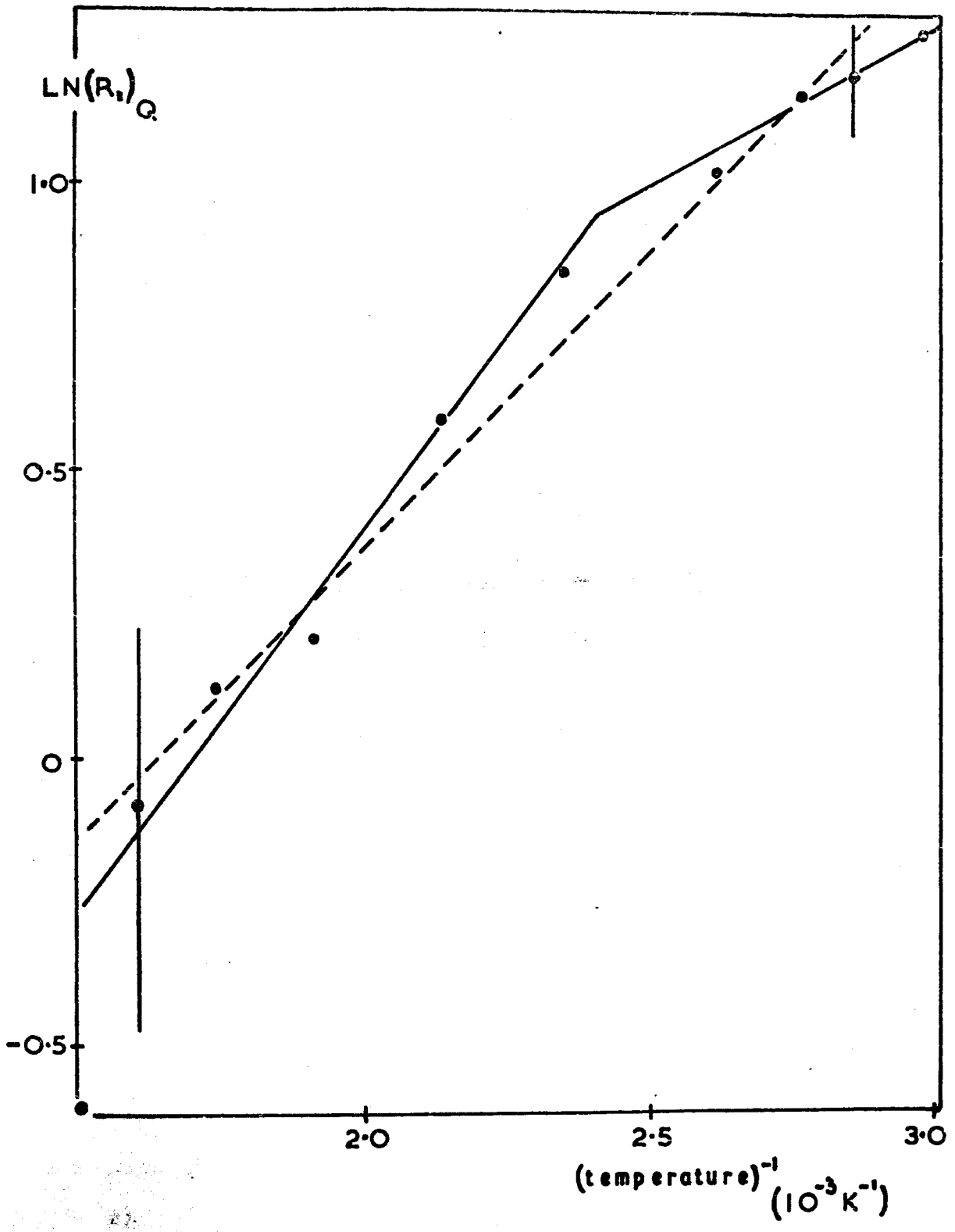

^{115}In $LN(R_1)_Q$ vs $(TEMPERATURE)^{-1}$ IN $Bi_{50}In_{50}$

in figure 5.11. This indicates that the relaxation rate temperature dependence could indeed arise from the reciprocal of the self-diffusion coefficient. It is interesting to note that the ^{115}In self-diffusion coefficient in pure In (Careri et al, 1958) agree in magnitude at 500 K, to within the experimental uncertainties, with the value in $Bi_{50}In_{50}$. Further its temperature coefficient is given by exp(- 1250/T) which shows that neither the self-diffusion coefficient nor its temperature dependence are strongly composition dependent.

b) Antimony i) $Bi_{50}Sb_{50}$. The Korringa product used in this case is that for pure Sb. The data are rather scattered due to poor signal to noise ratios, but yield a temperature dependence of exp(850 $\pm$ 500/T), see figure 5.12.a.

ii) $In_{50}Sb_{50}$. Whether the ^{121}Sb Korringa product remains constant or varies as the ^{115}In product the results are very similar, and give a temperature dependence of the quadrupolar relaxation rate of exp(900 $\pm$ 400/T), see figure 5.12.b. Isotopic separation of these data (Warren and Clark, 1969) gives a ^{121}Sb Korringa product which differs considerably from that used here, although not by more than the experimental uncertainty; nevertheless if this value is used the temperature dependence becomes exp(1200 $\pm$ 400/T). The self-diffusion coefficient temperature dependence has not been measured in pure Sb, but since it has a higher melting point than In it is expected that the temperature dependence will be stronger than in In (Saxton and Sherby, 1962). This tends to favour the latter choice of temperature dependence, which in turn suggests that the ^{121}Sb Korringa product is changing with composition in a manner independent of that of the ^{115}In product.

c) Bismuth i) $Bi_{50}In_{50}$. The two values of the ^{209}Bi Korringa product discussed above both yield linear relationships between $\ln(R_1)_Q$ and $(\text{temperature})^{-1}$. With the Korringa product constant the temperature dependence of the relaxation rate is exp(670 $\pm$ 70/T),

figure 5.12.a

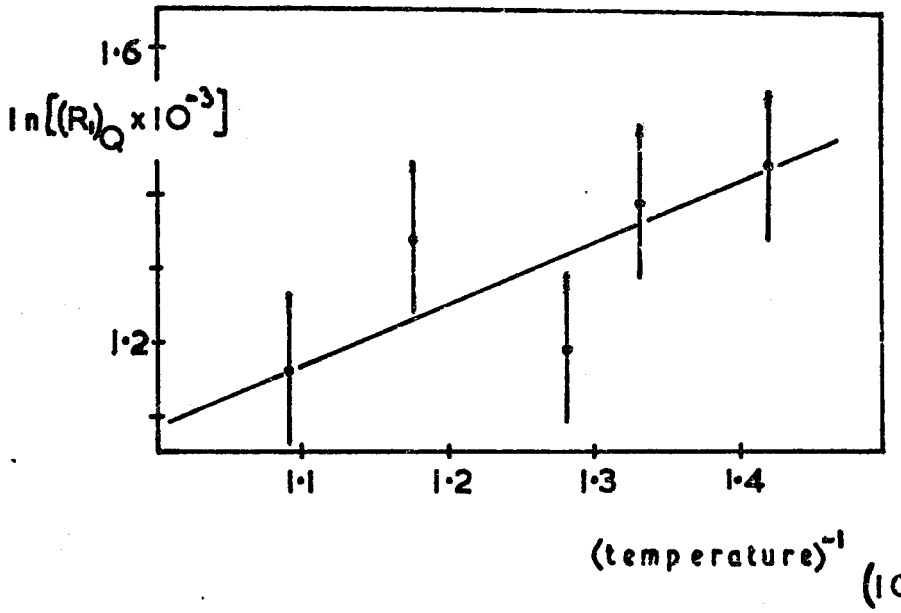

^{121}Sb LN $(R_t)_Q$ vs (TEMPERATURE)$^{-1}$ IN $Bi_{50}Sb_{50}$

figure 5.12.b

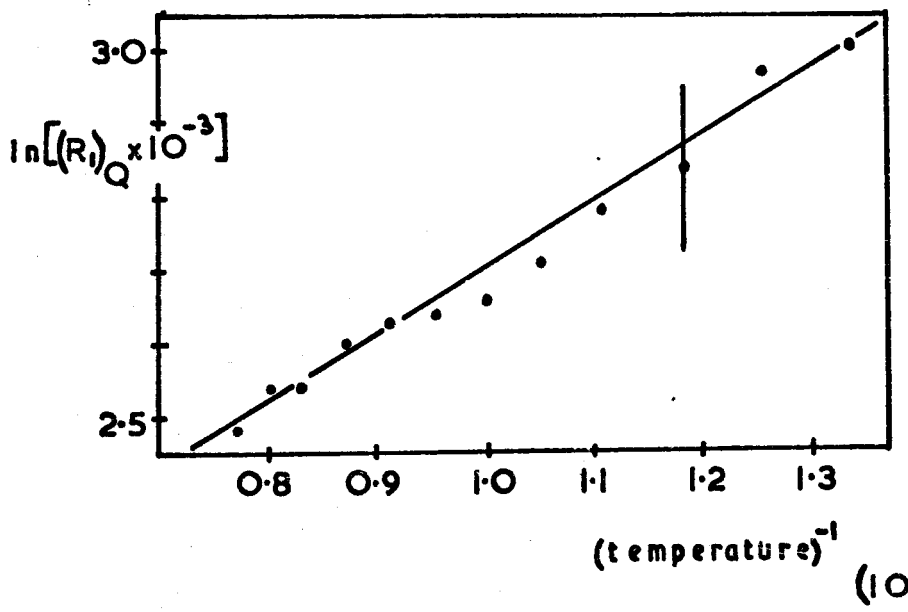

^{121}Sb LN$(R_t)_Q$ vs (TEMPERATURE)$^{-1}$ IN $In_{50}Sb_{50}$

see figure 5.13.a, and with the Korringa product varying it is given by exp(600 ± 60/T). These are to be compared with the temperature dependences of the Bi self-diffusion coefficient in this alloy (Petrescu, 1969a) exp(1500/T) and also with the temperature dependence of the viscosity of the alloy (Petrescu, 1969b) which is given by exp(680/T).

ii) $Bi_{50}Sn_{50}$. There is no information available on the behaviour of the ^{209}Bi Korringa product in this alloy and so it is assumed to be the same as that for pure Bi. The only possible line to fit the data, see figure 5.13.b, gives a temperature dependence of exp(490/T). There are some measurements of the ^{209}Bi self-diffusion coefficient in the eutectic alloy (43 at. % Sn) (Stavintsev and Rogov, 1969) but these are over such a limited temperature range that no conclusions can be drawn about the temperature dependence.

iii) $Bi_{50}Sb_{50}$. The melting point of this alloy is high (780 K) and so the data are available over only a very limited range, and are poor in quality. The temperature dependence is estimated to be exp(780 ± 700/T), as shown in figure 5.14.a.

iv) $Bi_{50}Pb_{50}$. Here also two possible values for the ^{209}Bi Korringa product have been considered. As discussed in section 5.4.4.f neither appear to give good fits to the composition dependence data; with the Korringa product constant which was the more acceptable choice the temperature dependence is exp(850 ± 100/T), see figure 5.14.b. If the Korringa product varies similarly to that of Pb the temperature dependence is exp(1100 ± 100/T).

v) Pure Bi. Resonance linewidth measurements have been analysed to give the temperature dependence of the ^{209}Bi quadrupolar relaxation rate as exp(2200 ± 200/T) (Heighway, 1970); however the experimental data are not linear when plotted against $(\text{temperature})^{-1}$. Above the melting point, 544 K, the rates are small and the uncertainties large, the temperature dependence is weaker, given by exp(900 ± 400/T).

figure 5.13.a

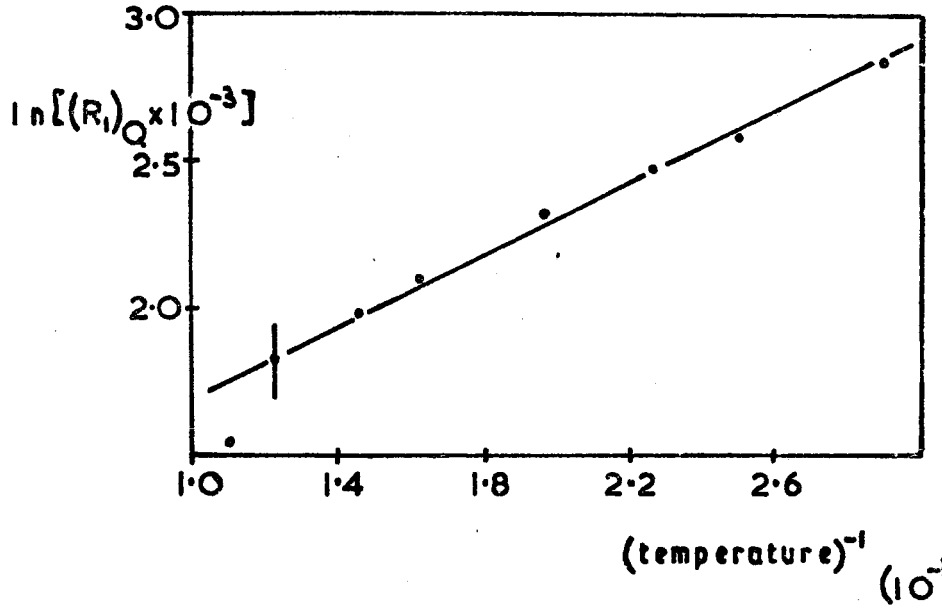

^{209}Bi LN $(R_1)_Q$ vs (TEMPERATURE)$^{-1}$ IN $Bi_{50}In_{50}$

figure 5.13.b

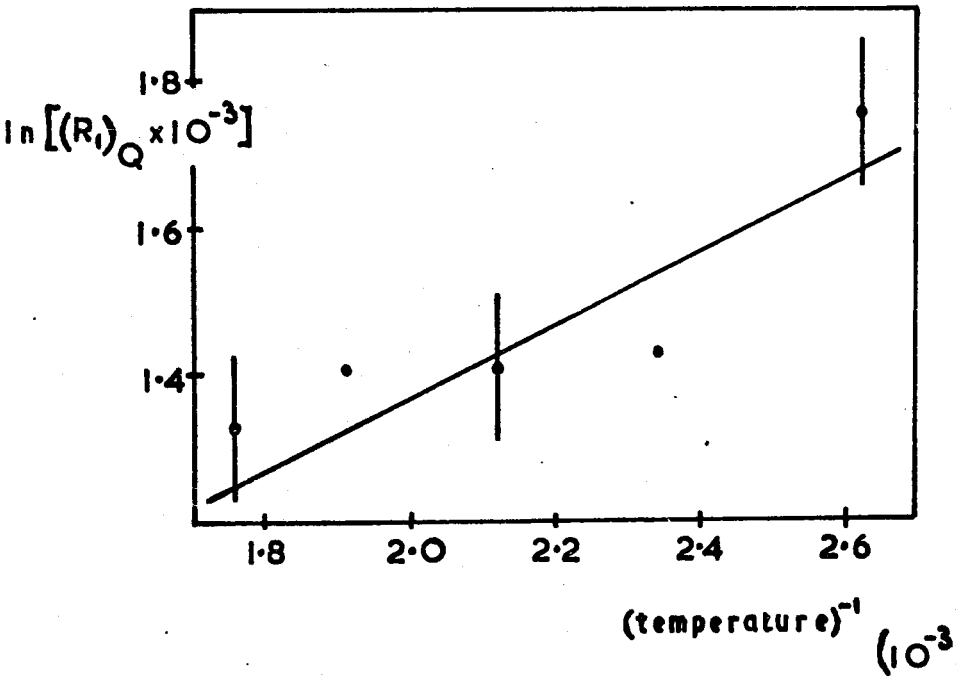

^{209}Bi LN $(R_1)_Q$ vs (TEMPERATURE)$^{-1}$ IN $Bi_{50}Sn_{50}$

figure 5.14.a

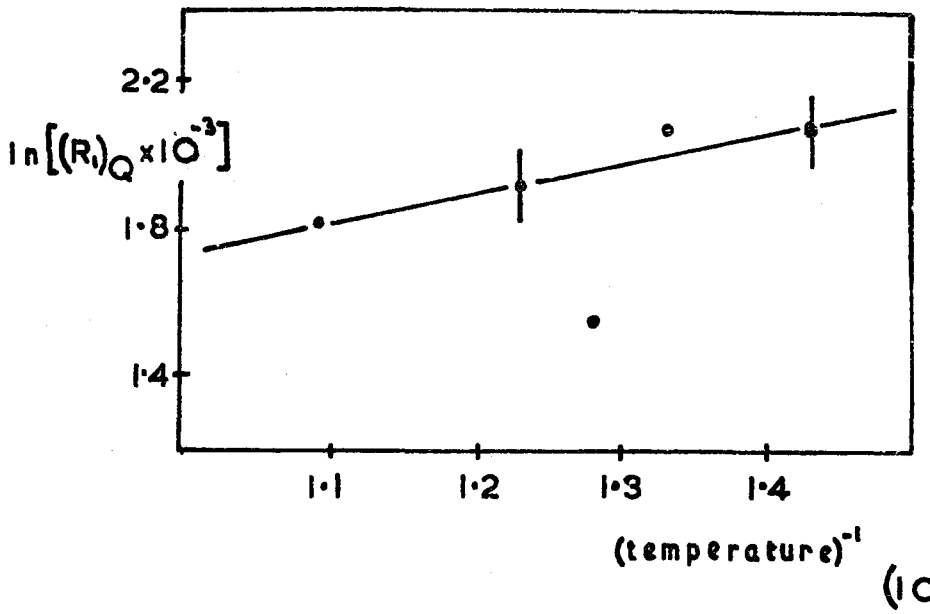

^{209}Bi LN$(R_1)_Q$ vs (TEMPERATURE)$^{-1}$ IN $Bi_{50}Sb_{50}$

figure 5.14.b

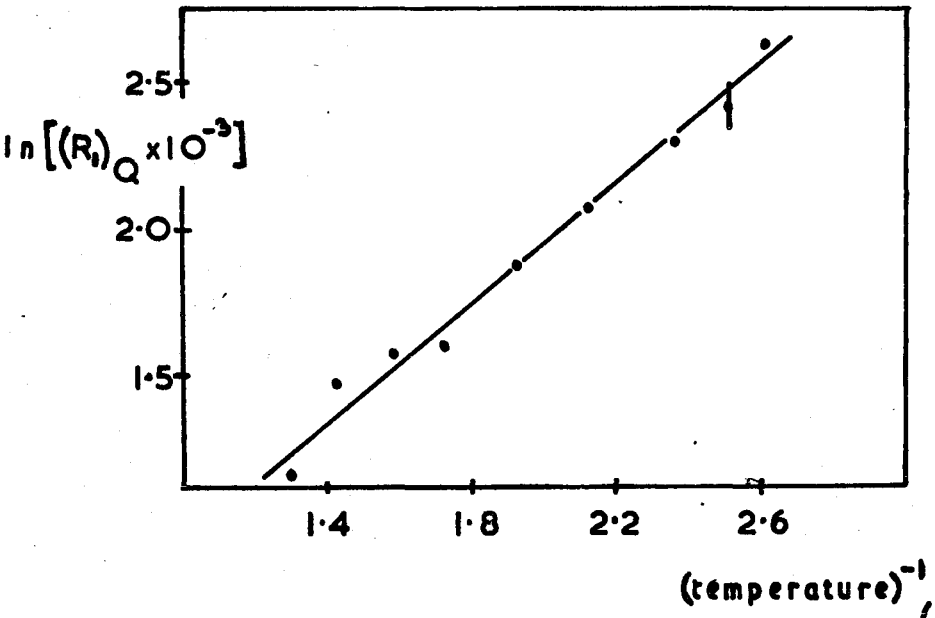

^{209}Bi LN$(R_1)_Q$ vs (TEMPERATURE)$^{-1}$ IN $Bi_{50}Pb_{50}$

It is only in the supercooled region that the gradient increases to give as an overall average the value quoted above. The experimental data are in good agreement with relaxation rate measurements reported (Rossini and Knight, 1970) which suggests that the Arrhenius form is not the best description for self-diffusion processes.

Two measurements of the self-diffusion coefficients and its temperature dependence are reported; Larson (1969) gives the temperature dependence as $\exp(-900 \pm 300/T)$ in the temperature range 550 K to 750 K, whereas Petrescu and Petrescu (1970) give it as $\exp(-1250 \pm 60/T)$ in the temperature range 550 K to 1000 K.

These values give a good indication of the experimental uncertainties in self-diffusion coefficient measurements currently available, and it is seen that within the limits of these uncertainties quadrupolar relaxation rate temperature dependences are in agreement with the appropriate self-diffusion coefficient temperature dependences.

5.4.6 Summary of α values The values of α determined for the systems mentioned above will now be tabulated. Those for Ga, In and Sb will be presented first.

Table 5.5

^{69}Ga, ^{115}In and ^{121}Sb α values in some alloys

Nucleus	System	α
^{69}Ga	Ga-In	1.7 ± 0.3
^{115}In	Ga-In	0.3 ± 0.15
^{115}In	Bi-In	0.3 ± 0.15
^{121}Sb	Bi-Sb	0.65 ± 0.15
^{121}Sb	In-Sb	1.7 ± 0.3

The ^{209}Bi values will be presented in the form of a section of the periodic table so that an examination may be made for possible valence

dependence.

Table 5.6

^{209}Bi α values in Bi - X

In		Sn	Sb
(a)	(b)	(a)	(a)
2.5 ± 0.4	2.8 ± 0.4	1.7 ± 0.3	2.5 ± 0.4
		Pb	Bi
		(a)	
		2.2 ± 0.4	

(a) Korringa product constant (b) Korringa product varying

The validity of the simplifying assumptions and the general interpretation of these values will now be discussed, in section 5.5.

5.5 Discussion of the Sholl theory

It is seen in section 5.4 that the Sholl theory can be used to obtain reasonable correlation with experimental observations in both composition and temperature dependences. Some further consideration must now be given to the validity of the simplifying assumptions made, and to the magnitude of the individual terms required to achieve quantitative agreement between theory and experiment. The three simplifying assumptions (see section 5.3.3) concerning the self-diffusion coefficients, the radial distribution functions and the interatomic potentials will be considered first. Then the magnitude of the two integrals I_1 and I_2, and the effect on them of altering the Fermi level by alloying will be discussed. Finally some remarks will be made concerning the multiplying factor $F(Q,T,I_1)$.

5.5.1 Self-diffusion coefficients

There are relatively few published data on self-diffusion in pure liquid metals, and even less in binary alloys. A basic technique is to place a capillary

containing the sample into a reservior of the sample which also contains a radioactive tracer, subsequent analysis of the sample in the capillary enables the self-diffusion coefficient to be measured. There are several other techniques available (see Edwards et al, 1968) but from the scatter of the experimental results it has been estimated (Wilson, 1965) that uncertainties can be as large as 50% in pure metals, and as much as 100% in some alloy measurements. In the case of binary alloys it is also possible to measure interdiffusion coefficients of the two constituents and from these using Darken's relation (Darken, 1948) the self-diffusion coefficients can be estimated. A further method by which mass transport has been investigated is electrotransport, the study of atom motion in the presence of an electric field; self-diffusion coefficients may be obtained by observing back diffusion when the field is removed.

The experimental results reported in pure Ga, Cd, In, Sn and Bi at around 600 K all lie in the range (2 to 4)x $10^{-9} m^2 s^{-1}$. Measurements of self-diffusion of impurity atoms in liquid Bi and also in liquid Pb (Onoprienko et al., 1967) find that there is little or no apparent dependence of diffusivity on valence difference between solvent and solute atoms or on atomic size; the coefficients reported at around 700 K almost all lie in the range (2 to 5)x $10^{-9} m^2 s^{-1}$. Extensive investigations of composition dependences have been carried out in the Cd-Pb system (Cranfield and Trimble, 1967) and in the In-Sn system (Paoletti and Vicentini-Missoni, 1961). In each case the self-diffusion coefficients of both constituents have been measured, and at 600 K all have values which vary little with composition and lie in the range (2 to 3)x $10^{-9} m^2 s^{-1}$ Neither of these systems have an intermetallic compound in their solid phase diagrams, but there is one in the In-Sb system at $In_{50}Sb_{50}$ (Hansen, 1958). This system has not been investigated fully but the self-diffusion coefficient for In in $In_{50}Sb_{50}$ has been reported (Petrescu et al, 1968) to be 5 x $10^{-9} m^2 s^{-1}$ at 800 K. Comparing this to the value in pure In at

800 K (Careri et al, 1958) of $6 \times 10^{-9} m^2 s^{-1}$ it is concluded that self-diffusion measurements do not show the existence of any marked change in liquid alloys whose composition corresponds to a solid state compound. It is interesting to note that in cases where self-diffusion coefficients have been measured over a wide range of temperatures deviations are often reported from Arrhenius type temperature dependence, which suggests that energy activated diffusion may not be strictly applicable to mass transport in liquid metals.

Two results have been reported which do not fall into the general pattern suggested above. The self-diffusion coefficient of Sn in Cu is reported to rise from normal values at less than 0.1 at. % Sn by two orders of magnitude by the addition of 1.0 at. % Sn (Gerlach et al, 1970). Since this is such an enormous change its validity must be in question. The second case is that of Tl in Hg (Foley and Liu, 1964) at 300 K, here the self-diffusion coefficient of Tl is reported to have decreased by a factor of 2.5 in going from 1 at. % Tl to 41 at. % Tl. It is possible that this change could become less marked at higher temperatures. Bi-Sn is a system discussed above, in section 5.4, in which quadrupolar relaxation is found to occur. Inter-diffusion measurements have been reported for this system (Buell and Shuck, 1970) in the range 580 K to 680 K, and it is shown that if it is assumed that the self-diffusion coefficients of the constituents vary linearly with composition good agreement is obtained between the inter-diffusion coefficients predicted from the Darken relationship and those observed experimentally.

From these few results and others mentioned it appears that self-diffusion coefficients in liquid metals lie in a narrow range of values which do not change appreciably on alloying. Thus it can be seen that the assumption that the self-diffusion coefficients do not contribute appreciably to the composition dependence of quadrupolar relaxation is a reasonable one.

5.5.2 Radial distribution functions The radial distribution function, g(r), has already been defined in section 1.1.3. Since g(r) gives the probability of finding two atoms separated by a distance r it must also give the amount of interference between incident X-ray radiation scattered by an atom through angle θ, and the radiation scattered by other atoms. We define $a(K) = I_a(\theta)/I_o(\theta)$ where $I_a(\theta)$ is the intensity of scattered radiation per atom from the liquid and $I_o(\theta)$ is the scattered intensity from one isolated atom. g(r) may be obtained with limitations from experimental observations by performing a Fourier transform on a(K). Neutron scattering experiments may also be used to obtain g(r) but in this case the expressions are more complex since the scattering process is inelastic. It is quite difficult in practice to obtain accurate g(r) by transforming a(K) due to truncation errors which arise from the experimental upper limitation to K; random errors in a(K) give a cumulative error in the transform which appear most marked at low values of r. It is also possible in principle to calculate a(K) or g(r) theoretically if a suitable interatomic potential can be found; the scarcity of experimental data has led to this being attempted (Ashcroft and Lekner, 1966).

The a(K) expression can be generalised to cover binary alloys, but now three partial interference functions are required. To obtain these experimentally is a much more complex problem than for pure metals and has only been carried out in one case so far (Enderby et al., 1967). To obtain these functions three separate experiments are required, and in some cases the data have been analysed by performing a Fourier transform on the total scattered intensity, which only yields an average over the three functions. It can be seen that the g(r) obtained from transforming experimental results must be examined with some caution.

Results for pure metals will be considered first. Nearest neighbour distances, given by the position of the first peak in g(r)

give good agreement with the smallest interatomic distance in the corresponding solid. Data on the majority of the metals considered in this work are presented and discussed (Waghorne et al., 1967). Most of these show a shoulder on the large angle side of the principal experimental diffraction which is interpreted as demonstrating departure from simple random mixing. Since this is still open to question the main peak is taken as giving the mean interatomic distance and the available values are tabulated.

Table 5.7

Mean interatomic distances in some liquid metals

Metal	Al	Ga	In	Sn	Pb	Bi
r	0.296 nm	0.277 nm	0.317 nm	0.327 nm	0.340 nm	0.332 nm

The variation of these values covers a range of some 20% and since in the Sholl theory the potential is screened out very rapidly it would seem that the first peak in g(r) is the most significant. Hence the approximation that all g(r) are the same may not be a very good one; although in none of the alloys considered is the difference as large as 20%.

There are few data available on liquid alloys, but these will also be considered. The case of Cu-Sn has been mentioned above (Enderby et al. 1967); here by three separate experiments the three partial interference functions were found. The $a_{Cu-Cu}(K)$ and $a_{Sn-Sn}(K)$ were similar to those for the pure metals but the $a_{Cu-Sn}(K)$ was not a linear interpolation between those of the constituents, however the three partial interference functions were found to be practically independent of composition.

An analysis of the X-ray scattering data for the Bi-In system is available (Isherwood and Orton, 1969) and since this is one of the systems discussed above it is of particular interest. It was assumed that the partial interference functions $a_{Bi-Bi}(K)$ and $a_{In-In}(K)$ were the same as

for the pure metals and independent of composition, which enabled $a_{Bi-In}(K)$ to be evaluated. The first main peak position of the total scattered intensity is found to vary linearly as a function of composition changing by about 6% over the range c = 0 to c = 1. The partial interference function $a_{Bi-In}(K)$ is found to coincide with that of the total scattered intensity, within the experimental error. It seems that in this case the approximation of setting all three g(r) equal is reasonable.

Data from several other alloy systems which are found to show asymmetric peaks with a pronounced shoulder are reviewed (Waghorne et al., 1967) and are interpreted as showing persistence of short-range order in the liquid; no conclusions are drawn about individual g(r).

Apart from these, other discussions of X-ray scattering data have been carried out on the assumption that $g_A(r) = g_B(r)$ (see for example Wagner and Halder, 1967) which produces reasonable agreement with experiment. From above it would seem that $a_{A-B}(K)$ lies somewhere between those of the two constituents, and so until more experimental data are available errors can be minimised by choosing g(r) so that it corresponds to the mean interatomic spacing for all the metals considered.

5.5.3 Interatomic electric field gradients Before the values obtained above are discussed it must be emphasised that they are all dependent to some extent on the behaviour of the Korringa product, least in the case of ^{121}Sb where the quadrupolar relaxation rates are greatest. Since the Korringa product appears to vary in a random way in going from one alloy system to another its variation cannot readily be allowed for.

If the Sholl theory assumption holds, namely that $(v_2)_{AB} = \alpha (v_2)_{AA}$, where $(v_2)_{AB}$ is the electric field gradient at an A type nucleus due to a neighbouring B type atom, then in any binary alloy of A and B atoms $\alpha(A)$ should equal the reciprocal of $\alpha(B)$. The data above, section 5.4.5,

enable this to be checked in three alloy systems

(a) Ga - In $\alpha(^{69}Ga) = 1.7 \pm 0.3$

$[\alpha(^{115}In)]^{-1} = 3.3 \pm 1.1$

(b) Bi - In $\alpha(^{209}Bi) = 2.5 \pm 0.4$

$[\alpha(^{115}In)]^{-1} = 3.3 \pm 1.1$

(c) Bi - Sb $\alpha(^{209}Bi) = 2.5 \pm 0.4$

$[\alpha(^{121}Sb)]^{-1} = 1.5 \pm 0.5$

This test is not entirely satisfactory since the choice of α is always ambiguous unless the composition dependence is available, this is true only for case (a). In case (b) the ^{209}Bi composition dependence makes $\alpha > 1$, but since (^{115}In) is estimated from the relaxation rate in $Bi_{50}In_{50}$ this value is ambiguous and so the $\alpha < 1$ value was chosen. In case (c) (^{209}Bi) was selected to agree with the $\alpha > 1$ obtained for Bi in the other cases, and hence the ^{121}Sb α value should be less than 1. Using the data for ^{121}Sb obtained earlier the choice of $\alpha < 1$ appears more reasonable $\alpha > 1$. Examining the results it can be seen that only in one case is agreement obtained to within the estimated uncertainties, but all are approximately right.

Next the magnitudes of the α values will be considered to see if any valence dependence is apparent. Size has been discounted by the assumption made in section 5.3.3 that all the $g(r)$ are the same. However two equivalent systems have been examined and both show quadrupolar relaxation. If the size of an atom is taken from the position of the first peak on experimental $g(r)$ curves then In is seen to be larger than Ga. A value for Sb is not available, but its neighbour in the periodic table, Sn, is only slightly smaller than Bi and so it is likely that Sb is in fact larger than Bi. In both Ga-In and Bi-Sb the atom which is taken to be larger has $\alpha > 1$, or in other words the electric field gradient at a nucleus due to the larger atom is greater than that due to the smaller one.

In all three cases where valence difference dependence can be considered, In-Sb, Bi-Pb and Bi-Sn the magnitudes are no greater than in the equivalent cases, and even appear to be less when the valence difference is two than when the valence difference is only one. In each case the constituent having the larger valence has $\alpha > 1$, namely the atom with the smaller 'valence' produces a greater electric field gradient at its nearest neighbour than does the larger valence atom. The expression for $v_2(r)$ is given in equation 5.13, and this is seen to contain A, the amplitude of the screened potential. This is given by (Sholl, 1967)

$$A = \frac{2 Z m e^3}{\pi \hbar^2 \epsilon^2(2 k_F)} \qquad \ldots\ (5.23)$$

where Z is the ion core valency,

m, e are the mass and charge of the electron,

$\epsilon(2k_F)$ is the dielectric function evaluated at $2k_F$.

The scaling factor α must arise from the different values of A, and hence of Z, so that $\alpha_A = (v_2)_{AB} / (v_2)_{AA} = Z_B / Z_A$; and this can be used to estimate the relative effective valencies of the different nuclei observed.

From this $Z_{In} / Z_{Bi} = 2.5 \pm 0.4$

and $Z_{In} / Z_{Sb} = 1.7 \pm 0.3$

which gives $Z_{Bi} / Z_{Sb} = 1.7/2.5 = 0.68$

and this compares favourably with the experimentally determined $Z_{Bi} / Z_{Sb} = 0.65$. From the α values a scale of effective valencies for liquid metals can be drawn up. Since the results are relative the value of In has been chosen to be 3 and the others calculated from it.

Table 5.8

Effective valences deduced from the values of α

Metal	Ga	In	Sn	Sb	Pb	Bi
Valence	1.0	3	2.2	1.8	2.7	1.2 or 0.9

These values are to be compared with those given by Faber (1966) in a summary of the effective valencies of a number of liquid metals, deduced from optical properties. There the values were within 20% of those predicted from the free electron picture, and hence are not in agreement with the values obtained here.

5.5.4 The magnitudes of I_1, I_2 and $F(Q,T,I_1)$

Sholl (1967) has calculated I_1 and I_2 for Ga and In. The g(r) used in each case were experimentally determined, and differ appreciably from each other. The values k_F used were $1.66 \times 10^{10} m^{-1}$ for Ga and $1.51 \times 10^{10} m^{-1}$, which are also appreciably different. Nevertheless the two computations only make I_1 for Ga some 40% larger than that for In, indicating that the integral is not especially sensitive to g(r) or to k.

To check this approximate calculations of I_1 have been made for a fixed g(r) and some values of k_F. I_1 appears almost independent of k_F in the region of interest, $(1.4 \text{ to } 1.8) \times 10^{10} m^{-1}$. This has been confirmed by calculations carried out by Sholl (private communication) in the course of the original work.

I_2 is an even more difficult term to consider. As Sholl has pointed out the errors in introducing the superposition approximation, which are worst when the ions are close together, mean that calculation of I_2 will be considerably less accurate than those of I_1. Sholl (1967) chooses, for this reason, to neglect I_2 in order to obtain a better fit to the experimental data. In this work to obtain a good fit to the much more comprehensive range of experimental values it is required that I_2 should be close to $-I_1$. Sholl (private communication) points out that although he is unable to show that I_2 is of opposite sign to I_1, the fact that the calculations give this for both In and Ga gives some encouragement. It does seem possible now that an experimental value of I_2 is available showing that I_2 is near to $-I_1$ that an estimate of the three-body

correlation function might be extracted, even although it is contained in an integration over r.

$F(Q,T,I_1)$ is defined in equation 5.22, and is given by

$$F(Q,T,I_1) = \frac{2I+3}{I^2(2I-1)} \left(\frac{A(1-\gamma_\infty)eQ}{\hbar} \right)^2 \frac{\pi \rho}{75\,D} I_1$$

Values of $F(Q,T,I_1)$ for three nuclei can be extracted from the fits which have been made to the experimental data.

Table 5.9

Values of $F(Q,T,I_1)$ deduced from experiment

Nucleus	$F(Q,T,I_1)$	Temperature
^{115}In	$24 \times 10^3 s^{-1}$	373 K
^{121}Sb	$80 \times 10^3 s^{-1}$	900 K
^{209}Bi	$11 \times 10^3 s^{-1}$	615 K

To obtain direct comparison the values must be extrapolated to a common temperature. The principal temperature dependence appears to arise from the self-diffusion coefficients and these have been discussed in section 5.4.5. Since this is least accurately known for Sb the other two values will be extrapolated to 900 K using as temperature dependence exp(1250/T) in each case.

Table 5.10

Values of $F(Q,T,I_1)$ at 900 K

Nucleus	^{115}In	^{121}Sb	^{209}Bi
F (in $10^3 s^{-1}$)	3.4	80	5

If the spin dependent term is evaluated, values for the quadrupole moments from the literature (Varian Associates, 1965) substituted and D, ρ are taken to be the same in all cases then the ratios of

$[A(1 - \gamma_\infty)]^2 I_1$ are obtained:-

In : Sb : Bi 8 : 90 : 43

Rossini and Knight (1970) estimate that I_1 for Sb or Bi is approximately one and a half times I_1 for In. On that basis the ratios of $A(1 - \gamma_\infty)$ may be estimated.

Table 5.11

Relative proportions of $A(1 - \gamma_\infty)$ for In, Sb and Bi

Atom	$A(1 - \gamma_\infty)$
In : Sb : Bi	2 : 5.5 : 4

A has been defined, equation 5.23, and has as principal variable Z, the ion core valency. Values for Z have already been deduced in this section and these ratios will be used to determine γ_∞; these cannot be any more reliable than the values of Z which have been found. From this the ratios of $(1 - \gamma_\infty)$ for In : Sb : Bi are 2 : 9 : 10. Sholl has estimated $(1 - \gamma_\infty)$ for In to be 78. Since this is for a screened ion it seems reasonable in comparison to the value 17 calculated by Sternheimer (1966) for an In^{3+} ion, as the anti-shielding factor decreases with increasing ionisation. On this basis $(1 - \gamma_\infty)$ for Sb is 350 and for Bi is 390.

Rossini and Knight (1969) have estimated $(1 - \gamma_\infty)$ for Sb and for Bi by multiplying the Sternheimer ionic anti-shielding values by a factor of three. They obtained 30 for Sb, and 150 for Bi; the value for Sb seems small in comparison to that for In. Heighway (1969) has estimated $(1 - \gamma_\infty)$ for Bi^{5+} to near to 80, so that the value for a screened ion could be 240. The values of $(1 - \gamma_\infty)$ deduced in this work appear to be overestimated due in the main to the choice of Z values.

In conclusion it must be pointed out that the value of I_1 calculated by Sholl leads to a value of $R_1 a$ which is some five times too small.

5.6 Summary

An attempt has been made to account for the general occurrence of greatly increased quadrupolar relaxation rates around 50 - 50 composition in binary liquid alloys, as compared to the values in pure metals. The physical phenomena responsible arise almost certainly in the fluctuations of the electric field gradients produced when a neighbouring ion of one type is replaced by an ion of a different type. This points to the importance of the I_2 term in Sholl's expression and of the three-body correlation function it contains. A full application of Sholl's extension of the theory to alloys becomes far too complex to serve as a basis for computation. By making several assumptions, not all of which are likely to be completely justified, it has been possible to express this extension in a form which is sufficiently simple to allow comparison with experiment. The result is that the required parabolic dependence of $(R_1)_Q$ on solute composition is produced providing the term I_2 is retained.

In Sholl's discussion of the pure metals Ga and In the predicted $(R_1)_Q$ values fitted experiment better if the term I_2 was ignored (being justified to some extent on the grounds that I_2 was considerably more uncertain than I_1). It now seems that this conclusion cannot be maintained since sufficiently pronounced parabolic dependence of $(R_1)_Q$ on composition cannot be obtained unless I_2 is negative and near in magnitude to I_1. Unfortunately the form of I_2 is so complex that it is impossible to discern an explanation for this conclusion. It could be argued that the form of the theory is inappropriate for meaningful comparison with experiment if the results depend so sensitively on the small difference between two large terms. However an alternative conclusion is put forward, namely that the sensitivity of I_2 to the three-body correlation function may provide a means of investigating that function; an opportunity which does not often present itself.

It must be admitted that in fitting the theory with experiment several quantities have been treated as adjustable parameters. As a result a point against this interpretation emerges in that the values of α, the relative field gradients, seem physically unreasonable. This could result from the use of an asymptotic expression for the field gradient in circumstances where the main contribution comes from small distances.

It has been suggested that other properties could give rise to the parabolic dependence of $(R_1)_Q$. Bonera et al. (1968) have attributed the effect in Ga-In to the assumed behaviour of the diffusion coefficient. However an extensive survey of the literature definitely rules out variation of D as the main cause; in fact D values turn out to be remarkably independent of composition. A further possibility was that I_1 might be sufficiently composition dependent through variation of the Fermi wavevector to produce the maximum in $(R_1)_Q$. Calculations indicate that this is not the case. Suggestions that the persistence into the liquid of compounds which exist in the solid might give rise to additional relaxation are ruled out since quadrupolar relaxation is equally effective in systems where no solid compound is known, for example Ga-In or Bi-Sb, as compared to systems where a compound does exist.

It is therefore concluded that the most likely interpretation of the data lies in the large field gradient fluctuations produced by exchange of unlike neighbours. Further experimental investigations could be centred on the ^{121}Sb nucleus since it is clearly more sensitive to quadrupolar relaxation than any of the other nuclei observed. Final confirmation must await evaluation of the I_2 term, and there seems little point in attempting this without including the refinement of differing partial radial distribution functions; generally such partial functions are not yet available.

References

Abragam, A., 1961, The Principles of Nuclear Magnetism.
(Clarendon Press : Oxford), 314.

Ashcroft, N. W. and Leckner, J., 1966, Phys. Rev., 145, 83.

Bloembergen, N., Purcell, E. M. and Pound, R. V., 1948, Phys. Rev.,
73, 679.

Bonera, G., Borsa, F. and Rigamonti, A., 1969, Colloque Ampere XV
(North Holland : Amsterdam), 359.

Borsa, F. and Rigamonti, A., 1967, Nuovo Cimento, 48, 194.

Buell, C. H. and Shuck, F. O., 1970, Met. Trans., 1, 1875.

Careri, G., Paoletti, A. and Vincentini, M., 1958, Nuovo Cimento, 10, 1088.

Cornell, D. A., 1967, Phys. Rev., 153, 208.

Cranfield, F. B. and Trimble, L. E., 1967, CFSTI Report No N 67, 29745.

Darken, L. S., 1948, AIME Trans., 175, 184.

Edwards, J. B., Hucke, E. E. and Martin, J. J., 1968, Met. Rev., 13, 1.

Enderby, J. E., North, D. M. and Egelstaff, P. A., 1967, Adv. in Phys.,
16, 171.

Faber, T. E., 1963, Solid State Commun., 1, 41.

Faber, T. E., 1966, Optical Properties and Electronic Structure of Metals
and Alloys, Ed. F. Abeles (North Holland : Amsterdam).

Foley, W. T. and Liu, M. T., 1964, Canad. J. Chem., 42, 2602.

Gaspari, G. D. and Das, T. P., 1968, Phys. Rev., 167, 660.

Gerlach, J. and Schwartz-Domke, W., 1970, Metall., 24, 1214.

Hanabusa, M., 1965, Tech. Report 470, Cruft Laboratory, Harvard University.

Hansen, M., 1958, The Constitution of Binary Alloys (McGraw Hill : New York).

Harrison, W. A., 1966, Pseudo-potentials in the Theory of Metals
(Benjamin : New York).

Heighway, J., 1969, Ph D Thesis, University of Warwick.

Heighway, J. and Seymour, E. F. W., 1971, J. Phys. F : Metal Phys., 1, 138.

Host, I. P., 1972, Ph D Thesis, University of Warwick.

Isherwood, S. P. and Orton, B. R., 1969, J. Appl. Cryst., 2, 219.

Jena, P., Das, T. P. and Mahanti, S. D., 1970, Phys. Rev. B, 1, 1160.

Korringa, J., 1950, Physica, 16, 601.

Larson, K. B., 1969, Ph D Thesis, Massachusetts Institute of Technology.

Mitchell, A. H., 1967, J. Chem. Phys., 26, 1714.

Moriya, T., 1963, J. Phys. Soc. Japan, 18, 516.

Moulson, D. J., 1966, Ph D Thesis, University of Leeds.

Nachtrieb, N. H., 1967, Adv. in Phys., 16, 309.

Narath, A. and Weaver, H. T., 1968, Phys. Rev., 175, 373.

Noer, R. J. and Knight, W. D., 1964, Rev. Mod. Phys., 36, 177.

Onoprienko, G. I., Kuzmenko, P. P. and Kharkov, E. J., 1967, Ukr. Fiz. Zh., 12, 39.

Oppenheim, I. and Bloom, M., 1961, Canad. J. Phys., 39, 845.

Paoletti, A. and Vicentini-Missoni, M., 1961, J. Appl. Phys., 32, 559.

Petrescu, N. et al., 1968, Rev. Roum. Chim., 13, 865.

Petrescu, N., 1969a, Electrochim. Metal., 4, 283.

Petrescu, N., 1969b, Rev. Roum. Chim., 14, 67.

Petrescu, N., 1970, Z. Metallkunde, 61, 19.

Pines, D., 1955, Solid State Physics (Academic Press : New York), 1, 367.

Rossini, F. A., Geissler, E., Dickson, E. M. and Knight, W. D., 1967, Adv. in Phys., 16, 287.

Rossini, F. A. and Knight, W. D., 1970, Phys. Rev., 178, 641.

Saxton, H. J. and Sherby, O. D., 1962, Am. Soc. Metals, Trans. Quart., 55, 826.

Sholl, C. A., 1967, Proc Phys. Soc., 91, 130.

Shyu, W. A., Das, T. P. and Gaspari, G. D., 1966, Phys. Rev., 152, 270.

Spokas, J. J. and Slichter, C. P., 1959, Phys. Rev., 113, 1462.

Stavintsev, P. A., and Rogov, V. I., 1968, Fiz. Met. Metall., 26, 1119.

Sternheimer, R. M., 1966, Phys. Rev., 146, 140.

Styles, G. A., 1964, Ph D Thesis, University of Leeds.

Styles, G. A., 1967, Adv. in Phys., 16, 275.

Townes, C. H., Herring, C. and Knight, W. D., 1950, Phys. Rev., 77, 852.

Varian Associates, 1965, NMR Table, 5th Edn.

Waghorne, R. M., Rivlin, V. G. and Williams, G. I., 1967, Adv. in Phys., 16, 215.

Wagner, C. N. J. and Halder, N. C., 1967, Adv. in Phys., 16, 241.

Warren, W. W. and Clark, W. G., 1969, Phys. Rev., 177, 600.

Wilson, J. R., 1965, Met. Rev., 10, 381.

Yafet, Y. and Jaccarino, V., 1964, Phys. Rev., 133, A1630.

CHAPTER SIX

NUCLEAR SPIN-LATTICE RELAXATION IN LIQUID BINARY ALLOYS CONTAINING TELLURIUM

6.1 Liquid semiconductors

The general properties of liquid semiconductors, liquids whose conductivities lie in the range $3 \times 10^{5} \text{ohm}^{-1}\text{m}^{-1}$ to $3 \times 10^{3} \text{ohm}^{-1}\text{m}^{-1}$ are outlined in section 1.1.2. Many of these liquids consist of binary alloys having a metallic component and a chalcogenide component, and so some alloys containing tellurium have been investigated as part of this work. There is, as yet, no complete theory to explain the electron transport properties observed in amorphous semiconductors, although a general model has been proposed (Cohen, Fritzche and Ovshinsky, 1969; Davis and Mott, 1970). This model has been extended to the case of liquid semiconductors, (Mott, 1971) and an outline of that work will now be given. The new work reported in this chapter represents an attempt to investigate the general predictions of the Mott theory.

6.1.1 The pseudogap model Two mechanisms for electronic conduction in solids have been described in the literature. In the first, which applies to crystalline structure, the electron is described by a wave function which has the periodicity of the lattice. The electron travels through the lattice with a mean free path, L, which is large compared to the interatomic spacing; L is determined by the scattering of the electron by impurities and by lattice vibrations. The second mechanism is that of thermally activated hopping; it is no longer possible to define a mean free path. The electron is in a localised state and so each time it moves it has to exchange energy with some source such as phonons.

In liquid metals the conductivity has been accounted for in the

n.f.e. theory (Ziman, 1961), where the electron is described by a plane wave, on the assumption that the scattering of an electron wave by each atom is small. The scattering factor is determined from neutron or X-ray diffraction experiments; this has led to remarkably good agreement in a number of liquid metals (see, for example, March, 1968, p 71). Ziman has given an expression for the conductivity,

$$\sigma = S_F e^2 L / 12 \pi^3 \hbar \qquad \ldots\ (6.1)$$

where S_F is the area of the Fermi surface,

L is the electron mean free path calculated from the n.f.e. theory.

Mott (1967) has considered the case where the interaction between the conduction electrons and the atoms is strong, and shows that the conductivity expression should be modified to

$$= S_F e^2 L\, g^2 / 12 \pi^3 \hbar \qquad \ldots\ (6.2)$$

where g is $N(E_F) / N(E_F)_{\text{free electron}}$

In the intermediate region as the conductivity decreases in different materials due to the increasing interaction the n.f.e. theory is expected to break down, since the Born approximation only holds for weak scattering. At first this is not found to happen, for example in liquid bismuth good agreement is obtained. This has been explained by Edwards (1962) who has shown, using second order perturbation theory that the true mean free path, L, is given by

$$L = L_z / g^2 \qquad \ldots\ (6.3)$$

This is basically because if the density of states decreases the probability of scattering also decreases. Hence there is a cancellation of the g^2 term. As the scattering becomes stronger so L must decrease. The lower limit will be reached when $L = a$, the interatomic spacing, since values smaller than this are not physically meaningful. When the

interaction is strong the Edwards theory will no longer work and the g^2 term will no longer cancel; the conductivity will then be given by equation 6.2.

Part of the problem is therefore to calculate g for the non-metallic case. The behaviour of the density of states as a function of energy has aroused considerable interest. Calculations based on a one dimensional model consisting of a random distribution of delta functions show that in the strong interaction case there is a considerable dip in the curve (Frisch and Lloyd, 1960).

Over a range of energies the ratio g drops considerably below unity. The problem in three dimensions has proved intractable so far. In solid semiconductors the band gap is a consequence of the structure of the material, and hence when a semiconductor melts the disorder is likely to produce a spread of energies, some of which will fall in the gap. Mott postulates that in this case a pseudogap is formed providing the structural changes are not too great, as for example in the case of PbTe.

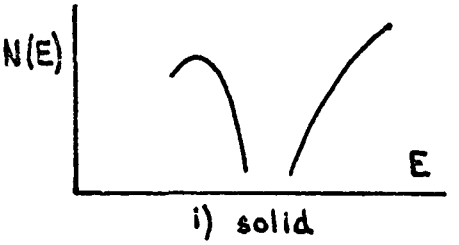

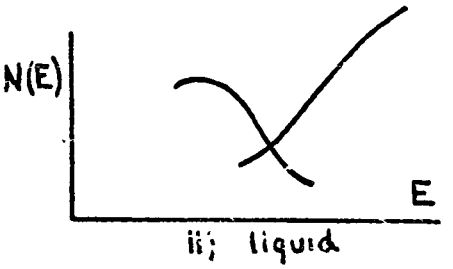

It is even possible that the gap will disappear altogether, and metallic behaviour will occur as in InSb.

Mott has also considered the conduction process when the density of states is well below the free electron value, as in the region of the pseudogap. Mott predicts, following the work of Anderson (1958), that when g is less than about one third, electrons in those states become localised. If the density of states at the Fermi energy is sufficiently below the free electron value such that the states at E_F are localised

there will be two processes leading to conduction. Current is carried by carriers excited into the extended states predominantly, but there is also a contribution from current carried by thermally excited hopping. Anderson considered a three dimensional crystalline array of potential wells whose depth varied in a random way. Conduction electrons placed on these sites interact (on the tight binding model) to form a single band of energy levels. Anderson then showed that, providing the spread in the potential is several times larger than the width of the energy band the electrons will be localised, and can only move with phonon assistance. The applicability of the theory to the case where the randomness is in the position of the atomic sites rather than in the depth of the wells is still an open question; Mott has used this theory being the only quantitative theory available at the time. In a liquid once the states have become localised it is unlikely that a hopping conduction process characterised by an activation energy is entirely satisfactory. Since the atoms are continually moving the electron can move without hopping, in a manner similar to that of a heavy ion in solution, but its mobility will still be several orders of magnitude less than if it is in a non-localised state.

Mott (1969) has considered the effect of the conduction electron character on the likelihood of localisation. It is shown that as a consequence the directional nature of non-s electrons these are much more likely to produce the spread of energies, due to random orientations, required to create localised states.

Other transport measurements should be able to provide additional information on the electronic behaviour in these materials. As has been pointed out in section 1.1.2 there is a conflict between the sign of the majority charge carrier predicted from Hall coefficient and thermopower measurements. Mott points out that the thermopower theory (Cutler and Mott, 1969) can be applied to amorphous materials, whereas the Hall

effect theory has not been developed to apply to these materials; another point of view is put forward in section 6.1.2. The thermopower measurements indicates that the majority of these materials are p-type; Mott explains this by assuming that the band of localised states below E_F is narrower than the localised band above E_F, so that there will be more mobile holes than electrons.

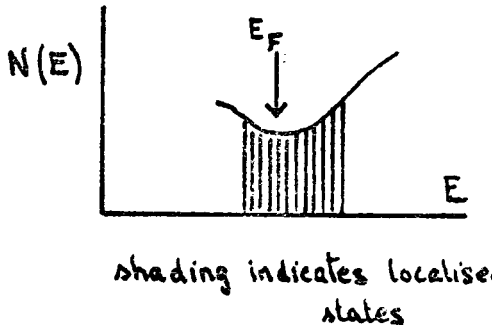

6.1.2 The dilute metal model Another model has been proposed (Enderby and Simmons, 1969) in which the transport properties are explained in general terms. It is assumed that the Hall coefficient is indeed a useful measure of the sign and density of the current carrier, it is then postulated that molecular groups are formed in the liquid of some critical composition; generally at stoichiometry, together with excess of one or other of the constituents. The bonding electrons in these groups form a narrow band of virtual bound states separated in energy from the conduction band; hence the number of free electrons will be depleted causing a peak in the Hall coefficient as the composition nears the critical value.

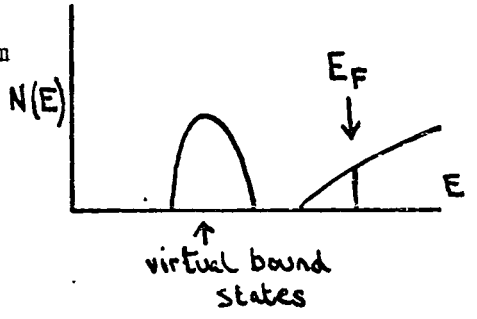

The resistivity of any arbitrary alloy is discussed in terms of liquid binary metal theory (Faber and Ziman, 1965) assuming that the conduction electron states are extended states at all compositions,

$$1/\sigma = m v_F / ne^2 \left[\frac{1}{\Lambda_0} + \frac{1}{\Lambda_1} \right]$$

where v_F is the velocity of Fermi surface electrons,

n is the free electron density.

Λ_o and Λ_1 are the contributions to the electronic mean free path from the molecular groups and from the excess atoms respectively. If Λ_1 is expressed using partial wave theory (Ziman, 1960) it is possible to derive an expression for the energy dependent resistivity, $\rho(E)$. This is then used to derive an expression for the thermopower which is compared to the experimental data. A rapid variation in the conduction electron scattering with change in Fermi energy is predicted; since this scattering will depend on the nature of the 'impurities' the different variations in resistivity with composition on each side of the critical composition can be explained.

In further calculations, by taking Λ_o to be 20×10^{-9}m where this is deduced from the conclusion that the limiting value of k_F is found from $k_F \Lambda_o > 1$; Mott, 1967) it is possible to estimate the width of the virtual bound state band; it is found to be 0.2 e_v in $TeTl_2$.

A modification to this theory has been put forward (Enderby and Collings, 1969) where it is postulated that the energy dependent scattering arises from the molecular groups. This has the advantage of predicting a maximum in the resistivity at the critical composition without the need to make special assumptions about the scattering properties of the constituents.

The experimental results will now be reviewed in the light of these theories.

6.2 Te-Tl

6.2.1 The Te-Tl system

One of the most suitable alloy systems to choose for investigation with the available apparatus is Te-Tl. The liquidus line on the phase diagram, see figure 6.1 shows that over most of the composition it is possible to melt the alloys within the temperature range of the spectrometer furnace. There is a region of

figure 6.1

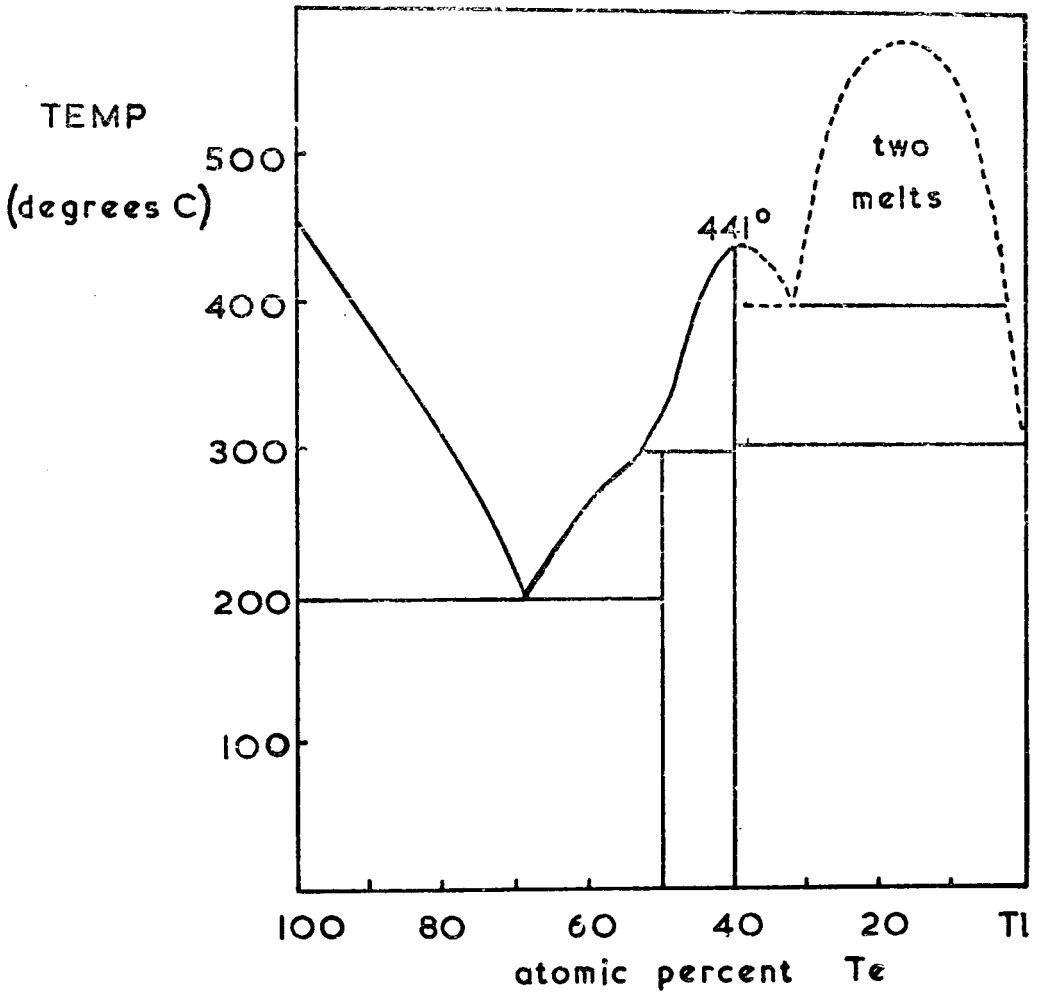

Te-Tl PHASE DIAGRAM (ff HANSEN)

liquid immiscibility when the Te content lies between 0 and 30 at. %, and it is this region that is inaccessible. Further, since ^{125}Te and ^{205}Tl (both of which nuclei it was intended to investigate) have nuclear spin one half, there can be no relaxation which is electric quadrupolar in origin; this will simplify the interpretation of relaxation rate measurements. On the other hand the small abundance and nuclear moment of ^{125}Te made it certain that considerable efforts would be required to extract the resonance adequately from the noise.

The electron transport properties of Te-Tl have been extensively investigated and show interesting behaviour. The conductivity is found to vary rapidly with concentration and has a pronounced minimum at $TeTl_2$, see figure 6.2. The temperature coefficient of the conductivity, which is positive in alloys from Te to $TeTl_2$, is greater at around $TeTl_2$ than at any other concentration. (Cutler and Mallon, 1966; Enderby and Walsh, 1966). The thermopower shows unusal behaviour, being p-type from Te_{100} to $TeTl_2$, when it undergoes a change of sign, becoming n-type on the Tl rich side of $TeTl_2$ (Cutler and Mallon, 1966). The Hall coefficient has been measured across the composition range and is found to remain negative throughout and has a large sharp peak at $TeTl_2$ (Enderby and Walsh, 1966; Cutler and Field 1968).

In the present study magnetic suceptibility measurements have been made on several alloys, see table 4.13, and figure 6.3. There is a rapid decrease in χ_t, see section 1.1.4, as the Te content is reduced towards $TeTl_2$; this behaviour is discussed in more detail in section 6.2.3. In addition the ^{125}Te nuclear magnetic resonance shift has been measured as a function of temperature and composition in the range 100 to 30 at. % Te, see table 4.11. A typical isotherm, see figure 6.4, shows a rapid decrease as the Te content is reduced. These results are discussed in more detail in section 6.2.4. Nuclear spin-lattice relaxation rates have been measured in the same range of compositions and those results are tabulated

figure 6.2

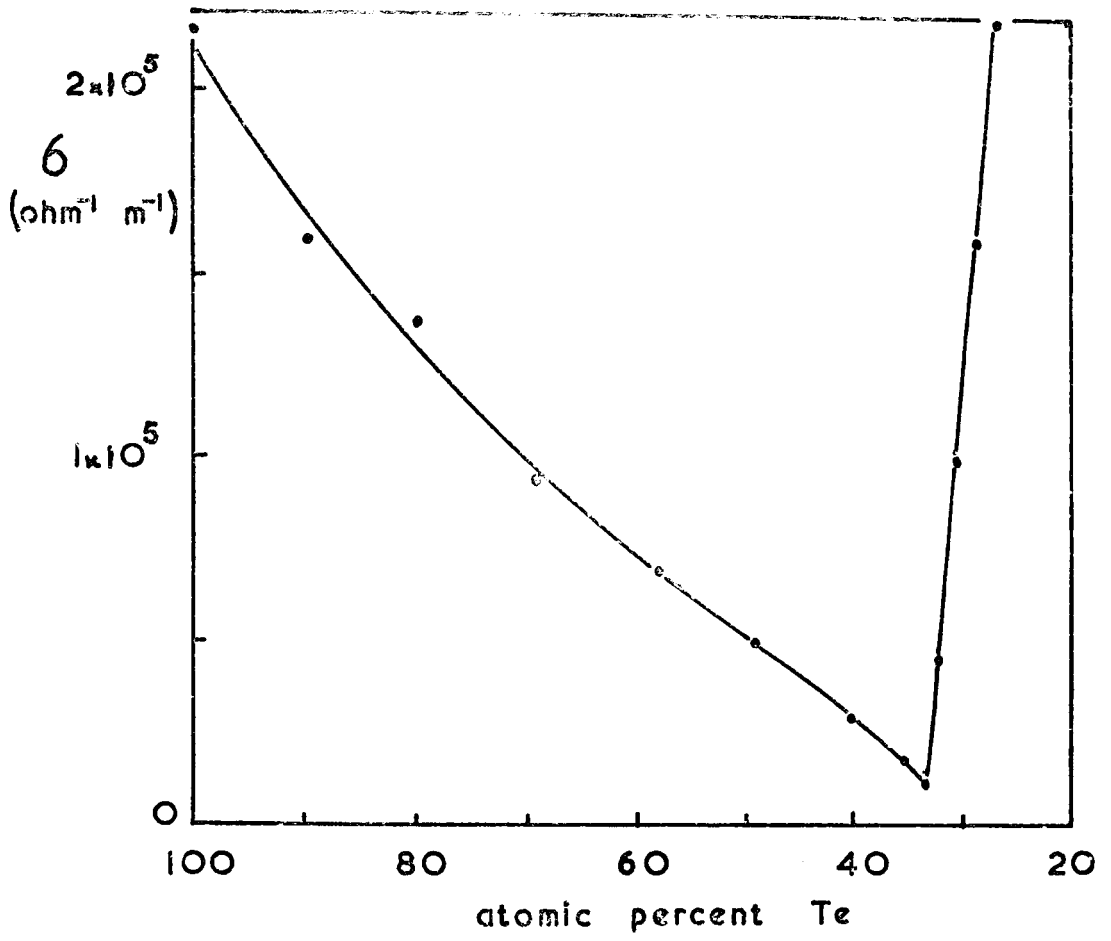

CONDUCTIVITY AS A FUNCTION OF

COMPOSITION IN Te–Tl AT 773 K

figure 6.3

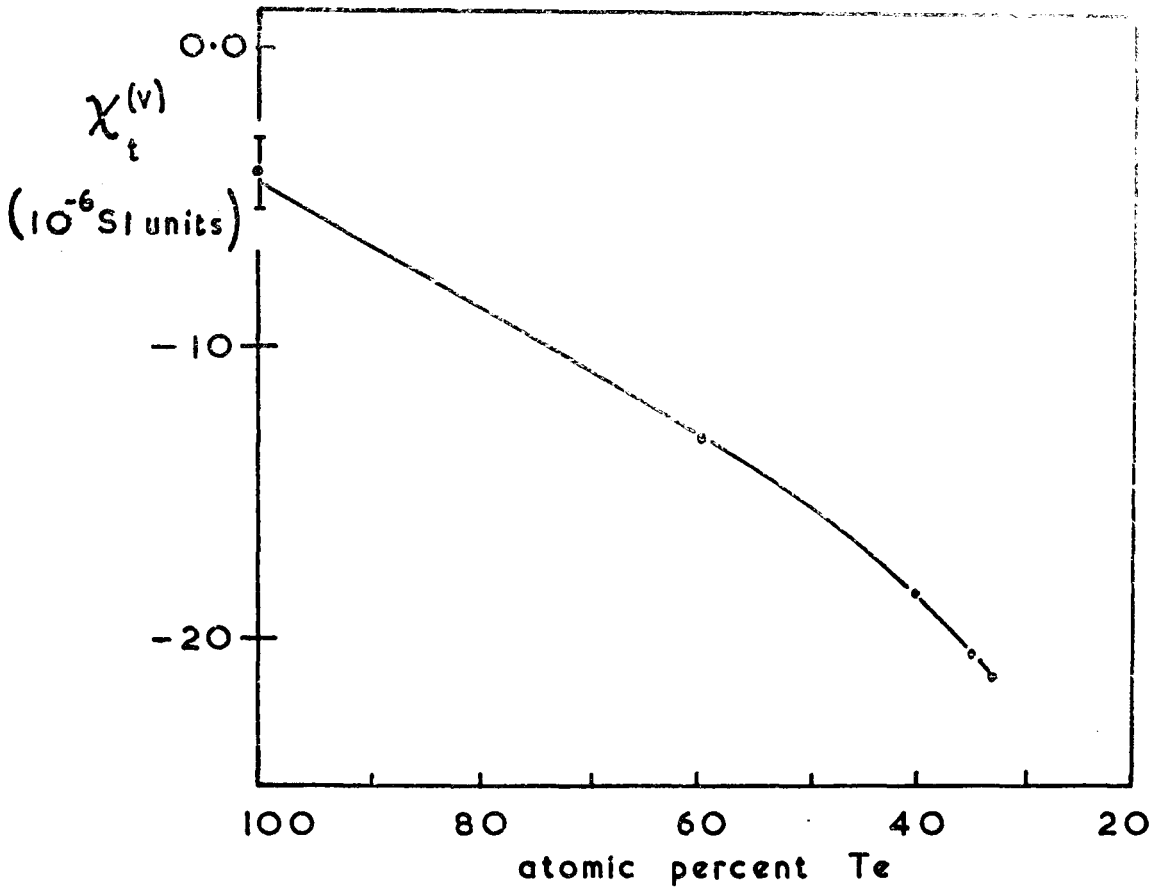

TOTAL VOLUME SUCEPTIBILITY AS A FUNCTION OF COMPOSITION IN Te–Tl AT 773 K

Figure 6.4

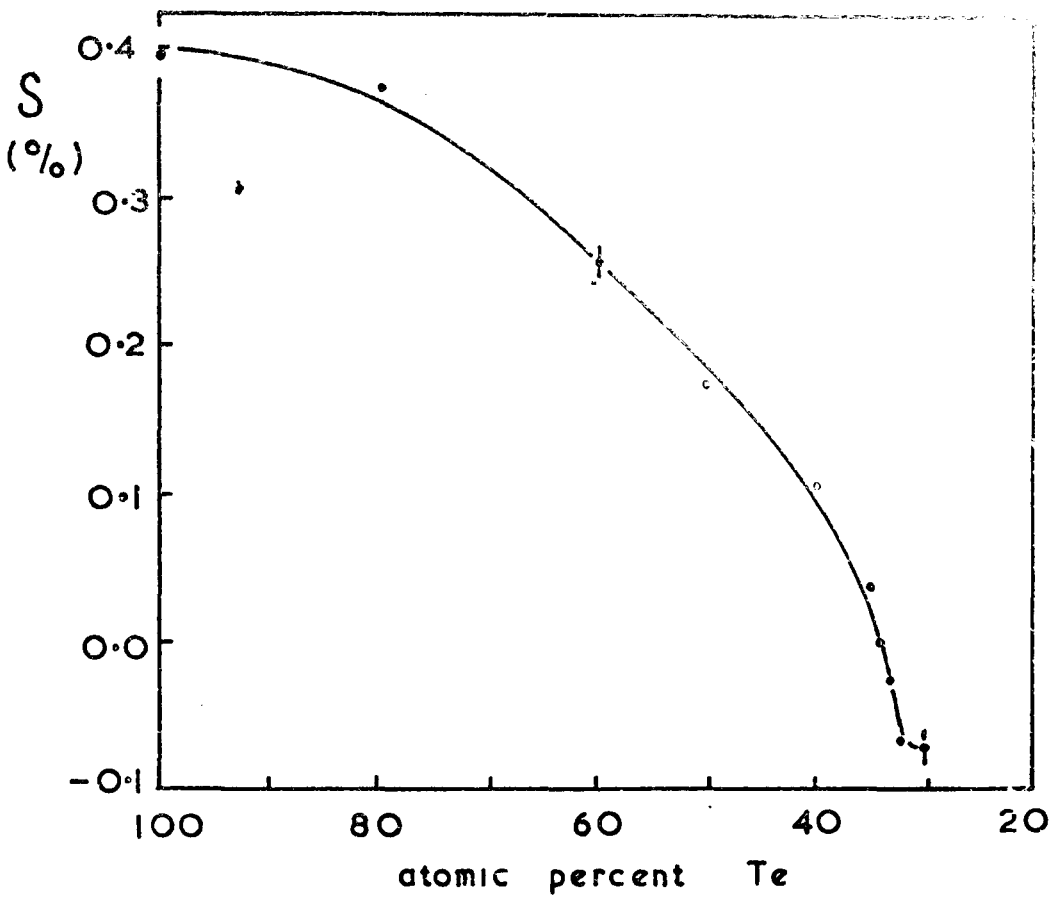

^{125}Te RESONANCE SHIFT AS A FUNCTION OF COMPOSITION IN Te–Tl AT 773K

in table 4.12. These relaxation rates are found to be enhanced over the rate which is predicted by the Korringa relationship by an amount which increases rapidly near the composition $TeTl_2$, see figure 6.7 and section 6.2.5 for further discussion.

The similarity between the general form of the conductivity, suceptibility and resonance shift measurements as a function of concentration suggests strongly that the density of states at the Fermi energy decreases steadily as Tl is added, until the composition $TeTl_2$ is reached. A detailed theory of the electron transport behaviour in Te-Tl has been proposed by Cutler (1971). This theory will now be outlined.

6.2.2 The Cutler Model This model gives a possible mechanism for the composition and temperature dependences of the density of states observed in Te-Tl.. It is basically a structural model, and applies specifically to chain structures, as may exist in alloys of Te or Se with monovalent metals. It is similar to the dilute metal model of section 6.1.2 in that conduction is through bands of extended states.

The conductivity and thermopower of the Te-Tl system behave in quite different ways on different sides of the composition $TeTl_2$. On the Tl rich side these quantities vary rapidly with composition but have small temperature dependences. A model has been proposed (Cutler and Petersen, 1971) which treats the alloys as dilute metallic solutions of Tl^{3+} ions in a matrix of stable $TeTl_2$ molecules.

On the Te rich side of $TeTl_2$ the conductivity and thermopower change rapidly with temperature but only slowly with composition, so thermal processes are more important here. From the fact that the conductivity is lowest at $TeTl_2$, and since crystalline Te is known to exist in a chain-type structure a model is proposed by Cutler (1971) which pictures alloys in this range to be made up from chains of the form $Tl\text{-}(Te)_n\text{-}Tl$, the Tl atoms fulfilling the role of chain-enders.

The starting point used to deduce a model for the electronic structure is the states corresponding to these molecules. The Te atom has two s and four p electrons in its outer shell; the s-electrons are ignored, being lower in energy, and hybridisation is not considered at this stage for simplicity. A Te-Te molecular bond orbital is formed by a linear combination of atomic p-orbitals in the bond direction which gives two bonding states, since spin states are included, denoted by σ and two more states higher in energy, antibonding states denoted by σ^*. Hence a Te atom forms two covalent bonds with other Te atoms or Tl atoms. As the Te content increases, causing the number of Te-Te bonds to increase, the conductivity increases and if this arises from broken bonds it must be easier to break a Te-Te bond than to break a Te-Tl bond. Therefore the σ bond corresponding to Te-Tl will be lower in energy than the σ bond for Te-Te. The two non-bonding p-electrons left at a Te site must remain at about their original energy, and are referred to as π electrons. These discrete energies will be broadened into bands by overlap with neighbouring atoms as in the tight binding case.

With no bonds broken all the states in the σ and π bands are filled, and the Fermi level lies at the top of the π band, as shown in figure 6.5. When a bond breaks the bonding electron will return to its original energy, in the π band but will bring two allowed states thus creating one vacant state, or hole, in the π band. Hence this model shows how p-type conduction arises, and how the density of states at the Fermi level increases with temperature.

This model differs from conventional semiconductor theory in this mechanism proposed for the increase in conductivity with temperature. Instead of electrons being thermally excited across a band gap more states are generated in the valence band.

Cutler has adapted the thermodynamic theory for polymer equilibrium (Flory, 1944) to the case for short chains, and using this has calculated

figure 6.5

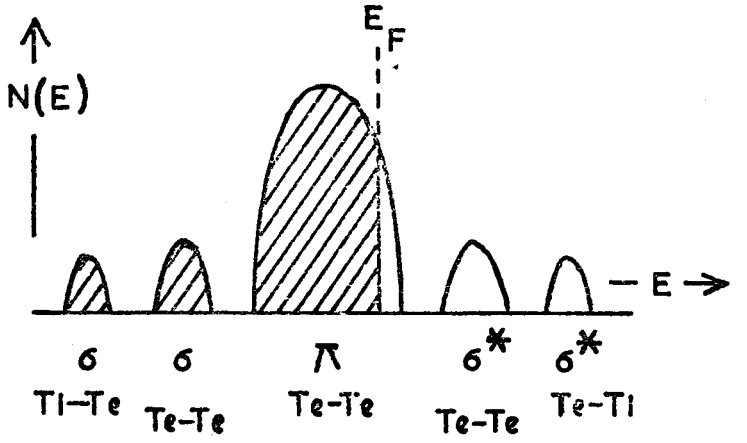

High ~~temperature~~ temperature

(some bonds broken)

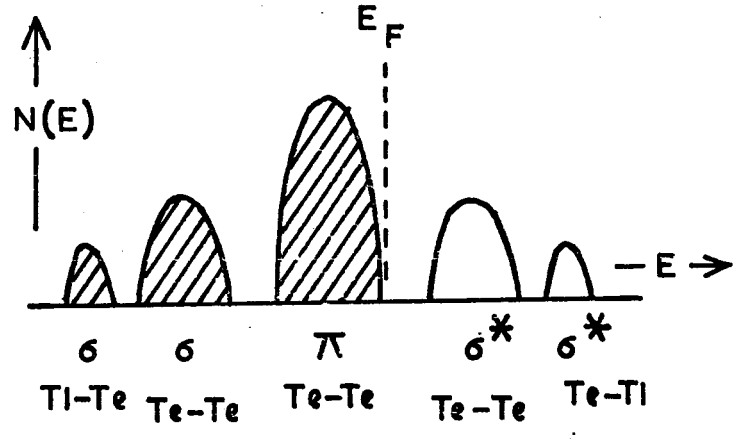

Low ~~temperature~~ temperature

(some bonds broken)

THE CUTLER MODEL FOR THE

DENSITY OF STATES IN Te-Tl

the fraction of broken bonds as a function of concentration and of temperature. Calculations of conductivity from these data give good agreement with the experimental results.

6.2.3 Discussion of the Magnetic Suceptibility Measurements

The total observed suceptibility is made up of three principal contributions, namely the suceptibilities of the ion cores, χ_c, and of the electronic Pauli spin paramagnetism, χ_p, and Landau orbital diamagnetism, χ_d.

$$\chi_t^{(m)} = \chi_c^{(m)} + \chi_p^{(m)} + \chi_d^{(m)} \quad \ldots\ (6.4)$$

where the superscripts indicate that the suceptibility is measured per unit mass.

A method which has recently been proposed (Dupree and Seymour, 1972) in the case of liquid metallic alloys for extracting the electronic terms is to estimate the contributions from the ion cores in a particular alloy by taking a weighted sum of the suceptibilities of the constituent cores, using values for the cores which have been calculated by Angus (1932). In this case where tellurium and its alloys cannot be regarded as simple assemblies of ions this method cannot be applied.

Instead, in order to make an estimate of the electronic contribution to the total suceptibility the following three assumptions were made:-

(i) that the free electron result relating the spin suceptibility to the orbital suceptibility is still valid, namely

$$\chi_d = -1/3\,\chi_p$$

(ii) that it is possible to use the free electron expression for the spin suceptibility,

$$\chi_p^{(m)} = C\,N(E_F) \quad \ldots\ (6.5)$$

where C is a constant if the density is constant and $N(E_F)$ is the density

of states at the Fermi energy per unit volume.

(iii) that the principal temperature dependence of χ_t arises from changes in χ_p and χ_d due to the temperature dependence of $N(E_F)$.

The Mott formula for conductivity when there is a strong interaction between the conduction electrons and the ions, equation 6.3, can be expressed

$$= C' \{ N(E_F) \}^2 \qquad \ldots\ (6.6)$$

where C' is constant if S_F and L are constant.

It is possible to eliminate the density of states and the constants by writing

$$1/\sigma \ (d\sigma / dT) = 2 \ (1 / \chi_p^{(m)}) \ \{ d\chi_p^{(m)} / dT \} \qquad \ldots\ (6.7)$$

assumptions (i) and (iii) give

$$(d\chi_p^{(m)} / dT) = 3/2 \ (d\chi_t^{(m)} / dT) \qquad \ldots\ (6.8)$$

σ and $d\sigma / dT$ are available for several alloys from the work of Cutler and Mallon (1966) and hence $\chi_p^{(m)}$ may be evaluated.

Table 6.1

Estimate of $X_p^{(m)}$ at 800 K

at. % Te	$\frac{d X_t^{(m)}}{dT}$ (SI units K^{-1})	$\frac{d X_p^{(m)}}{dT}$ (SI units K^{-1})	σ ($ohm^{-1}m^{-1}$)	$\left(\frac{d\sigma}{dT}\right)^{-1}$ (ohm m K)	$\chi_p^{(m)}$ (SI units K^{-1})
34	5.8×10^{-13}	8.7×10^{-13}	140	1.5	3.6×10^{-10}
36	5.8×10^{-13}	8.7×10^{-13}	200	1.4	4.8×10^{-10}
40	5.8×10^{-13}	8.7×10^{-13}	240	1.8	7.5×10^{-10}
60	22.1×10^{-13}	33.1×10^{-13}	720	0.66	31.7×10^{-10}
100	49×10^{-13}	73×10^{-13}	2200	0.23	76×10^{-10}

It is seen that, as would be expected from the above models, the

conduction electron suceptibility decreases rapidly in going from Te_{100} to near $TeTl_2$; (only a small fraction of the change can be attributed to the change in density of the liquid).

Assumption (i) requires that the ratio of effective mass, m^*, to the electron mass, m, remains unity as in the free electron case. Since m^* reflects the interaction between the conduction electrons and the ions it is likely to be different from the free electron value here. Liquid bismuth and liquid antimony probably have values of m^* / m appreciably less than 1 (Dupree and Seymour, 1972) and it may be that the same is true for liquid tellurium. Since m^* affects χ_p and χ_d in inverse ways, the overall effect of reducing m^* is to reduce χ. It seems likely therefore that the values of $\chi_p^{(m)}$ above are overestimated, more so in the case of $TeTl_2$ than of Te_{100} where the conduction electron-ion interaction is not so strong; (of course a change in $N(E_F)$ due to filling up a pseudogap could well also change m^*. This possibility is ignored.) Further, on the dilute metal model a change in $N(E_F)$ would be accompanied by a change in S_F; for a free electron band the changes would be such that the factor on the right hand side of equation 6.7 would be 4 rather than 2. The qualitative conclusion that χ_p decreases rapidly near $TeTl_2$ is unaltered.

The estimated values of χ_c may now be found by subtracting χ_e from χ_t

Table 6.2

Estimate of $\chi_c^{(m)}$ at 800 K

at. % Te	34	36	40	60	100
$\chi_c^{(m)}$ (SI units)	-2.8×10^{-9}	-2.8×10^{-9}	-2.8×10^{-9}	-3.9×10^{-9}	-5.3×10^{-9}

The estimated value for $\chi_c^{(m)}$ for Te_{100} lies between the two values calculated by Angus, -1.8×10^{-9} SI units for a Te^{6+} core, and -6.8×10^{-9} SI units for a Te^{2-} core. The variation between these two

extremes will not be linear and so the degree of 'ionisation' of the Te nucleus cannot be evaluated, although this value for $\chi_c^{(m)}$ does imply that it cannot be fully ionised. The value calculated by Angus for a metallic Tl^{3+} nucleus is -2.4×10^{-9} SI units which is similar to the estimate for $\chi_c^{(m)}$ at $Te_{34}Tl_{36}$. Hence χ_c as a function of composition appears to deviate from linear behaviour, and although the uncertainties in the values of χ_c are too large to show any deviation conclusively it does suggest that the electrons involved in Te-Tl bonds appear to reduce the overall core diamagnetism.

6.2.4 Discussion of the ^{125}Te resonance shift measurements. The observed nuclear resonance shift is composed of three main contributions; that due to the direct contact interaction between the nucleus and the conduction electrons, S_s, that due to the polarisation of the s-type core electrons by the conduction electrons, S_{cp}, and a third contribution which arises from the orbital motion of the valence and conduction electrons, Δ.

The contact shift has been expressed in section 5.2,

$$S_s = (2/3)\,\Omega\, P_F\, \chi_p^{(v)} \qquad \ldots\ (6.9)$$

Core polarisation shifts, S_{cp}, are a much more complex problem. These have been discussed in section 5.2.2 where it is concluded that S_{cp} varies from element to element but is likely to lie in the range $\pm 15\%\ S_s$. Since both S_s and S_{cp} are proportional to χ_p they will be included in a single term and the observed resonance shift will be expressed

$$S = \beta\, \chi_p^{(v)} + \Delta \qquad \ldots\ (6.10)$$

If as a first approximation β and Δ are assumed to be independent of temperature they may be found by comparison of the temperature dependence of S and of $\chi_p^{(v)}$. A comparison of conductivities with S using

temperature as the implicit variable will also enable Δ to be estimated.

a) Calculation of β and Δ using suceptibility measurements. Values of $\chi_p^{(v)}$ and its temperature dependence were calculated from the experimental values $\chi_p^{(m)}$ using density measurements available for all the alloys (Kanda 1967). Then by differentiating equation 6.10 with respect to temperature β is first deduced; hence Δ can be found for each alloy.

Table 6.3

Estimate of β from suceptibility measurements

at. % Te	$\frac{dS}{dT}$ (K^{-1})	$\frac{d\chi_p^{(v)}}{dT}$ (SI units K^{-1})	β (SI units)
34	2.5×10^{-6}	7.3×10^{-9}	340
36	2.5×10^{-6}	7.5×10^{-9}	330
40	4.9×10^{-6}	7.7×10^{-9}	640
60	4.9×10^{-6}	27×10^{-9}	180

Table 6.4

Estimate of Δ at 800 K from suceptibility measurements

at. % Te	S (%)	$\beta\chi_p^{(v)}$	Δ (%)
34	- 0.01	0.06×10^{-2}	- 0.07
36	+ 0.04	0.12×10^{-2}	- 0.08
40	+ 0.12	0.39×10^{-2}	- 0.27
60	+ 0.27	0.37×10^{-2}	- 0.10

b) Calculation of Δ using conductivity measurements.

The resonance shift may be expressed in terms of the density of states by

substituting for χ_p in equation 6.9 giving

$$S = \beta a N(E_F) + \Delta \quad \ldots\ (6.11)$$

where a is a constant (the alloy density times C, see equation 6.5. Since the conductivity has already been given in terms of $N(E_F)$ in equation 6.6 plotting S against $\sigma^{\frac{1}{2}}$ will yield Δ. The gradient of this plot will depend on a and on C', defined in equation 6.6; both are constant for a particular alloy but could depend on composition hence the graphs for different alloys need not all have the same gradient. However when plotted on the same axis, see figure 6.6 alloys having Te concentrations of 40, 45 and 60 at. % respectively all appear to be on the same straight line with intercept

$$\Delta = -0.15 \pm 0.03\ \%$$

The data points for $Te_{35}Tl_{65}$ do not lie on this line but do have the same intercept, within the uncertainity quoted. In this region the conductivity is changing very rapidly and a change of less than 1% in the Te content would put the points on to the common line; hence it cannot be said that the change of slope is significant.

c) Discussion of the values of β and Δ. In Te_{100} β was found to be 160 SI units but has not been included in table 6.3 since the uncertainty in this value is very large due to the difficulty in extracting accurate values from published graphs of σ and χ_t.

A calculation of β for a Te^{6+} ion has been made (Heighway and Seymour, 1971) by representing a conduction electron at the Fermi energy by a single orthogonalised plane wave. The value obtained was β = 350 SI units. Comparison of the values for β indicates that the conduction-electron wavefunction density at the nucleus is not violently composition dependent and that the change in S must be largely due to the composition dependence of $N(E_F)$.

It is now possible to investigate the fractional s-character in this wavefunction. It is useful to introduce a factor ξ given by

Figure 6.6

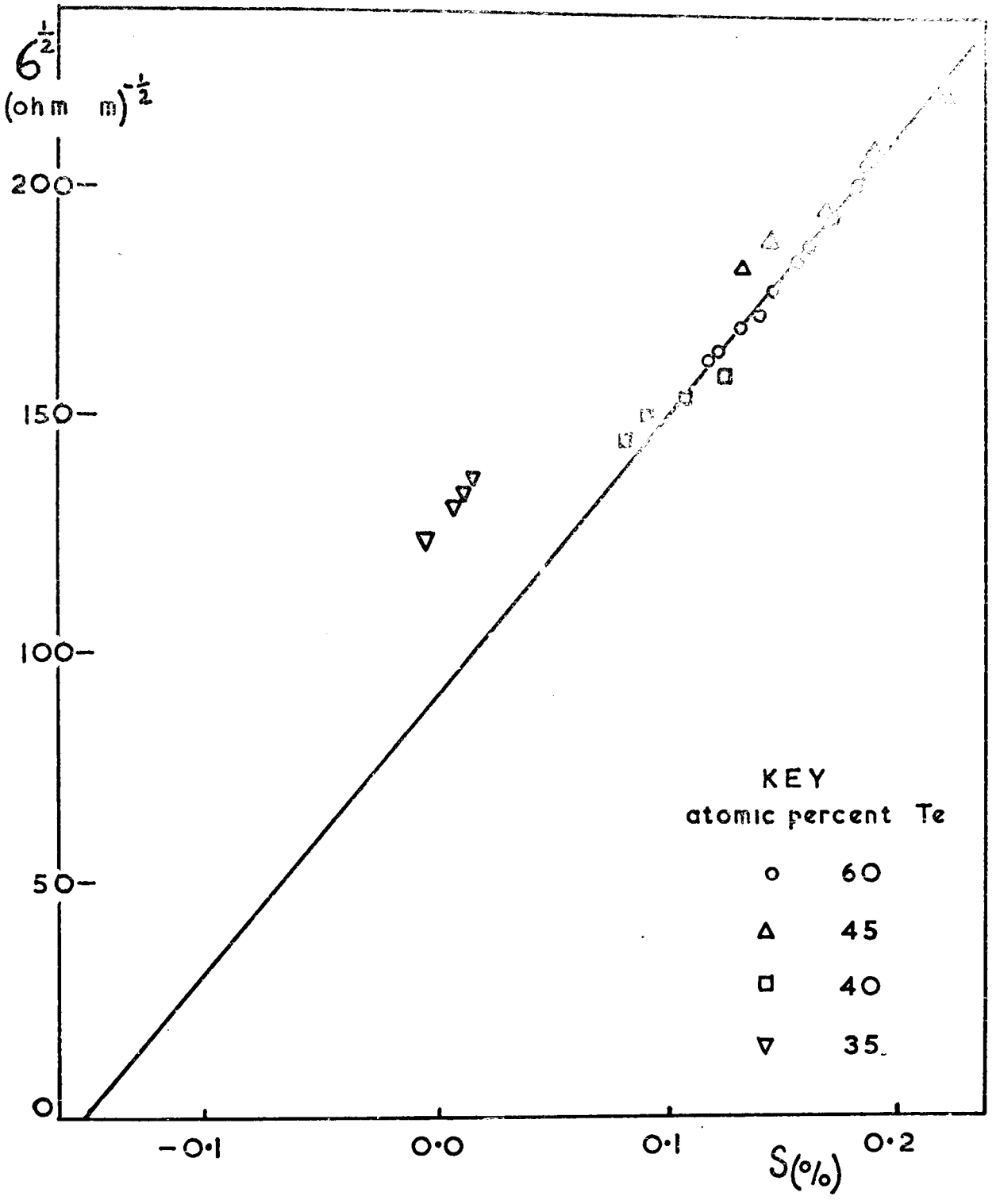

^{125}Te RESONANCE SHIFT vs (CONDUCTIVITY)$^{\frac{1}{2}}$ FOR SOME Te–Tl ALLOYS AT DIFFERENT TEMPERATURES

$$\xi = P_F / P_A$$

where P_A is the density at the nucleus of the outermost shell s electrons in a free atom. ξ can be estimated from the above OPW calculation of P_F and the tabulated 5 s atomic wavefunction for the neutral atom given by Herman and Skillman (1963). Extrapolating the Te 5 s function to $r = 0$ gives $P_A = 25$ in atomic units, and hence in this case $\beta = 4100$ SI units.

$$\xi = \frac{350}{4100} = 0.08$$

Alternatively ξ can be estimated from experiment. If the core polarisation part of β is neglected then β is simply $2/3\ \Omega\ P_F$, then taking the maximum observed shift and using the free electron value for χ_p this gives $P_F = 1.5$ in atomic units. P_A can be estimated from the observed atomic hyperfine splitting constant, a_s. Bennett, Watson and Carter (1970) found $P_A = 33.6$ atomic units; hence $\xi = 0.045$. The agreement between these two values indicates that the conduction electron wavefunction in Te has about 5% s-character, and this proportion does not change much on adding Tl. This implies that the p-character must be large which is in keeping with the predictions of the Cutler model.

The values of Δ derived above indicate clearly the existence of a negative chemical shift near $TeTl_2$. The general interpretation of the resonance shift measurements is that as the density of states falls, either due to reduction of the Te content or a reduction in temperature then $\chi_p^{(v)}$ diminishes and the resonance shift tends to Δ, which has its origin in the orbital motion of the Te-Tl bonding electrons. The largest negative shifts observed occurred in $Te_{31}Tl_{69}$ and $Te_{33}Tl_{67}$ at temperatures around 64.0 K and were $S = -0.11 \pm 0.01\%$. Hence taking $\Delta = -0.15\%$ in the range of 33 to 60 at. % Te as given by the S vs $\sigma^{\frac{1}{2}}$ analysis is in good agreement with the experimental results and if

anything overestimates the magnitude of Δ. The average of the values of Δ calculated from the S vs χ analysis is $\Delta = -0.13 \pm 0.05\%$ which is in agreement with the conclusion above. This value for the ^{125}Te chemical shift is reasonable in the light of the value of - 0.24% observed in semiconducting $Pb_{45}Sn_5Te_{50}$ at room temperature (Claridge and Moore, unpublished) and - 0.1% for ^{125}Te in the amorphous state of $Te_{81}Ge_{15}As_4$ (Senturia, Hewes and Adler; 1970).

There is little change of resonance shift on going from $Te_{33}Tl_{67}$ to $Te_{31}Tl_{69}$ which suggests that the electronic environment of the Te nuclei is no longer changing rapidly as Te content decreases; (as would be expected on the dilute metal model of $TeTl_2$ molecules with free Tl atoms). The temperature dependence of the shift is the same in both alloys and so the mechanism by which the density of states increases with temperature has not changed.

6.2.5. Discussion of the ^{125}Te spin-lattice relaxation rate measurements. The observed spin-lattice relaxation rates do not show any marked dependence on concentration and hence it appears that the Korringa relationship does not hold in these alloys, since the behaviour of the resonance shift predicts that the rate should decrease steadily as the tellurium content decreases from 100 to 33 at. %.

The Korringa relationship can be expressed from section 5.2 as

$$R_1 = \frac{4\pi k}{\hbar} \left\{ \frac{\gamma_n}{\gamma_e} \right\}^2 T S_s^2 \Big/ K(\alpha) \qquad \ldots\ldots (6.13)$$

Where S_s is the part of the resonance shift which arises from the direct contact interaction. As discussed in the previous section it is not possible to disentangle the core polarisation part from the contact part, but this should cause about 20% uncertainity in R_1 at most.

The chemical shift, Δ, has been estimated above to be - 0.15% in

alloys near $TeTl_2$ and hence must arise from the Te-Tl bonds. This shift must decrease as the Tl content decreases and has been taken to be - 0.15% for alloys in the range $Te_{31}Tl_{69}$ to $Te_{60}Tl_{40}$, and arbitrarily to be - 0.07% for $Te_{80}Tl_{20}$ and 0% for Te_{100}. Using these values for Δ and the observed shifts to evaluate S_s, the Korringa relationship has been used to calculate relaxation rates for each alloy at each temperature of observation.

Table 6.5

^{125}Te nuclear spin-lattice relaxation rates

Alloy (at. % Te)	T (kelvins)	$(R_1)_{observed}$ ($10^3 s^{-1}$)	$(R_1)_{Korringa}$ ($10^3 s^{-1}$)	$\frac{(R_1)_{observed}}{(R_1)_{Korringa}}$
100	695	5.2 ± 1.1	3.1	1.7
	778	6.7 ± 1.3	4.8	1.4
80	523	2.1 ± 0.4	0.96	2.2
	625	5.4 ± 1.5	2.5	2.2
60	473	1.8 ± 0.3	0.68	2.7
	573	3.0 ± 0.7	1.8	1.7
	690	5.0 ± 2.5	3.6	1.4
45	563	3.1 ± 0.4	1.0	2.9
	663	5.0 ± 2.5	1.8	2.8
40	719	4.3 ± 1.1	1.5	3.0
36	741	4.6 ± 1.3	0.93	5.1
35	737	5.2 ± 1.9	0.56	9.5
34	718	6.7 ± 2.2	0.36	19
33	705	1.0 ± 0.25	0.10	10
	841	1.7 ± 0.3	0.38	4.5
31	662	0.74 ± 0.2	0.42	18
	831	1.0 ± 0.2	0.32	3.1

Comparison of the observed relaxation rates with those calculated from the Korringa relationship, see table 6.5 and figure 6.7, suggests that some other relaxation mechanism must also be present to account for the additional rates observed in most alloys, or else the Korringa formulation fails. Electric quadrupolar relaxation is already ruled out since the ^{125}Te nuclear spin is one half, so other possible mechanisms must be considered.

If there is a hyperfine field due to polarisation of the core electrons not only will this affect the value of $(R_1)_{Korringa}$ through the magnitude of the observed shift, but it will also produce nuclear spin relaxation in its own right. This mechanism has been discussed in section 5.2.2 where it has been shown to be ineffective in comparison to the direct contact interaction, and also, since it depends on $N(E_F)$ it must get less effective on going towards $TeTl_2$ and so cannot explain the data.

The relaxation rate arising from the orbital motion of p-type electrons has been derived by Obata (1963) using the tight binding approximation, a model suitable for these alloys.

$$(R_1)_{orb} = \frac{8\pi kT}{\hbar} \left(\gamma_e \gamma_n \hbar^2 \left\langle r^{-3} \right\rangle \frac{N(E_F)}{N V} \right)^2 \quad \ldots\ (6.14)$$

where N is the number of atoms per unit volume,

V is the valency,

r is the electron-nucleus separation.

For any of the alloys, say $Te_{36}Tl_{64}$ the density of states may be found from the value of $\chi_p^{(v)}$ using the free electron expression for the spin suceptibility. As discussed earlier it is not possible to say how many free electrons there are in these alloys, but if it is only one per atom say then at 740 K.

$$(R_1)_{orb} = 620\ s^{-1}$$

figure 6.7

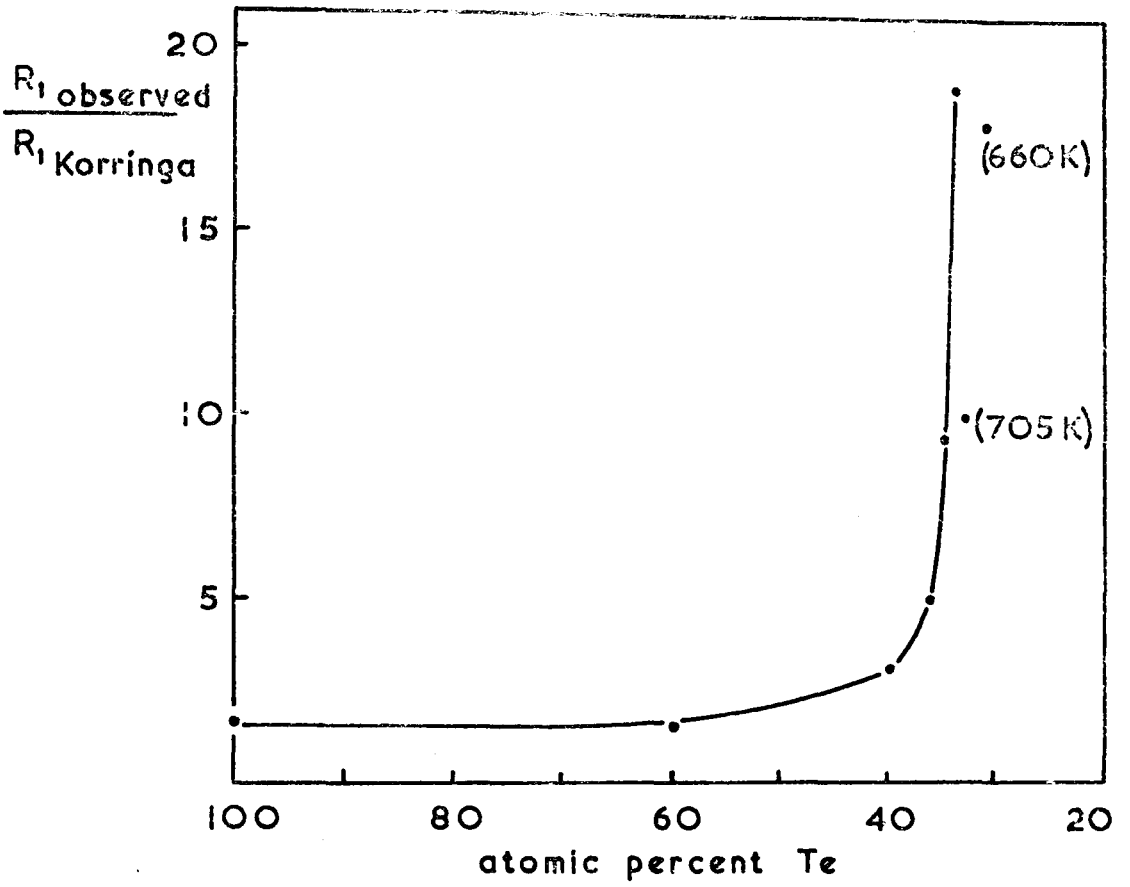

ENHANCEMENT OF THE ^{125}Te SPIN-LATTICE RELAXATION RATE AS A FUNCTION OF CONCENTRATION IN Te-Tl AT 730 K

If the valency is larger then equation 6.14 predicts a smaller R_1 and therefore this process is too weak to explain the apparent extra relaxation rate.

There are also several mechanisms which arise from ionic motions, tumbling motion of molecules or the change in environment of a Te nucleus by moving from say a $TeTl_2$ molecule to become a free ion. Since a chemical shift is known to exist its effect will be considered first. This shift can cause relaxation if it is anisotropic by reorientation due to molecular motion. Abragam (1961) has derived an expression for this process

$$(R_1)_{cr} = \frac{6}{40} \gamma_n^2 B_0^2 \delta_z^2 (1 + \eta^2/3) \tilde{J}(\omega_L) \quad \ldots\ (6.15$$

where δ_z is the largest component of the chemical shift,

η is the shift asymmetry parameter (where $0 < \eta < 1$),

$\tilde{J}(\omega_L)$ is the component at ω_L of the fourier transform reduced correlation function for the chemical shift interaction.

The interaction may be typified by a correlation time τ_c and in the case where this is short compared to the Larmor period $1/\omega_L$ as it will be here $\tilde{J}(\omega_L) = \tilde{J}(0) = 2\tau_c$. Typical τ_c for molecular rotation in liquids are of order 10^{-11}s. Bensoussan (1967) has measured the chemical shift in a single crystal of Te and found a paramagnetic shift characterised by $\delta_x = \delta_y - 0.05\%$, $\delta_z = + 0.11\%$. The estimate of chemical shift in liquid $TeTl_2$ above is - 0.15% so for the purposes of this calculation $|\delta_z| = 0.15\%$ and $\eta = 0$ will be used. It is found that $(R_1)_{cr} = 2 \times 10^{-2} s^{-1}$, which is far too small to be of interest.

The same expression can be used to evaluate the relaxation rate which could arise if the chemical shift was modulated due to chemical exchange, causing the chemical shift to vary between 0.15% and 0. The correlation time for this process is not known, but it will be at its most

effective when comparable to the Larmor period, 10^{-7}s. If it were even longer two resonance lines corresponding to the two environments would be seen, but only a single line was seen. With $\tau_c = 10^{-7}$s the rate $(R_1)_{ce} = 100\ s^{-1}$. The Te-Te bond lifetime has been estimated by Cabane and Friedel (1971) in Te_{100} to be of order 10^{-12}s and so the value of $(R_1)_{ce}$ above is clearly very much an upper limit.

The normal dipole-dipole coupling can cause relaxation in the presence of molecular rotation. $\tau_c = 10^{-11}$s as used above is short compared to the Larmor period and so the suitable expression for the relaxation of Te nuclei in $TeTl_2$ molecular groups is given (Abragam, 1961)

$$(R_1)_r = \frac{\gamma_{Te}^2 \gamma_{Tl}^2 \hbar^2}{b^6} \tau_c \qquad \ldots\ (6.16$$

where b is the inter-molecular distance, here estimated to be 3×10^{-10}m.

The calculation gives $(R_1)_r = 10^{-4}s^{-1}$ which is negligible.

A further interaction is the scalar spin-spin coupling where two unlike nuclear spins are indirectly coupled via the conduction electrons. The relaxation rate in $TeTl_2$ due to chemical exchange of Tl ions can be calculated using an expression derived by Abragam (1961)

$$(R_1)_{sc} = \frac{2A^2}{3} S(S+1) \frac{\tau_2}{\left[1 + (\omega_{Te} - \omega_{Tl})^2 \tau_2^2\right]} \qquad \ldots\ (6.17$$

where A is the scalar coupling constant,

S is the Tl spin,

τ_2 is the correlation time for chemical exchange of the Tl ions.

A is estimated to be 2×10^4rad s^{-1} in the metallic phase of InTe (Brog, Jones and Milford, 1966). It is not known what value τ_2 has and although it could be as small as 10^{-12}s the relaxation rate is largest

when $\tau_2(\omega_{Te} - \omega_{Tl}) = 1$. Even in this case $(R_1)_{sc} = 4\ s^{-1}$ which again is too small to be important.

Finally it is suggested, see section 6.2.5, that the Tl spin-lattice relaxation rate is as rapid as $10^5 s^{-1}$ so this could cause relaxation of the Te nuclei via the indirect spin-spin coupling. The previous formula is applicable but now $\tau_2 = 1/T_1\,(Tl) = 10^{-5}s$. This gives $(R_1)_{sT_1} = 10^{-2}s^{-1}$, and so is even less effective.

It is apparent that none of the possible relaxation mechanisms so far considered, even at their most effective, can account for the increase in relaxation rate over that calculated from the resonance shift measurements. Another explanation must be sought as to why the relaxation rate has been enhanced, particularly in the range of composition near $TeTl_2$. It is in this region that the density of states at the Fermi energy is low and so according to the Mott model it is possible that the conduction electrons are becoming localised.

Warren (1971) has considered this possibility and suggests that nuclear spin-lattice relaxation will be sensitive to localisation of conduction electrons. His work will be discussed in detail below (section 6.5.2); however the main principle will be outlined here.

In the short correlation time limit ($\omega_L \tau_c \ll 1$) the nuclear spin-lattice relaxation rate due to perturbation which is a random function of time, $\mathcal{H}_1$, has been shown in section 1.1.2 to be given by

$$R_1 \simeq 1/\hbar^2 \overline{|\mathcal{H}_1|^2}\ \tau_c$$

where τ_c is the correlation time for the interaction.
When the interaction is the contact interaction between the nuclear spins and the conduction electrons the relaxation rate is given by

$$R_1 = 1/\hbar^2 \left[(8\pi/3)\,\gamma_e\,\gamma_n\hbar^2\right]^2 (\Omega P_F)^2 (kT/E_F)\,\tau_c \qquad \ldots\ (6.18)$$

The factor (kT / E_F) is included because only electrons within kT of the Fermi energy can absorb the nuclear energy as it relaxes. This equation can be combined with the resonance shift expression, equation 6.9 to give a form of the Korringa relationship

$$R_1 = (\gamma_n / \gamma_e)^2 \ (kT\, E_F / \hbar^2) \ S_s^2 \ \tau_c \qquad \ldots\ (6.19)$$

In materials where the electron mean free path is long, the time which a conduction electron spends in the vicinity of a particular nucleus does not depend on the mean free path, since it is just the time taken to transverse the unit cell. The Fermi velocity is given by Bloembergen (1954)

$$v_F = 2a\, E_F / Z\hbar$$

where Z is the number of conduction electrons per atom,

a is the nearest neighbour distance.

Hence the electron-nucleus correlation time is

$$\tau_c = a / v_F = \hbar / E_F \qquad \ldots\ (6.20$$

Substituting this into equation 6.19 gives the usual Korringa relationship to within a numerical factor. Warren points out that the pseudogap theory predicts that in these materials where the scattering is large, the mean free path is of the order of the interatomic spacing, so if the density of states is reduced sufficiently the electron remains for a longer time in the vicinity of one nucleus, τ_c will increase and formula 6.19 predicts that there will be an enhancement of the relaxation rate.

This provides a plausible explanation for the observations of the ^{125}Te spin-lattice relaxation times in the Te-Tl system. As Tl is added to Te the density of states decreases to the point where, at around $Te_{40}Tl_{60}$, the electrons begin to increase their time of stay in the vicinity of a particular nucleus and the relaxation rate is enhanced over the simple Korringa value. This enhancement increases until $Te_{33}Tl_{67}$ is

reached, and in $Te_{31}Tl_{69}$ it is still observed although not quite so marked as in $Te_{33}Tl_{67}$. It is of course to be expected that since there will be a spread of concentrations in any liquid alloy due to thermal motions the effect will be observed in a range of alloys.

It is difficult to deduce when localisation as such occurs for there is no satisfactory criterion. These results show that 730 K when the resonance shift, and hence the density of states is reduced to about one half of the value in Te_{100} there is some small indication of the onset of localisation. By the time the density of states has dropped by a factor of 7 the enhancement factor is 10. The uncertainty in the enhancement factor must be large to judge from the values in high Te concentrations where a factor of 1 is expected, but the value is 2 or more. In good liquid metals the factor is less than 1 but this is due mainly to electron-electron interactions which have not been included in the Korringa expression. Electron-electron interactions are expected to be small here and so the discrepancy must arise from uncertainties in S_s measurements, in possible core-polarisation effects and in the value for the chemical shift. The uncertainties in R_1 measurements will also contribute appreciably.

Mott has estimated that when the conductivity has fallen to $(20 \pm 7) \times 10^3 \text{ohm}^{-1}\text{m}^{-1}$ localisation can occur, which corresponds to alloys with Te content between 32 and 35 at. %, or as far as 40 at. % at around 700 K when the uncertainty is included, which agrees well with the R_1 observations.

The conduction process for fully localised electrons is by hopping, so presumably the jump time for the electrons will be of the order of the phonon vibration period, about 10^{-12}s or longer; alternatively the lifetime of the local configuration could be the dominant time. In the nearly free electron case the correlation time τ_e is given by $\hbar N(E_F) = 10^{-15}$s, so fully localised electrons could be expected to

produce relaxation enhancement factors of the order of 10^3. (Alternatively the effective field fluctuations due to a localised electron could be produced by the electron spin-lattice relaxation; such times vary widely but would be 10^{-9}s or longer.) Hence in this case only the onset of localisation is being observed.

6.2.6 The search for the ^{205}Tl resonance The first search for the ^{205}Tl nuclear resonance was made in $Te_{60}Tl_{40}$ using the pulse spectrometer, but no signal was observed. Several other alloys were tried but in none of them was any signal seen. This was surprising and disappointing since it had been hoped that information extending that derived from the ^{125}Te resonance would have been obtained. The ^{205}Tl resonance is about six times larger than the ^{125}Te resonance in $Te_{60}Tl_{40}$, and even if the relaxation rate was as low as 100 s^{-1} it should have been visible. The response time of the spectrometer sets an upper limit on relaxation rates that can be detected of around $R_1 = 50{,}000\ s^{-1}$. It is concluded that

$$R_1\ (^{205}Tl) > 50 \times 10^3 s^{-1}$$

To check this conclusion the $Te_{60}Tl_{40}$ alloy was investigated using a Varian VF 16 wide-line CW spectrometer. Again no resonance was seen, and again there is an upper limit to the linewidth (which is proportional to the relaxation rate) that can be detected. This arises in the first instance from the maximum modulation that can be used, in this particular case 1 mT. Secondly if the line is wide, and of small intensity it will be obscured by the noise. The combination of these factors implies that $R_1\ (^{205}Tl) > 100 \times 10^3 s^{-1}$. To ensure that the spectrometer was performing satisfactorily the ^{125}Te nuclear resonance was observed, but due to poor signal to noise the linewidth could not be measured.

Finally a search was made in solid $Te_{60}Tl_{40}$ and here the ^{205}Tl resonance was observed. The resonance shift varied from 0.27% at room temperature to 0.41 ± 0.03% at a few kelvins below the melting point (540 K), indicating that the density of states is well below the free-electron value. The Korringa relationship predicts $(R_1)_s$ = $(12 \pm 3) \times 10^3 s^{-1}$ at 520 K. The resonance line, which is Lorentzian in shape, at 520 K had a measured width of not much greater than the modulation width but applying a correction (Smith, 1964) the true line-width is estimated to be $(3.0 \pm 0.3) \times 10^{-4}$ T. This corresponds to a spin-spin relaxation rate of $R_2 = (40 \pm 8) \times 10^3 s^{-1}$ which suggests that some other process, probably self-diffusion of the nuclei is causing the additional spin dephasing rate.

Difficulty in observing the ^{205}Tl nuclear resonance arises due to its large γ_n value and hence rapid 'Korringa' relaxation. The resonance has been reported in pure liquid Tl (Moulson, 1966) and has a resonance shift of 1.56% which corresponds to a relaxation rate $(R_1)_s = 200 \times 10^3 s^{-1}$. Hence if the resonance shift in $Te_{60}Tl_{40}$ increases by a factor of 3 or more on going to the liquid state and if the Korringa relation continues to hold the spin-lattice relaxation rate will be too large for the resonance to be observable on this spectrometer. This increase in resonance shift could arise from a change in the wave function character at the Tl nucleus on melting and if it is the case it is likely to occur in other Te-containing alloys. An investigation of the Cu resonance in $Cu_{50}Te_{50}$, for example, should show the same behaviour. The alternative possibility that partial localisation is increasing $(R_1)_s$ at this composition is discounted in view of the results for ^{125}Te.

These observations are borne out by a recent report (Warren, 1972) that $R_1 = 200 \times 10^3 s^{-1}$ for ^{205}Tl in $Te_{33}Tl_{67}$ at 700 K. It was also reported that the resonance was unobservable for Tl concentrations below 66 at. % due to R_1 increasing to beyond the limit of resolution of the

spectrometer.

6.3 $Cu_{50}Te_{50}$

6.3.1 The Cu-Te system

The solid phase diagram for this system shows considerable similarity to that for Te-Tl (Hansen, 1958) except that, since Cu melts at a much higher temperature than Tl the liquidus is lifted considerably in temperature. Both have a eutectic at around 70 at. % Te, a eutectic at around 30 at. % Te and both have a region of solid immiscibility from about 4 at. % Te up to 30 at. % Te.

The conductivity (Dancy, 1965) has a singularity at around Cu_2Te, and has a positive temperature coefficient there. Although the temperature dependence of the conductivity does become negative on the Te rich side of Cu_2Te it becomes positive again by 42 at. % Te and remains so right through to 100 at. % Te. The magnitudes of the conductivities are rather larger than for Te-Tl, for example at 970 K in $Cu_{50}Te_{50}$, $= 200 \times 10^3\ \Omega^{-1}m^{-1}$, whereas in $Te_{50}Tl_{50}$, $= 70 \times 10^3\ \Omega^{-1}m^{-1}$.

The thermopower (Dancy, 1965) has a rounded maximum of about 100 $\mu V.(\text{kelvins})^{-1}$ which peaks at a few % on the Te rich side of Cu_2Te. The large positive thermopower if interpreted on conventional semiconductor theory indicates that the charge carriers are holes. The Hall coefficient has been measured in $Cu_{50}Te_{50}$ (Enderby and Simmons, 1969) and is negative which, from conventional theory, indicates electronic conduction.

If there is any correlation between the properties of a liquid and the existence of compounds in the solid state which explains the behaviour in Te-Tl then the properties described above indicate that the same behaviour should be observed in the Cu-Te system.

6.3.2 Discussion of the magnetic resonance measurements

The purpose of the investigation was to observe the behaviour of the NMR of the Cu nuclei on melting. Alloys with Te content less than 50 at. % were ruled out since their melting points were too high for the spectrometer furnace. $Cu_{50}Te_{50}$ is available at 99.99% purity (Koch Light Laboratories) and melts at 895 K, so it was chosen. The temperatures were too high to allow the ^{125}Te resonance to be observed satisfactorily but the resonance of both ^{63}Cu and ^{65}Cu were measured thus enabling isotopic separation of relaxation contributions to be carried out.

The ^{63}Cu and ^{65}Cu nuclei both have spin $I = 3/2$ and hence can be relaxed both via the nuclear magnetic dipole and electric quadrupole interactions with the lattice. It has been shown in section 5.3 that the parts of the observed relaxation rate due to each of these mechanisms may be resolved when relaxation rates of two isotopes can be measured. The ratio of the magnetic rates of the two nuclei is given by the ratio of the squares of the gyromagnetic ratios, and the ratio of the quadrupolar relaxation rates by the ratio of the squares of their quadrupole moments. Providing these two ratios are not the same it is simple to deduce an expression for each rate in terms of the observed rates and of these ratios.

The results of resonance shift and spin-lattice relaxation rate measurements on ^{63}Cu and ^{65}Cu in $Cu_{50}Te_{50}$ are displayed in table 4.14. The results of the isotopic separations are displayed in table 6.6 and some are shown in figure 6.8. The uncertainties are large due to the fact that the observed relaxation rates in the two isotopes are similar in magnitude.

These results, which show a general trend of magnetic relaxation increasing with temperature, and quadrupolar relaxation decreasing with increasing temperature as would be expected, will now be discussed individually.

Table 6.6

Magnetic and quadrupolar contributions to the relaxation rate in CuTe

Nucleus	T (kelvins)	$(R_1)_M$ (s^{-1})	$(R_1)_Q$ (s^{-1})
^{63}Cu	700	150 ± 750	1050 ± 750
	850	40 ± 300	1000 ± 300
	950	680 ± 400	220 ± 400
	1040	1090 ± 350	(0 + 170)
	1120	400 ± 400	500 ± 400
^{65}Cu	700	180 ± 800	900 ± 800
	850	40 ± 350	860 ± 350
	950	780 ±	190 ± 440
	1040	1250 ± 400	(0 + 240)
	1120	470 ± 440	420 ± 440

a) Magnetic relaxation. The behaviour of each isotope is similar and ^{63}Cu will be considered in detail since it is the stronger resonance, and more resonance shift measurements were made on it. Direct comparison of the observed shifts, (of order 0.04%) with those in pure liquid Cu, (0.26 ± 0.003)% (Warren and Clark, 1970) suggests that the density of states at the Fermi energy is reduced by a factor of around six from the free-electron value. However if the Cu nuclei experience a chemical shift comparable to that which exists in $Te_{50}Tl_{50}$ at the Te nuclei, of say - 0.1% then K_s (^{63}Cu) = 0.14% and the reduction in the density of states would only be by a factor of two. This neglects any possible change in the conduction electron wave function character. Unfortunately the conductivity data are insufficient to enable the chemical shift to be found from a $\sigma^{\frac{1}{2}}$ vs S analysis.

figure 6.8

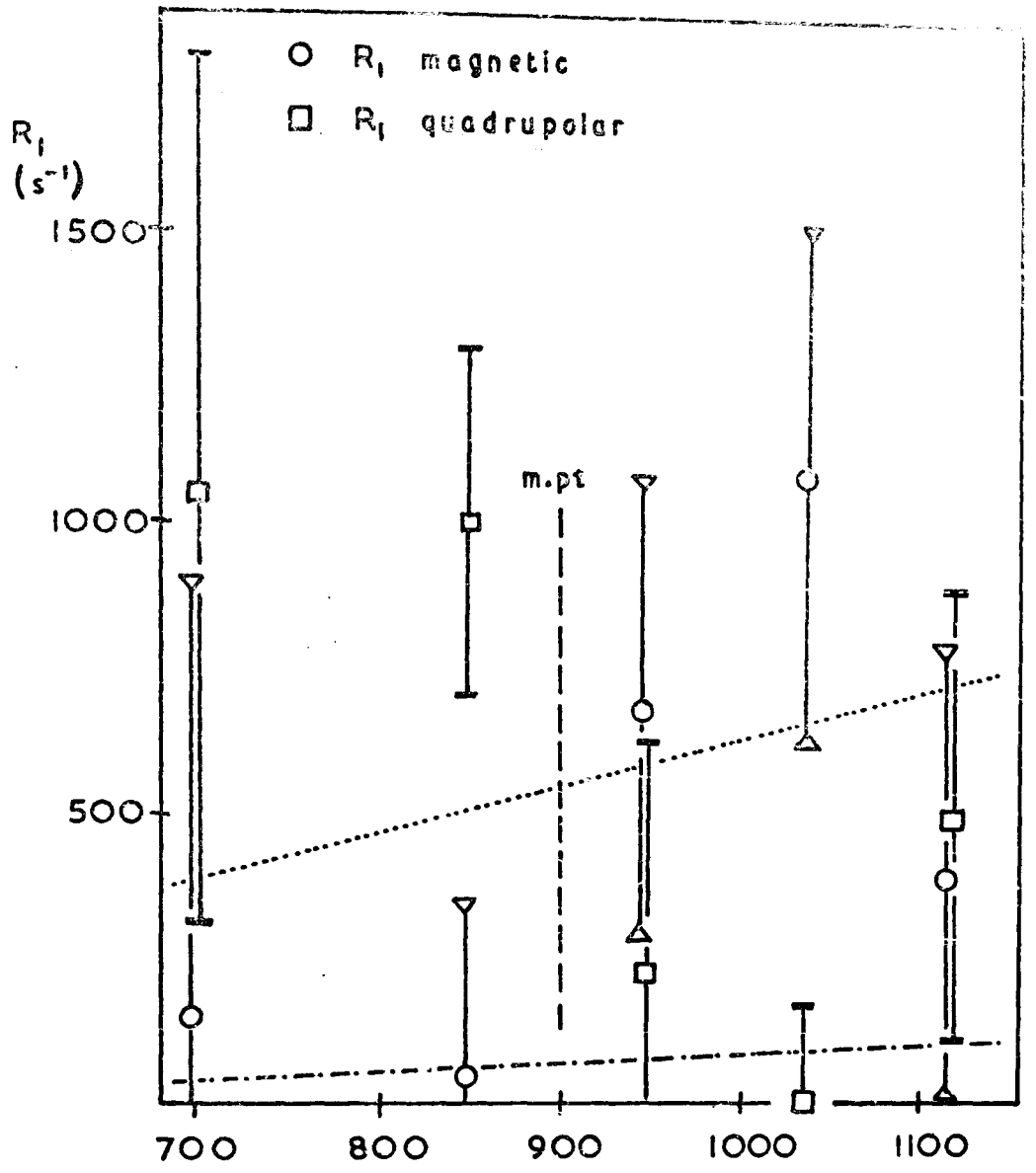

^{63}Cu MAGNETIC AND QUADRUPOLAR RELAXATION RATES AS A FUNCTION OF TEMPERATURE IN $Cu_{50}Te_{50}$

$(R_1)_{Korringa}$ -·-·-·-·-

$(R_1)^*_{Korringa}$ .....

(assuming a chemical shift of -0·1%)

In table 6.7 the magnetic relaxation rates are compared with those calculated from the observed resonance shifts by the Korringa relationship, and also with a rate $(R_1)^*_M$ calculated on the assumption that there is a chemical shift of - 0.1% present.

Table 6.7

^{63}Cu magnetic relaxation rates in CuTe

Temp (kelvins)	$(R_1)_M$ observed (s^{-1})	$(R_1)_M$ Korringa (s^{-1})	$(R_1)^*_M$ Korringa (s^{-1})
700	150 ± 750	29	370
850	40 ± 300	34	440
950	680 ± 450	39	500
1040	1090 ± 350	56	610
1120	400 ± 400	90	730

If there is no chemical shift these measurements show that the density has fallen by a factor of six, and that the magnetic relaxation rate is enhanced, in the liquid, by factor of between four and ten. Both these values point to onset of electron localisation; however the conductivity is well above the level set by Mott for the start of localisation. Thus a more satisfactory explanation of these measurements is that a chemical shift of around - 0.1% exists. More extensive measurements of conductivity and of resonance shift as a function of temperature are required to prove its existence.

b) Quadrupolar relaxation. The three points in the liquid do not show a clear trend. All that can be said is that there is some quadrupolar relaxation of magnitude 200 to 400 s^{-1} roughly. In pure liquid Cu the rate has been estimated as $(R_1)_Q \leq 60\ s^{-1}$ (Warren and Clark, 1970) and so the behaviour observed in liquid metal alloys is also seen here where the quadrupolar relaxation is considerably enhanced by alloying.

In conclusion it must be pointed out that no marked change in either resonance shift, or in relaxation rate was observed on melting and so the behaviour of the ^{205}Tl resonance goes unexplained.

6.4 Bi_2Te_3

6.4.1 The Bi-Te system The solid equilibrium phase diagram (Hansen, 1958) is rather different, and much simpler than those for the two previous systems; the liquidus line being one broad hump across most of the range. There is no miscibility gap, and only one solid compound is found to exist, Bi_2Te_3.

The conductivity at 860 K shows a steady increase from $220 \times 10^3 ohm^{-1}m^{-1}$ at Te to $720 \times 10^3 ohm^{-1}m^{-1}$ at Bi (Enderby and Walsh, 1966), but some structure is detected in the conductivity isotherms with a minimum in the conductivity at 65 at. % Te and another near 50 at. % Te (Glazov, Chizevskaya and Glagoleva, 1969). The Hall coefficient is found to be small and negative, varying smoothly across the concentration range, and similar behaviour is observed in the thermopower (Enderby and Walsh, 1966); all of which indicates metallic rather than semiconducting behaviour.

The temperature coefficient of conductivity is positive down to 40 at. % Te and then becomes steadily more negative as the Te content is reduced (Glazov et al., 1969). It seems that although the Bi_2Te_3 liquid alloy has a positive temperature coefficient of conductivity none of the other properties characteristic of the materials described earlier exist here, and hence an investigation of the NMR properties could prove interesting, particularly since In_2Te_3 and Ga_2Te_3 are known to show liquid semiconductor behaviour.

6.4.2 Discussion of the magnetic resonance measurements

a) ^{125}Te The measurements were carried out at a single

temperature, about 25 kelvins above the melting temperature (878 K) and gives a resonance shift, see table 4.15, which is in keeping with the large density of states at the Fermi energy predicted by the conductivity measurements. The Korringa relationship gives the spin-lattice relaxation rate $(R_1)_s = 5.1 \times 10^3 s^{-1}$ which compares well with the observed rate $(R_1)_{observed} = (5.0 \pm 2.5) \times 10^3 s^{-1}$. Since there can be no quadrupolar relaxation in this case it is clear there is no appreciable deviation from the Korringa relationship.

b) ^{209}Bi The resonance shift observed is about two-thirds of that observed in pure liquid Bi, which agrees with the conclusion that this alloy is metallic in character. The Korringa relationship here predicts $(R_1)_s = 8.4 \times 10^3 s^{-1}$, but this is much lower than the observed rate $(R_1)_{observed} = (40 \pm 15) \times 10^3 s^{-1}$. However since the nuclear spin is 9/2 it is probable that the additional rate is due to quadrupolar relaxation. The solid equilibrium phase diagram for Sb-Te is very similar to that for Bi-Te and it is found that Sb_2Te_3 also behaves in a metallic fashion (Warren, 1971). The NMR measurements, which are discussed in section 6.5.2, show that the electric quadrupolar relaxation rate in Sb_2Te_3 comprises about 85% of the observed rate.

From all points of view, with the exception of the temperature dependence of the conductivity, and even that is explicable in terms of the partial structure factors, this alloy is metallic in character.

6.5 Other NMR measurements

6.5.1 Te Resonance shift measurements of ^{125}Te in liquid Te have been reported (Cabane and Froidevaux, 1969) in the temperature range 743 K to 923 K. These showed a linear increase from 0.38% to 0.48% which is in complete agreement with the results reported here. The spin-lattice relaxation rate was also measured near the

melting point, 740 K, $R_1 = (5 \pm 1.3) \times 10^3 s^{-1}$ and this is also in good agreement with this work.

6.5.2 In_2Te_3, Ga_2Te_3 and Sb_2Te_3

a) In_2Te_3 (Warren, 1971). The ^{115}In resonance shift is near zero in the solid but begins to increase with temperature from about 150 kelvins below the melting point. There is only a small change on melting, and the shift continues to increase, appearing to reach a constant value at some 500 kelvins above the melting point; the ^{125}Te resonance shows similar behaviour although rather smaller in magnitude. This is interpreted as showing a steady increase in the density of states at the Fermi energy as the temperature increases and tending to a limiting value, due to a gradual disappearance of the ordered structure without any marked change in the short range order on melting.

The ^{115}In nuclear spin-lattice relaxation rate is very large near the melting point, being about two orders of magnitude greater than the rate calculated from the Korringa relationship, but decreases as the temperature is raised and approaches the Korringa value at the highest temperature of observation. These measurements are interpreted, as outlined in section 6.2.5, as being direct evidence of the onset of localisation of the conduction electrons, since the electron-nucleus correlation time must increase as the temperature is decreased to cause the increasing enhancement of the relaxation rate. This interpretation is open to query, firstly since quadrupolar relaxation could be a large contributor, but since the observed rate is more than an order of magnitude larger than the rate for ^{115}In in In_2Sb_3 it is unlikely to be wholly quadrupolar in origin. It is also possible that the relaxation rate derived from the Korringa relationship could be too small if some negative chemical shift exists, this does not appear to have been considered by Warren. Using conductivity data (Glazov et al., 1969) a plot of

$\sigma^{\frac{1}{2}}$ vs resonance shift has been tried, but the scatter was too large to be able to draw a satisfactory line through the data. By considering the observations at high temperatures it can be seen that a chemical shift of more than - 0.2% would give a Korringa relaxation rate larger than the observed rate and thus sets the possible upper limit. If this value is used it increases the Korringa rate by a factor of about three and so the enhancement of the relaxation would be reduced to about thirty. This is still too large to be explained in any terms other than of an increase in the degree of localisation of the conduction electrons.

The quantity g is estimated by comparing the ^{115}In resonance shift in In_2Te_3 with its value in the pressure stabilised metallic phase InTeII (Brog, Jones and Milford, 1966).

$$g = \frac{N(E_F)}{N(E_F)_{F.e.}} \simeq \frac{S\ (^{115}\text{In in } In_2Te_3)}{S\ (^{115}\text{In in InTeII})}$$

A plot of g against log (relaxation rate enhancement factor) with temperature as the implicit variable shows a change of slope at around $g = 0.18$, with enhancement increasing more rapidly as g falls below this value. When g is plotted against conductivity a similar change is observed at about the same g value, the conductivity is seen to decrease more rapidly as g falls below 0.18. Warren suggests that this marks the transition from conduction by extended states to conduction in weakly localised states when $g > 0.18 \pm 0.03$.

b) Ga_2Te_3 (Warren, 1971). The solid state structure and binary alloy phase diagram are similar to those of In_2Te_3; the NMR behaviour is also similar. Two Ga isotopes were observed and the magnetic and quadrupolar contributions to the relaxation rate were resolved. This confirmed that the major part of the enhanced relaxation rate was magnetic in origin. Again Warren has not considered the existence of a chemical shift but in this case an attempt to correlate

conductivity and resonance shift data indicate that the chemical shift for Ga in Ga_2Te_3 is zero. There are no suitable Ga resonance shift data available in comparable but metallic material so values of g were estimated by comparing the ^{71}Ga resonance shifts in Ga_2Te_3 with a shift value calculated using a wave function density obtained from an optical hyperfine splitting and the free electron value for the density of states. This yields very similar behaviour to In_2Te_3, showing a transition in the region of $g = 0.18 \pm 0.03$.

c) Sb_2Te_3 (Warren, 1971). The binary phase diagram for Sb-Te has no liquid immiscibility gap and so differs from the two previous systems. The conductivity of Sb_2Te_3 is around $190 \times 10^3 ohm^{-1}m^{-1}$ at a few kelvins above the melting point and hence is almost two orders of magnitude greater than for the two alloys in a) and b).

The NMR behaviour is also very different. The ^{121}Sb and ^{123}Sb resonance shifts are large and metallic in the solid, and do not change appreciably on melting. The nuclear spin relaxation rate is an order of magnitude smaller than the ^{115}In relaxation rate in In_2Te_3 although it does decrease as the temperature is increased. From isotopic separation it is shown that the main contribution to the relaxation rate is quadrupolar, which explains the temperature dependence of the relaxation. The magnetic part of the relaxation rate fits the Korringa rate to within the experimental error, hence it is concluded that in this material there is no significant localisation of the conduction electrons.

6.6 Summary

The Te-Tl system has been investigated in some detail. Comparison of the suceptibility and conductivity with the resonance shift shows that there is little change in the conduction electron wavefunction as the composition is altered; rather the decrease in suceptibility, resonance shift and conductivity in going from pure Te towards TeTl arises

from a decrease in the density of states at the Fermi energy. A model for the electron behaviour in Te-Tl which has been postulated by Cutler to explain the variation of the density of states describes the conduction in terms of p-electrons; this is borne out to some extent by these measurements in that the s electron component is shown to be a few percent of the conduction electron wavefunction.

The predictions which the two general models for liquid semiconductors make concerning the principal parameters measured must now be considered. The resonance shift measures the magnitude of the average local field of the conduction electrons at the nucleus. On either model this field will change at any particular nucleus many times in a single Larmor period, hence the measurements cannot distinguish between the models. On the other hand the outstanding feature of the measurements reported here is the enhancement of the ^{125}Te spin-lattice relaxation rates which has been observed in Te-Tl alloys near to the composition $TeTl_2$ over the rates calculated from the resonance shifts using the Korringa relationship. These measurements appear to provide a basis for some conclusion regarding the models. In considering the observed enhancement a point concerning the calculated values of the relaxation rate must be made; namely that the calculated relaxation rate depends on the size and sign of the chemical shift contribution to the observed shift. Two calculations of the chemical shift one from the suceptibility measurements, the other from conductivity data give consistent values which are in line with similar measurements in other materials. In fact the values taken for the chemical shifts are the larger of these two sets of calculations, so that the enhancement may be even greater than the estimates given in this work. To explain the enhancement, all other sources of additional relaxation having been considered and discounted as being too ineffective it is necessary to postulate that the conduction electron-nucleus correlation time increases as the Te content decreases towards 33 at. %.

In the dilute metal model the conduction process is metallic, through a conventional conduction band, and there is no indication that the electron should spend any longer in any unit cell than in a normal metal. In the pseudogap model the conduction is also in a conventional band until the density of states at the Fermi energy reduces to some critical value, below which the electron states are localised. There is a spread of compositions in any liquid alloy due to the thermal motions and hence it is expected that the appearance of localisation will be a gradual process as the Te content decreases. This is just what is observed and, although it is difficult to say where localisation begins, there is some evidence of it by the time the density of states has fallen to about 30% of the free electron value. This behaviour is similar to that described by the pseudogap model and must therefore be taken as evidence in its favour. Further, Mott has shown that localisation is only likely to occur with electrons in p or higher states; the deductions concerning the wavefunction character are consistent with this conclusion.

In CuTe where the conductivity is some three times larger than in TeTl the resonance shift is small and the relaxation rate shows no large enhancement. This behaviour is similar to that of TeTl, and had it been possible to extend the range of observation it is likely that localisation would have been detected.

In Bi_2Te_3 the conductivity, resonance shift and relaxation rates are all typically metallic; whereas Warren reports that in In_2Te_3 and Ga_2Te_3 there is evidence of localisation although there is none in Sb_2Te_3. An explanation for these two categories of behaviour may come from the model proposed for Te-Tl. There it is suggested that molecular groups persist in the liquid, and this is supported by the observation of a chemical shift; the retention of some form of solid grouping in the liquid implies that the solid behaviour must be important. This is given weight by the fact that those alloy systems which show some evidence for

localisation have a region of liquid immiscibility and rather similar solid phase diagrams; those which are metallic have simpler phase diagrams. This offers a starting point for further investigations of localised electron states in liquid semiconductors.

References

Abragam, A., 1961, The Principles of Nuclear Magnetism (Claredon Press : Oxford).

Anderson, P. W., 1958, Phys. Rev., 109, 1492.

Angus, W. R., 1932, Proc. Roy. Soc., A 136, 569.

Bennett, L. H., Watson, R. E. and Carter, G. C., 1970, Journal of Research of the National Bureau of Standards - A Physics and Chemistry, 74 A, 569.

Bensoussan, M., 1967, J. Phys. Chem. Solids, 28, 1533.

Brog, K. C., Jones, W. H. and Milford, F. J., 1966, Phys. Rev., 144, 245.

Cabane, B. and Froidevaux, C., 1969, Phys. Lett. A, 29, 512.

Cabane, B. and Friedel, J., 1971, J. Phys., 32, 73.

Cohen, M. H., Fritzsche, H. and Ovshinsky, S. R., 1969, Phys. Rev. Lett., 22, 1065.

Cutler, M., 1971, Phil. Mag., 24, 381.

Cutler, M. and Field, M. B., 1968, Phys. Rev., 169, 632.

Cutler, M. and Mallon, C. E., 1966, J. Chem. Phys., 37, 2677.

Cutler, M. and Mott, N. F., 1969, Phys. Rev., 181, 1336.

Cutler, M. and Petersen, R. L., 1970, Phil. Mag., 21, 1033.

Dancy, E. A., 1965, Trans. Met. Soc. AIME, 233, 270.

Davis, E. A. and Mott, N. F., 1970, Phil. Mag., 22, 903.

Dupree, R. and Seymour, E. F. W., 1972, Physics and Chemistry of Liquid Metals. Ed. S.Z. Beer. (Marcel Dekker : New York), 461.

Edwards, S. F., 1962, Proc. Roy. Soc., A 267, 518.

Enderby, J. E. and Collings, E. W., 1970, J. Non-Cryst. Solids, 4, 161.

Enderby, J. E. and Simmons, C. J., 1969, Phil. Mag., 20, 125.

Enderby, J. E. and Walsh, L., 1966, Phil. Mag., 14, 991.

Faber, T. E. and Ziman, J. M., 1965, Phil. Mag., 11, 153.

Flory, P. J., 1944, J. Chem. Phys., 12, 425.

Frisch, H. L. and Lloyd, S. P., 1960, Phys. Rev., 120, 1175.

Glazov, V. M., Chizevskaya, S. N. and Glagoleva, N. N., 1969, Liquid Semiconductors. (Plenum Press : New York).

Hansen, M., 1958, The Constitution of Binary Alloys. McGraw Hill.

Heighway, J. and Seymour, E. F. W., 1971, Phys. kondens. Materie, 13, 1.

Herman, F. and Skillman, S., 1963, Atomic Structure Calculations. (Prentice Hall, Englewood Cliffs, N. J.).

Kanda, F. A., 1967, USAEC Report NYO - 2731/8.

March, N. H., 1968, Liquid Metals (Pergamon Press Ltd : London).

Mott, N. F., 1967, Adv. in Phys., 16, 49.

Mott, N. F., 1969, Phil. Mag., 19, 835.

Mott, N. F., 1971, Phil. Mag., 24, 1.

Obata, Y., 1963, J. Phys. Soc. Japan, 18, 1020.

Senturia, S. D., Hewes, C. R. and Adler, D., 1970, J. Appl. Phys., 41, 430.

Smith, G. W., 1964, J. Appl. Phys., 35, 1217.

Warren, W. W., 1971, Phys. Rev. B, 3, 3708.

Warren, W. W., 1972, J. Non-Cryst. Solids, 8/9.

Warren, W. W. and Clark, W. G., 1970, Phys. Rev. B, 1, 24.

Ziman, J. M., 1960, Electrons and Phonons (Clarendon Press : Oxford).

Ziman, J. M., 1961, Phil. Mag., 6, 1013.

APPENDIX

The extension of the Sholl theory of quadrupolar relaxation to the case of binary alloys.

The starting point of the theory is the quadrupolar relaxation rate expression, equation 5.8. The potential part of the quadrupolar Hamiltonian, equations 5.12 and 5.13 expressed in terms of the screened potential, equation 5.11, is used to calculate the spectral density, equation 5.14.

In an alloy the potential describing the interaction depends on whether the atom pairs are AA or AB, so now

$$F^{(m)}(t-\tau)\,F^{(-m')}(t) = \sum_{\lambda\mu} U_m^{\lambda}\left\{\underline{r}(t-\tau)\right\}\,U_{m'}^{\mu *}\left\{\underline{r}_{\mu}(t)\right\} \qquad \ldots\ldots (A.1)$$

the ensemble average of this is

$$\begin{aligned} g_{mm'}(\tau) = &\iint U_m^A(\underline{r}_o)\,U_{m'}^{A*}(\underline{r}_1)\,P_{AAA}(\underline{r}_o, t-\tau; \underline{r}_1, t)\,d\underline{r}_o\,d\underline{r}_1 \\ &+ \iint U_m^B(\underline{r}_o)\,U_{m'}^{B*}(\underline{r}_1)\,P_{ABB}(\underline{r}_o, t-\tau; \underline{r}_1, t)\,d\underline{r}_o\,d\underline{r}_1 \\ &+ \iint U_m^A(\underline{r}_o)\,U_{m'}^{B*}(\underline{r}_1)\,P_{AAB}(\underline{r}_o, t-\tau; \underline{r}_1, t)\,d\underline{r}_o\,d\underline{r}_1 \\ &+ \iint U_m^B(\underline{r}_o)\,U_{m'}^{A*}(\underline{r}_1)\,P_{ABA}(\underline{r}_o, t-\tau; \underline{r}_1, t)\,d\underline{r}_o\,d\underline{r}_1 \end{aligned} \qquad \ldots\ldots (A.2)$$

Where $P_{AAB}(\underline{r}_o, t-\tau; \underline{r}_1, t)\,d\underline{r}_o\,d\underline{r}_1$ is the probability of finding an ion of type A in $d\underline{r}_o$ at $\underline{r}_o$ at time $t-\tau$ and an ion of type B in $d\underline{r}_1$ at $\underline{r}_1$ at time t given that there is one of type A at the origin. These probabilities are expressed

$$\begin{aligned} P_{AAA}(\underline{r}_o, t-\tau; \underline{r}_1, t) = &\; g_{AA}(\underline{r}_o)\,c\rho\,P_A(\underline{r}_o, t-\tau; \underline{r}_1, t) \\ &+ \int {}^{(3)}_{AAA}(\underline{r}_o, \underline{r}_2)\,P_A(\underline{r}_2, t-\tau; \underline{r}_1, t)\,d\underline{r}_2 \end{aligned} \qquad \ldots\ldots (A.3)$$

$$P_{ABB}(\underline{r}_o, t-\tau; \underline{r}_1, t) = g_{AB}(r_o)(1-C)\rho\, P_B(\underline{r}_o, t-\tau; \underline{r}_1, t) + \int \rho^{(3)}_{ABB}(\underline{r}_o, \underline{r}_2)\, P_B(\underline{r}_2, t-\tau; \underline{r}_1, t)\, d\underline{r}_2 \quad \ldots. (A.4)$$

$$P_{AAB}(\underline{r}_o, t-\tau; \underline{r}_1, t) = \int \rho^{(3)}_{AAB}(\underline{r}_o, \underline{r}_2)\, P_B(\underline{r}_2, t-\tau; \underline{r}_1, t)\, d\underline{r}_2 \quad (A.5)$$

$$P_{ABA}(\underline{r}_o, t-\tau; \underline{r}_1, t) = \int \rho^{(3)}_{ABA}(\underline{r}_o, \underline{r}_2)\, P_A(\underline{r}_2, t-\tau; \underline{r}_1, t)\, d\underline{r}_2 \quad (A.6)$$

where ρ is the atom number density,

C is the fractional concentration of A type atoms,

g_{AA} is the AA radial distribution function,

g_{AB} is the AB radial distribution function,

$\rho^{(3)}_{AAA}(\underline{r}_o, \underline{r}_2)$ is the three particle correlation function : the probability of finding A ions at $\underline{r}_o$, and $\underline{r}_2$ given an A type ion at the origin.

$P_A(\underline{r}_o, t-\tau; \underline{r}_1, t)\, d\underline{r}_o\, d\underline{r}_1$ is the probability of finding an ion of type A in $d\underline{r}_o$ at $\underline{r}_o$ at time $t-\tau$ and the same ion in $d\underline{r}_1$ at $\underline{r}_1$ at time t.

The three particle correlation function is expressed using the superposition approximation.

$$\rho_{AAA}(\underline{r}_o, \underline{r}_2) = C^2\rho^2\, g_{AA}(r_o)\, g_{AA}(r_2)\, g_{AA}(r_{o2}) \quad \ldots. (A.7)$$

$$\rho_{ABB}(\underline{r}_o, \underline{r}_2) = (1-C)^2\rho^2\, g_{AB}(r_o)\, g_{AB}(r_2)\, g_{BB}(r_{o2}) \quad \ldots. (A.8)$$

$$\rho_{AAB}(\underline{r}_o, \underline{r}_2) = C(1-C)\rho^2\, g_{AA}(r_o)\, g_{AB}(r_2)\, g_{AB}(r_{o2}) \quad \ldots. (A.9)$$

$$\rho_{ABA}(\underline{r}_o, \underline{r}_2) = C(1-C)\rho^2\, g_{AB}(r_o)\, g_{AA}(r_2)\, g_{AB}(r_{o2}) \quad \ldots. (A.10)$$

Following Oppenheim and Bloom (1961)

$$g_{AA}(r_o)\, P_A(\underline{r}_o, t-\tau; \underline{r}_1, t) = g^{\frac{1}{2}}_{AA}(r_o)\, g^{\frac{1}{2}}_{AA}(r_1)\, \psi_A(\underline{r}_o, \underline{r}_1, \tau) \quad \ldots. (A.11)$$

and

$$g_{AB}(r_o)\, P_A(\underline{r}_o,\, t - \tau;\, \underline{r}_1,\, t) \;=\; g_{AB}^{\frac{1}{2}}(r_o)\, g_{AB}^{\frac{1}{2}}(r_1)\, \psi_B(\underline{r}_o,\, \underline{r}_1, \tau) \quad \ldots\ (A.12)$$

$$\text{where } \psi_A \;=\; (8\pi D_A \tau)^{-3/2} \exp\left\{-(\underline{r}_1 - \underline{r}_o)^2 / 8 D_A \tau\right\} \quad \ldots\ (A.13)$$

D_A is the self-diffusion coefficient of ion A.

Substituting equations A.3 and A,13 into equation A.2 gives

$$g_{mm'}(\tau) \;=\; C\rho A_{mm'}(\tau) + C^2 \rho^2 B_{mm'}(\tau) + (1 - C)\rho\, C_{mm'}(\tau)$$

$$+ (1 - C)^2 \rho^2 D_{mm'}(\tau)$$

$$+ C(1 - C)\rho^2 \left[E_{mm'}(\tau) + F_{mm'}(\tau)\right] \quad \ldots\ (A.14)$$

where $A_{mm'}(\tau)$ and $B_{mm'}(\tau)$ are integral expressions of U_m, the $g(r)$, and are defined by Sholl (1961). The terms C, D, E and F are similar in form but have changes of D_B for D_A, $g_{AB}(r_{o2})$ for $g_{AA}(r_{o2})$ and so on.

The relaxation rate can now be expressed

$$(R_1)_Q \;=\; \frac{2I + 3}{I^2(2I - 1)} \left(\frac{eQ\,(1 - \gamma_\infty)}{\hbar}\right)^2 \frac{\pi\rho}{75} \;\times$$

$$\Big[\left\{C / D_A\right\} I_1(v_2^A,\, v_2^A,\, g_{AA},\, g_{AA})$$

$$+ \left\{C^2 / D_A\right\} I_2(v_2^A,\, v_2^A,\, g_{AA},\, g_{AA},\, g_{AA},\, g_{AA})$$

$$+ \left\{(1 - C) / D_B\right\} I_1(v_2^B,\, v_2^B,\, g_{AB},\, g_{AB})$$

$$+ \left\{(1 - C)^2 / D_B\right\} I_2(v_2^B,\, v_2^B,\, g_{AB},\, g_{AB},\, g_{AB},\, g_{BB})$$

$$+ \left\{C(1 - C) / D_B\right\} I_2(v_2^A,\, v_2^B,\, g_{AA},\, g_{AB},\, g_{AB},\, g_{AB})$$

$$+ \left\{C(1 - C) / D_A\right\} I_2(v_2^B,\, v_2^A,\, g_{AB},\, g_{AA},\, g_{AA},\, g_{AB}) \Big] \quad \ldots\ (A.15$$

$$\text{where } I_1(v_2^A,\, v_2^B,\, g_{AA},\, g_{AB}) \;=\; \int_0^\infty v_2^A(\underline{r}_o)\, G(r_o)\, dr_o \quad \ldots\ (A.16$$

and

$$G(r_o) = g_{AA}^{\frac{1}{2}}(r_o) / r_o \left[\int_0^{r_o} v_2^B(r_1)\, g_{AB}^{\frac{1}{2}}(r_1)\, r_1^4\, dr_1 + r_o^5 \int_{r_o}^{\infty} \left\{ v_2^B(r_1) / r_1 \right\} g_{AB}^{\frac{1}{2}}(r_1)\, dr_1 \right]$$

$$2\pi\rho\, I_2(v_2^A, v_2^B, g_{AA}, g_{AB}, g_{AB}, g_{BB}) = \int_0^{\infty} v_2^A(r_o)\, g_{AA}(r_o)\, r_o^2\, dr_o \int_0^{\infty} G(r_2)\, dr_2 \int_{-1}^{+1} \left\{ g_{BB}(r_{o2}) - 1 \right\} P_2(z)\, dz \quad \ldots\ (A.17)$$

where $P_2(z)$ is defined in equation 5.16.

If we now make the assumptions that $g_{AA} = g_{AB} = g_{BB}$ and also that $v^B = \alpha\, v^A$ then equation 5.19 appears.